JSTR
ASEAN Journal of Scientific and Technological Reports
Vol. 25 No. 4
October - December 2022
ISSN 2773-8752 (online)

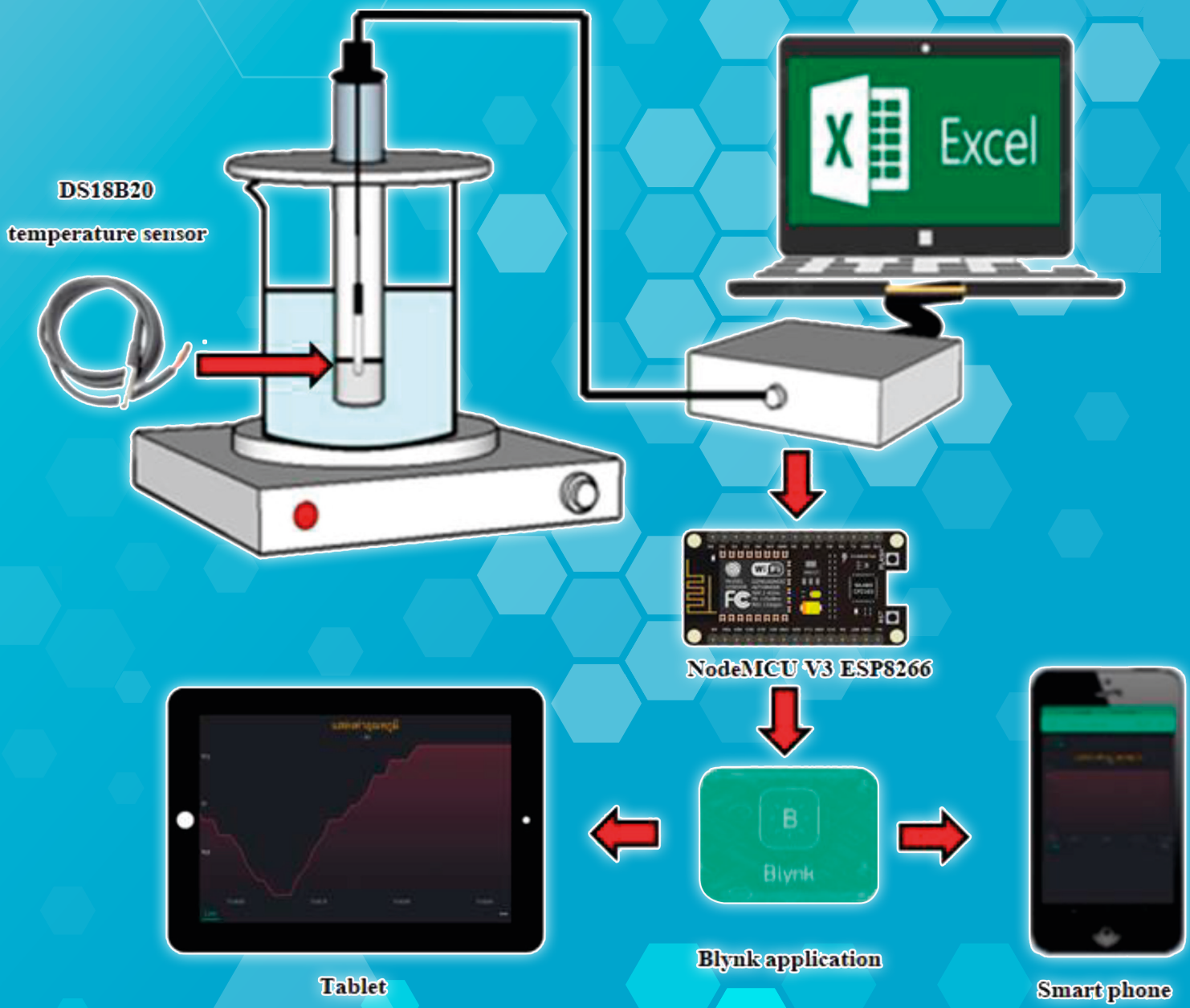

ASEAN Journal of Scientific and Technological Reports (AJSTR)

Contact Us Research and Development Institute Thaksin University
222 M. 2 Ban-Prao sub-district, Pa-Pra-Yom district, Phatthalung province, Thailand
Tel. 0 7460 9600 # 7242 , E-mail: aseanjstr@tsu.ac.th

Editorial

The ASEAN Journal of Scientific and Technological Reports (AJSTR) Vol. 25 No. 4 (October-December 2022) ISSN 2773-8752 is the fourth issue under AJSTR. This issue published 9 worth-reading research articles. These exciting research articles were reviewed and answered by experts from various universities and institutions. We sincerely hope that some of the research papers will help guide and motivate our active researchers to produce and create more valuable research shortly. The AJSTR has served our energetic readers and customers on an international level.

For this reason, all selected and accepted research articles will be written and organized in English. From now on, the AJSTR and a new editorial team are ready to organize, manage, publish, and deliver all good quality articles written in well-organized English to the world of academic society. I would like to introduce AJSTR's editorial board members as below.

Assoc. Prof. Dr. Sompong O-Thong

Journal Editor-in-Chief

List of Contents

Contents Page

Water Quality Improvement by Wild Bacilli Isolated from Marine Environments 1
Rungnapa Keawkong, Onanong Siriboon, Sunipa Chankaew, Yutthapong Sangnoi and Arnon Uppabullung

Plasma Instability During ITBs Formation with Pellet Injection in Tokamak 11
Ponkris Klaywittaphat, Thawatchai Onjun, Roppon Picha, Jiraporn Promping and Boonyarit Chatthong

Corrosion of Low Carbon Steel in Chloride Containing Environment 21
Tosapolporn Pornpibunsompob, Sittha Saidarasamoot, Sawitri Phabjanda, Teeratas Pornyungyuen, Apirath Gositanon, Suradet Chalermboon and Ploypilin Nakaracha

"Water Quality Management Guidelines to Reduce Mortality Rate of Red Tilapia (*Oreochromis niloticus x Oreochromis mossambicus*) Fingerlings Raised in Outdoor Earthen Ponds with a Recirculating Aquaculture System Using Machine Learning Techniques" 30
Putra Ali Syahbana Matondang, Wara Taparhudee, Ruangvit Yoonpundh and Roongparit Jongjaraunsuk

An Experimental Set for Studying the Changing State of Matter with Smart Learning Media Displayed Through the IoT System for Smart-Lab 42
Jiraporn Chomanee, Nisagorn Nakarang, Sek Handee, Patchara Choksuriwong, Supagorn Katathikarnkul and Tanchanok Poonsin

The Effect of Acacia mangium Leaf Feed on Apparent Metabolizable Energy, Growth Performance, and Carcass Composition of Broiler Chickens 50
Saichon Lerdsuwan, Warrapong Nalinanon and Duangjai Pisuttharachai

Effects of Different Potting Media on the Growth of Commercial Cacti 59
Kittiphan Ritthidechrat and Chamaiporn Anuwong

Effect of Supplementation Yeast Fermented *Acacia mangium* Leaf in Diets on Growth Performance, Carcass Quality, and Haematology of Climbing Perch *(Anabas testudineus)* 68
Warrapong Nalinanon, Saichon Lerdsuwan and Duangjai Pisuttharachai

Impact of Using Blue Crab Shell Powder (BCSP) on Alteration of EC, pH, Leaf Greenness, and Growth of Cucumis melo var. Hamigua TA215 Seedlings 79
Pimpan Pimonrat, Dowroong Watcharinrat, Nattapong Chanchula and Pornpimol Pimolrat

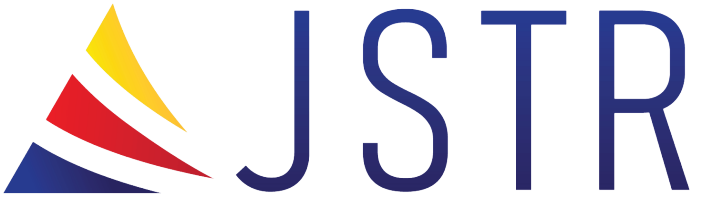

ASEAN Journal of Scientific and Technological Reports

JSTR
ASEAN Journal of Scientific and Technological Reports

Research article

Water Quality Improvement by Wild Bacilli Isolated from Marine Environments

Rungnapa Keawkong[1], Onanong Siriboon[2], Sunipa Chankaew[3], Yutthapong Sangnoi[4, 6*] and Arnon Uppabullung[5, 6]

[1] Faculty of Natural Resources, Prince of Songkla University, Hat Yai, Songkhla, 90110, Thailand; saifon_sila5366@hotmail.com
[2] Faculty of Natural Resources, Prince of Songkla University, Hat Yai, Songkhla, 90110, Thailand; moodang_aqua@hotmail.com
[3] Faculty of Natural Resources, Prince of Songkla University, Hat Yai, Songkhla, 90110, Thailand; chan.sunipa@gmail.com
[4] Faculty of Natural Resources, Prince of Songkla University, Hat Yai, Songkhla, 90110, Thailand; yutthapong.s@psu.ac.th
[5] Faculty of Natural Resources, Prince of Songkla University, Hat Yai, Songkhla, 90110, Thailand; arnon.u@psu.ac.th
[6] Discipline of Excellence in Sustainable Aquaculture, Prince of Songkla University, Hat Yai, Songkhla 90110, Thailand
* Correspondence: yutthapong.s@psu.ac.th

Abstract: Huge feed volume and shrimp density loading in the intensive shrimp culture decreased water quality. Ammonia and nitrite, which are toxic substances, are occurred from feed and shrimp excretion. *Bacillus* and related genera (class Bacilli) are bacteria capable of transforming ammonia to nitrite and then nitrite to nitrate by nitrification. In this study, wild marine Bacilli were isolated from samples collected from seagrass beds Andaman Sea, Thailand. Bacilli strains were obtained by using the heat-shock method. Three bacilli bacteria were consisting of *Bacillus* sp. BC02 (DNA-based), *Bacillus* sp. BC05 (morphology-based) and *Virgibacillus* sp. BC06 (DNA-based) was obtained. This study aims to investigate these isolates in shrimp wastewater improvement compared with the commercial seed of *Bacillus* spp. product (PM-1). Seven wastewater treatments were separately tested by adding different formulas of bacteria. Each treatment was added for 1% (w/v) of 10^7 CFU/mL density and incubated for 7 days. Treatment of BC02+BC05 showed a significant TSS decrease (66.56%) and produced the highest nitrate concentration. The highest increase of OTP (84.97%) was found in the treatment of BC02+BC05+BC06. PM-1 product has presented the best BOD lessening (54.35%) and showed a non-significant reduction of ammonia (98.60%) with the highest nitrite (0.685 ± 0.009 mg/L) at the end of the experiment. *Virgibacillus* (BC06) has resulted in the highest significant reduction of COD (60.39%). Thus, it might be summarized that three marine isolates of *Bacillus*, *Virgibacillus*, and commercial PM-1 product have excellent potential to improve wastewater quality with no significant diferent. Marine *Bacilli* can be substitution used for commercial PM-1 products.

Keywords: *Bacillus*; *Virgibacillus*; Wastewater improvement, OTP, BOD, COD

Citation:
Keawkong, R.; Siriboon, O.; Sangnoi , Y.; Uppabullung, A.; Chankaew, S. Water Quality Improvement by Wild Bacillus Isolated from Marine Environments. *ASEAN J. Sci. Tech. Report.* **2022**, *25*(4), 1-10. https://doi.org/10.55164/ajstr.v25i4.247454.

Article history:
Received: September 28, 2022
Revised: November 7, 2022
Accepted: November 8, 2022
Available online: November 20, 2022

1. Introduction

Intensive shrimp culture has been popular in recent years. High-density rearing is necessary to use high protein feed for shrimp. This leads to a continuous increase of uneaten feed, feces, and wastes at the bottom of the pond according to

time and declines in water quality [1-2]. High ammonia and nitrite are some of the improper water qualities and are toxic to shrimp, which should be controlled [3]. In the huge pond, water exchangeable takes a lot of time and increase energy cost. Water discharging brings loads rich in nutrients and organic matter to surrounding environments [4]. And it creates a risk of the pathogen spreading to other farms and environments [5]. The microorganisms have been applied in shrimp culture as a biological process for managing these problems [1, 6]. Microorganisms should not be pathogenic bacteria, working as biodegradable organic matter, and removal of ammonia and nitrite in culture pond. Most microorganisms are Bacillus spp. as they role in nitrification and produce enzymes (i.e., amylase, lipase, and protease) that can decompose organic matter [1, 7-10]. Moreover, *Bacillus* spp. has been described as promoting the growth of green algae and diatoms in shrimp ponds. At the same time, they can control toxin-producing algae groups (blue-green algae and dinoflagellates) [11]. Furthermore, the advantage of the genus *Bacillus* is endospore formation which makes it comfortable to prolong shelf-life, storage, transport, and application in shrimp farms [12]. Although several commercial Bacillus products are currently used for water improvement in marine shrimp aquaculture, they are probably not marine species. This may result in being less effective in improving saline water quality. Therefore, the isolation of *Bacillus* from the marine origin is necessary because they may have more efficiency in enhancing water quality in marine shrimp aquaculture [9-10]. Thus, this study aimed to isolate wild marine bacteria, *Bacillus* spp. and *Virgibacillus* sp., apply them to improve water quality in shrimp ponds, and compare the efficiency with commercial Bacillus spp. (PM-1) product. Additionally, untapped, promising, and novel marine bacterial strains may be found for wastewater treatment.

2. Materials and Methods

2.1 Isolation of marine Bacilli

The samples, including soil and seawater, were collected from seagrass beds at Libong Island, Trang province, Andaman Sea, Thailand. Targeted marine *Bacilli* were isolated by the heat-shock method [13]. One gram of soil and 1 mL of water samples were taken to each tube. The tubes were heated at 80 ℃ for 20 minutes and immediately shocked in ambient water. The soil sample was diluted with 10 mL of sterilized seawater. Then all sample solutions were diluted by 10 folds serial dilution. Each 0.1 mL of dilution was spread out on Nutrient Agar (NA) plates with an additional 3.2% sea salt, and plates were incubated at 37 ℃ for 24 hours. Single colony on plates was picked up by loop and streaked on fresh NA plates (3.2% sea salt) 2-3 times until pure isolates were obtained. Bacilli cells were observed by the unique characteristics of gram-negative, rod shape, endospore-forming, and positive catalase testing [10]. Then, DNA extraction of each strain was done using a commercial DNA extraction kit (Genomic DNA mini kit, Geneaid). Their 16S rRNA genes were amplified by PCR using a set of universal primers 27F (5′-AGAGTTTGATCATGGCTCAG-3′) and 1492R (5′-GGTTACCTTGTTACGACTT-3′). After PCR product purification by GF-1 AmbiClean Kit (PCR/Gel) (Vivantis), DNA sequencing was determined with the same primers by Macrogen manufacturing [9]. DNA sequences were compared within GenBank/EMBL/DDBJ database using the Blast program. A phylogenetic tree of marine isolates and related species was constructed by the MEGA 11 program [14].

2.2 Optimal salt requirement of marine Bacilli

Each strain of candidate *Bacilli* was cultured in Nutrient Broth (NB) with 3.2% sea salt by inoculating a 1-loop of bacteria into a 10 mL tube containing NB (3.2% sea salt) shaking at 110 rpm for 24 hours. 1 mL of each isolate was transferred into a tube containing 9 mL of NB at different salinity levels of 0, 5, 10, 15, 20, 25, 30, 35, and 40 ppt. All tubes were shaken at 110 rpm for 24 hours, and measured cell density was using a spectrophotometer at 600 nm wavelength.

2.3 Water improvement efficiency

The water treatment efficiency of isolated marine Bacilli was compared with PM-1. A commercial bacterial product consisted of 3 *Bacillus* species (*B. subtilis*, *B. licheniformis*, and *B. megaterium*). One gram of PM-1 seed product was mixed with 2.5 L water, 5 g shrimp feed, and 50 mL molasses, then closed the cover. Air has been blowing continuously for 36 hours. Seed starters of isolated marine Bacilli and PM-1 were carried in a 250 mL flask with NB (3.2% sea salt), shaking at 110 rpm for 24 hours. After that, each isolated Bacilli's cell suspension was started at a concentration of 10^7 CFU/ml. Then, 70 mL (1%) of each single strain suspension (PM-1, BC02, BC05, and BC06) was transferred into a 10-L glass jar containing 7 L of water from the shrimp

pond. Treatment BC02+BC05 was prepared at a 1:1 ratio (35:35 mL). Likewise, treatment BC02+BC05+BC06 was mixed in a 1:1:1 ratio (23.3 mL each). These mixture treatments were carried on under the same condition as a single treatment in a 10-L glass jar. The experiment was conducted for 7 days by air suppling for 24 hours in every treatment and water quality parameters were measured daily, including dissolved oxygen, salinity, temperature, ammonia, nitrite, and nitrate [15]. The total suspended solid was measured on days 1, 3, 5 and 7 of the following experiment [16]. Additionally, orthophosphate [15], BOD_5 [17], and COD [18] were analyzed at the initial and the end of the experiment.

2.4 Statistical Analysis

Variations in water quality parameters were investigated between treatments and control using Analysis of Variance followed Completely Randomized Design. Duncan's New Multiple Range Test and T-Test at 95% confidence levels were used to determine the mean difference among the treatments. These analyses were performed using the R program.

3. Results and Discussion

3.1. Wild marine Bacilli

Bacilli bacteria were isolated from water and soil samples collected on seagrass beds at Libong Island, Trang province, which was manipulated by the heat-shock method. Although fourteen isolates were gram-positive and showed rod shape, only 3 isolates found endospore forming, consisting of BC02, BC05, and BC06 (Figure 1). Endospore formation is a unique characteristic of *Bacillus* when environmental conditions are far from optimal, e.g., high temperature and dry. Utilizing this capability will therefore make the isolation process easier. In addition, endospore-forming *Bacillus* is proficient for further use in shrimp ponds. The three Bacilli isolates were selected to study the water improvement efficiency further.

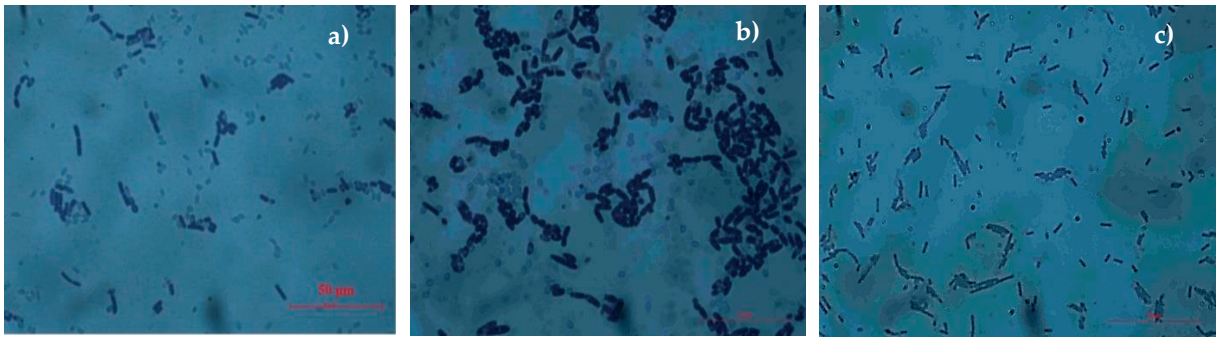

Figure 1. Characteristic of three marine endospore-forming Bacilli; a) BC02, b) BC05, and c) BC06.

As a result of partial 16S rDNA sequencing, *Bacillus* sp. BC02 showed a similarity of about 95% to *Bacillus thuringiensis* (Figure 2). The bacteria *B. thuringiensis* was widely known that they inhabited soil and produced specific proteins to kill insects. Therefore, *B. thuringiensis* has been widely used as a biocontrol of insect pests in agriculture [19]. However, [20] reported the isolation of marine *B. thuringiensis* from marine sediment. Then several publications of marine *B. thuringiensis* from marine sources were reported [21, 22]. In aquaculture, [23] reported the potential of marine *B. thuringiensis,* isolated from shrimp intestines, as a probiotic against a pathogenic bacterium in marine shrimp. Another research [24] published the isolation of *B. thuringiensis* from the goldfish intestine and screening it for use as a probiotic. In addition, there are some studies on the application of *B. thuringiensis* to inhibit parasitic nematodes in fish [25] or to control insects (mosquitoes) that as carriers of disease in water and wastewater [26]. However, no publication of *B. thuringiensis* directly used for water treatment. This research may first study *B. thuringiensis* for water treatment. Another isolate, BC06, has low similarity, about 83% related to the genus *Virgibacillus* (Class Bacilli). Genus *Virgibacillus* was reclassified, separating from the genus *Bacillus* in 1998 [27]. Although *Virgibacillus* can be isolated from marine and non-marine sources, they were reported as a halophilic bacterium [28-31]. The percentage of similarity result (83%) of partial 16S rRNA was deficient. Therefore, strain BC06 may require rearrangement when the 16S

rRNA gene full length is studied. In the case of strain BC05, the DNA extraction had a problem of low quantity and quality. Hence this isolate was still unidentified.

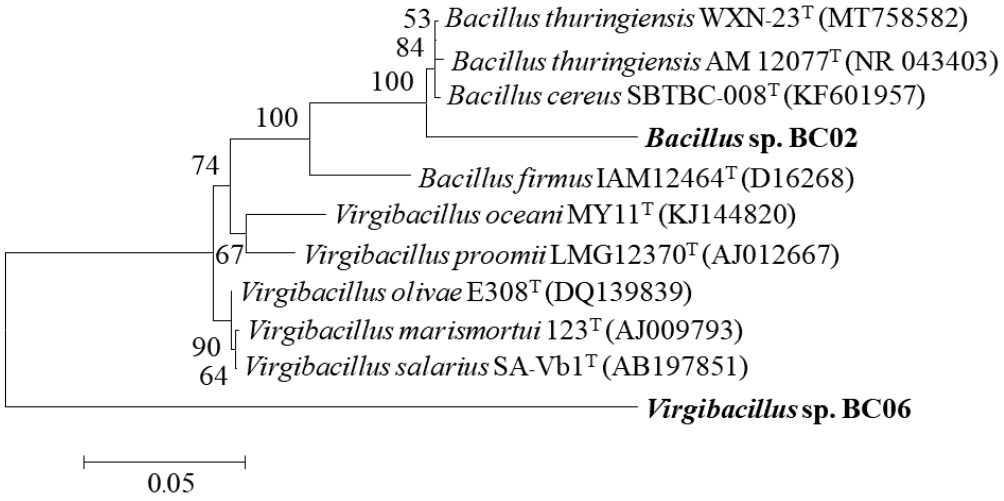

Figure 2. The phylogenetic tree of two marine Bacilli, BC02 and BC06, is based on partial 16S rDNA (Bar = 0.05 μm).

3.2. Salt tolerance for growth of marine Bacilli

Salt tolerance was conducted in 9 levels, including 0, 5, 10, 15, 20, 25, 30, 35, and 40 ppt. The result showed that strain BC02 has a wide range of optimal growth at 0-35 ppt, like strain BC05 has optimal growth at 0-30 ppt. In comparison, strain BC06 has a narrower range of optimal growth at 20 to 40 ppt. Three marine isolates in this study were obtained from marine sources. Therefore, they showed the character of a wide range of salt-tolerant, according to other studies [9-10]. These might result from the various physiological preferences of each strain.

3.3. Water quality improvement of marine Bacilli and PM-1 bacterial product

3.3.1. Total suspended solid (TSS)

All treatments showed no significant difference between each other on days 1 and 3, but they presented the same trends as TSS gradually decreased. While the end of the experiment, BC02+BC05 treatment was the lowest TSS (0.109 ± 0.009 mg/L) which has no significance (P>0.05) with treatments of BC05 and BC06 (0.1177 ± 0.0067 and 0.145 ± 0.029 mg/L, respectively). The TSS of control, BC02, BC06, BC02+BC05+BC06 and PM-1 were 0.182 ± 0.019, 0.145 ± 0.029, 0.1787 ± 0.034, 0.178 ± 0.0139 and 0.179 ± 0.062, respectively with no significance (P>0.05) as shown in Figure 3a. Conversely, they were significantly different (P<0.05) with BCO2+BC05. Adding all 3 marine Bacilli decreased TSS from 0.326 ± 0.000 mg/L to the range of 0.109±0.009 to 0.182 ± 0.019 mg/L (~ 44–66%) at the end of the study. Exceptionally, BC02+BC05 showed the lowest TSS. It might be because they have co-metabolism to degrade or trap the particle suspension in the water sample. The result was according to the study of *B. velezensis* that showed TSS removal of brewery wastewater for 55% [32]. In an aquaculture pond, the solid suspension will be overshadowed by light through water which affects the primary production process of water. The high suspension will directly harm aquatic animals by clogging their gills, leading to hard breathing, slow growth, late hatching, and growth of larvae. Therefore, using a couple of wild marine Bacilli (BC02+BC05) could reduce TSS and indirectly help promote the well-being of aquatic animals.

3.3.2. Orthophosphate concentration (PO_4^{3-})

Orthophosphate has been monitored in all treatments. The initial concentration of orthophosphate was 0.1224 ± 0.000 mg/L and continuously increased until the last day of the experiment with

the range of 0.1287 ± 0.0361 to 0.2264 ± 0.1165 mg/L. Treatment of BC02+BC05+BC06 was showed the highest quantity of orthophosphate (0.2264 ± 0.1165 mg/L), but has no significance (P>0.05) with treatments of control, BC02, BC05, BC06, BC02+BC05 and PM-1, which their orthophosphate volume were 0.1300 ± 0.0168, 0.1731 ± 0.0697, 0.1287 ± 0.0361, 0.1394 ± 0.0196, 0.1914 ± 0.0638 and 0.1345 ± 0.0452 mg/L, respectively (Figure 3b). Although the treatment BC02+BC05+BC06 was the highest PO_4^{3-}, major nutrients needed by most phytoplankton consist of nitrogen in the forms of nitrite (NO_3^-), ammonia (NH_4^+), and urea ($CO(NH_2)_2$). As well as phosphorus in orthophosphate (PO_4^{3-}) or soluble reactive phosphorus that are good soluble for instant utilization on phytoplankton and aquatic plants growth [1]. In the part of insoluble phosphorus will be slowly decomposed by bacteria and released into a soluble form. Several *Bacillus* species were mentioned about their ability in phosphate elimination, such as cellulolytic *Bacillus* species can reduce phosphate by 81% at the cell concentration of 10^9 CFU/g [33]. *B. subtilis*, *B. cereus*, and *B. licheniformis* showed phosphate reduction [34], and *B. velezensis* reduced total phosphorus in channel catfish pond by 19% [35]. Moreover, the mixture of *B. megaterium* and *B. subtilis* can remove total phosphorus by about 80.3% [36].

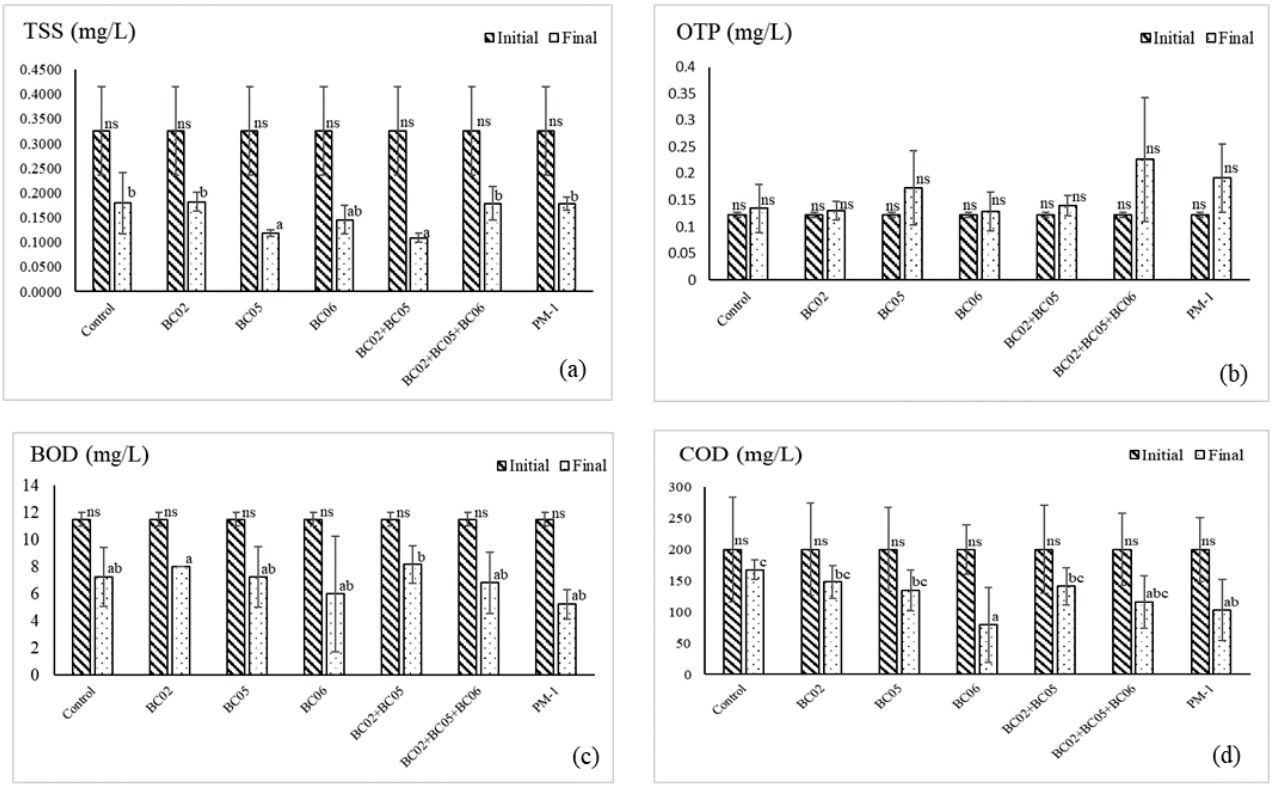

Figure 3. Water parameter variations during the experiment; (a) total suspended solid: TSS, (b) orthophosphate (PO_4^{3-}) concentration: OTP, (c) biological oxygen demand: BOD, (d) chemical oxygen demand: COD.

3.3.3. Biochemical oxygen demand (BOD_5)

The initial BOD_0 of all treatments was 11.50 ± 0.000 mg/L and tended to decrease until the 5-day incubation ended. The lowest BOD_5 was PM-1 treatment (5.25 ± 1.0897 mg/L), which showed 54.35% of BOD_5 decreasing. There was not significantly different (P>0.05) with treatments of BC02, BC05, BC06, BC02+BC05+BC06 and control (8.00 ± 0.0000, 7.25 ± 2.2500, 6.00 ± 4.2525, 6.83 ± 2.2684 and 7.25 ± 2.1794 mg/L, respectively), but was significance (P<0.05) with a treatment of BC02+BC05 (8.17 ± 1.3769 mg/L) (Figure 3c). Since the first day to the end of the 5-day experiment, Bacilli from both marine isolates and PM-1 can decrease BOD by approximately 36-54%, except BC02 and BC02+BC05 have 28-30% of BOD removal. BOD is the oxygen bacteria and other microorganisms require for organic degradation in water, with an optimal range of ≤ 6 mg/L. Only 5.25 (PM-1) and 6.00 (BC06) mg/L were found in this study, which was less than the standard BOD of

aquaculture effluent (≤20 mg/L). The result of Bacilli species was similar to the result of *B. velezensis, which showed 46% of BOD removal* [32]. While isolated cellulolytic *Bacillus* had reduced BOD by 90% [33], another *B. subtilis* was 93% of BOD removal [37].

3.3.4. Chemical oxygen demand (COD)

Initial COD in all treatments was 200.2933 ± 26.0721 mg/L and gently declined until the last day of the experiment. The treatment of BC06 was the lowest COD (79.3333 ± 45.2409 mg/L), and there was no significance (P>0.05) with BC02+BC05+BC06 (115.8267 ± 31.6936 mg/L) and PM-1 treatment (103.1333 ± 33.7703 mg/L), but significantly different (P<0.05) with BC02, BC05, BC02+BC05 and control treatments (Figure 3d). Although there is no COD regulation in aquaculture effluent, COD levels below 120 mg/L are recommended for standard industrial effluent. According to this study, all treatments had lower COD than the standard industrial effluent. Only BC06 can reduce COD reached to about 60% as the best biodegradation in this study, while others diminished COD within 26-48%, and control without bacteria added resulted in only 16%. This might be because of the different species of *Bacillus*. For example, BC06 showed a high capability for organic degradation in high salinity conditions. [38] reported the isolation of *Bacillus* sp. LY from a membrane bioreactor (MBR), by testing water treatment efficiency for 24 days, can reduce COD up to 71.7%. Another study reported the COD removal efficiency of *B. velezensis* in a very high load of COD concentration (4,000 mg/L). Authors suggested that *B. velezensis* can remove COD volume by about 55% [32]. In addition, a COD reduction above 90% of another *Bacillus* was described by [33] and mentioned *B. subtilis* had an 80% COD decrease [37]. Furthermore, *B. flexus* and *B. licheniformis* were suggested as effective species for COD, removing about 70-80% [39]. *Bacillus* spp. has a good ability for COD removal because it can produce several digestive enzymes, surfactants, hydrocarbons, phenols, fatty acids, and ketones to decompose organic matter as nutrients for growth [39].

3.3.5. Concentrations of Ammonia (NH_4^+), Nitrite (NO_2^-) and Nitrate (NO_3^-)

On the first day, ammonia concentration was 0.7389 ± 0.0840 mg/L and showed diminished trends in all treatments. Despite the increased concentration of all treatments on day 2, it lightly decreased from day 3 to the end of the experiment (day 7). The treatment of PM-1 has presented the lowest ammonia removal percentage (98.60%) and has no significance (P>0.05) with treatments of control, BC02, BC05, BC06, BC02+BC05, and BC02+BC05+BC06, which their ammonia removal was 71.13, 80.26, 97.30, 76.16, 64.14 and 90.13%, respectively (Figure 4a, 4b). Reduction trends resulted in nitrite concentration of every treatment on day 1 with the initial value of 0.0030 ± 0.0002 mg/L. From day 2 until the last day, nitrite slowly rose. PM-1 has produced the highest nitrite (0.6851 ± 0.0087 mg/L) and is not significantly different (P>0.05) from others (Figure 4c). In the case of nitrate, initial nitrate was 0.0143±0.0034 mg/L and gently raised since day 1, except for BC02, BC02+BC05+BC06, and PM-1, have slightly decreased on day 3. Then again, they all increased on days 4 to 6. Only BC02+BC05+BC06 has resulted in a slight decline. At the end of the experiment, all treatments had higher nitrate than the initial as BC02+BC05 was the highest (0.4629 ± 0.0012 mg/L) and had significance (P<0.05) with control only (Figure 4d). All three strains of Bacilli showed 64.14–98.60% of ammonia removal ability while increasing nitrite from 0.0029 mg/L up to about 0.5623–0.6830 mg/L. The result suggested that the nitrification process was driven in this study. According to another study, a consortium of B. cereus, B. amyloliquefaciens, and Pseudomonas stutzeri can remove ammonia for 84.89%, whereas nitrite and nitrite nitrate concentrations were increased. The authors suggested that bacterial consortium contained both ammonia-oxidizing and nitrite-oxidizing bacteria [6]. *Bacillus* species were the miracle bacteria that can eliminate high strength of ammonium concentration. [9] reported that *Bacillus* sp. had an ammonium removal efficiency of 42.28% at a very high concentration (815.86 mg-N/L). However, ammonium removal efficiency will be decreased when the lack of carbon sources.

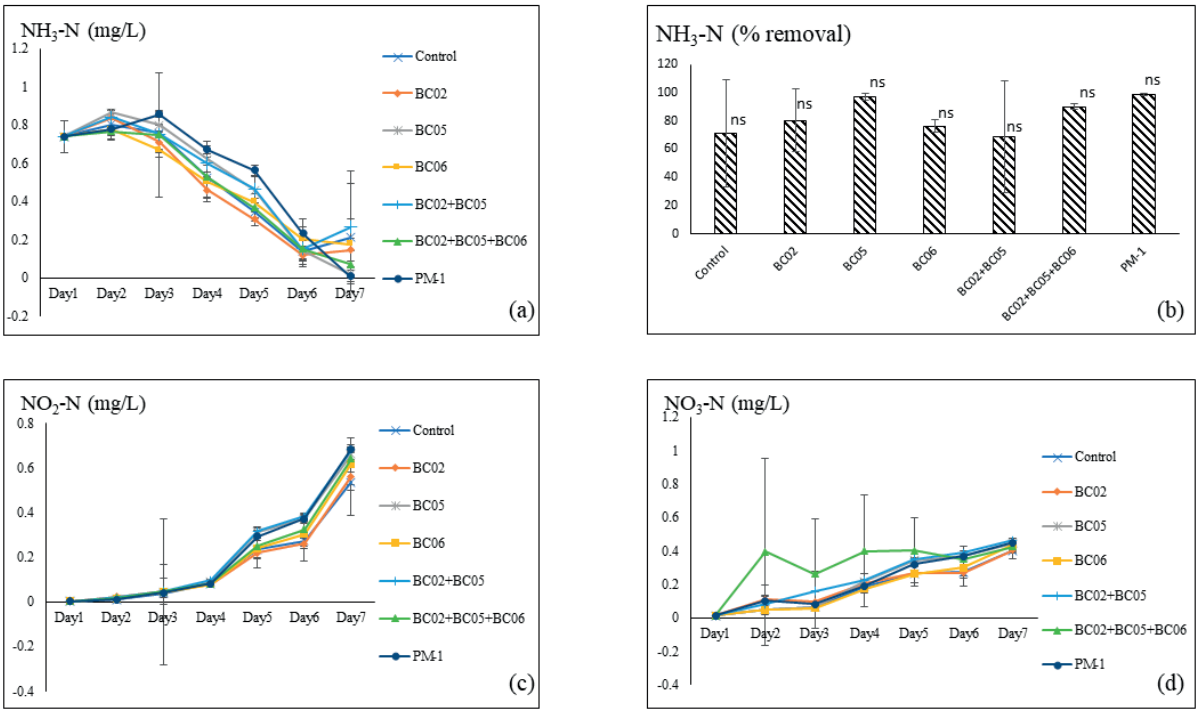

Figure 4. Water parameter variations along the experiment; (a) ammonia, (b) ammonium removal (%), (c) nitrite, (d) nitrate.

Nitrification of bacteria can transform ammonia to nitrite but cannot convert nitrite to nitrate as a full nitrification process. Ammonium oxidizing bacteria (AOB) will be altered ammonia to nitrite and continuously transform to nitrate by nitrite-oxidizing bacteria (NOB). Thus, three isolated marine Bacilli might be instead in the group of AOB, which can only converse ammonia to nitrite, agreed with [9] suggested that isolated *Bacillus* species could be ammonium oxidizing bacteria due to ammonium conversion characteristics. Additional research of *Bacillus* species for nitrogenous effluent treatment [7] reported *B. subtilis* A1 for water treatment capability for 120 hours with 33.51% ammonia removal and 20.4% of decreased nitrite. [40] also studied using *B. subtilis* (10^8 and 10^5 CFU/mL) in a shrimp pond. They described that *B. subtilis* with high concentration (10^8 CFU/mL) could control ammonia and nitrite better than with low concentration (10^5 CFU/mL). While [10] reported that the starter volume of *Bacillus* with 1% and 5% was no significance for ammonium removal efficiency. Besides the single culture of *Bacillus*, a mixture or consortiums of them were used for water treatment. For example, mixed Bacillus (B. megaterium and B. subtilis) reported efficiency of nitrogenous waste (ammonia, nitrite, and nitrate) reduction by approximately 35-76%. This result had good efficiency rather than compared mixture (*B. megaterium* and *B. coagulans*) [36]. Moreover, a consortium of *B. cereus*, *B. amyloliquefaciens*, and *Pseudomonas stutzeri* was studied with 84.89% of ammonium removal [6]. The consortium of microorganisms can be an advantage over single culture because they have cooperative interactions between the co-cultivated microorganisms that enhance the nutrient removal rate [6]. This study compares the water treatment efficiency of three Bacilli isolates, consisting of BC02, BC05, and BC06, with microbial seeds (PM-1), resulting in a decrease of total organic matter and an increase of orthophosphate in all isolates with no significance ($P>0.05$) compared with PM-1 product. PM-1 has shown high efficiency in decline BOD_5 with 54.35% while presenting only 48.51% COD removal, which was lower than BC06 (60.39%). Furthermore, PM-1 product has the utmost ability to diminish ammonia (98.60%) and raise nitrite (from 0.0029 to 0.6851 mg/L) since the initial day, but there was no significant difference ($P>0.05$) with 3 marine Bacilli isolates. Augmentation of nitrate has resulted in a mixed culture of BC02+BC05 that highest produced about 0.4629 mg/L from 0.01428 mg/L on the first day, which showed significantly ($P<0.05$) with control only. *Bacillus* spp. can improve water because it produces several enzymes to lyse nutrients and organic matter, which have been involved in nitrification/denitrification reactions. Furthermore, *Bacillus* species have suggested that they are proficient in maintaining water quality in aquaculture, which is simple

and cost-effective [1]. Other advantages: Bacillus species could reduce pathogenic microorganisms in aquaculture and control toxin-producing phytoplankton (blue-green algae and dinoflagellates) in shrimp farms [11].

4. Conclusions

Three marine Bacilli presented endospore-forming were isolated from soil and water samples on seagrass beds. Strain BC02 was identified as *Bacillus thuringiensis*, and BC06 was genus *Virgibacillus*. Unfortunately, strain BC05 could not be identified. These isolates have been utilized for shrimp water improvement at a density of 10^7 CFU/ml for 7 days. Bacilli utilization in water treatment caused better water quality as about a 50% decrease of TSS, COD, BOD, and NH_3, and only NO_3^- has significantly increased. Marine Bacilli isolates have no significant capabilities compared to commercial PM-1 product. Therefore, these Bacilli isolates can develop into an alternative microorganism product with efficiency equal to commercial PM-1. Therefore, these Bacilli isolates have the potential to become a substitute microbial product with a level of efficacy comparable to that of commercial PM-1. Further research should be done to determine how marine Bacilli and PM-1 can enhance the water quality in shrimp ponds.

5. Acknowledgements

We would like to thank Aquatic Science and Innovative Management Division for supporting the budget, equipment, and laboratory for analysis.

Author Contributions: Conceptualization, Y.S; methodology, Y.S.; software, S.C.; formal analysis, R.K., O.S., and S.C.; investigation, R.K., and O.S.; writing—original draft preparation, R.K., and O.S.; writing—review and editing, Y.S. and A.U.

Funding: This research received no external funding.

Conflicts of Interest: The authors declare no conflict of interest.

References

[1] Hlordzi, V.; Kuebutornye, F. K. A.; Afriyie, G.; Abarike, E. D.; Lu, Y.; Chi, S.; Anokyewaa, M. A. The use of *Bacillus* species in maintenance of water quality in aquaculture: A review. *Aquac. Rep*. 2020, *18*, 100503.

[2] Iber, B. T.; Kasan, N. A. Recent advances in shrimp aquaculture wastewater management. *Heliyon*. 2021, *7*, e08283.

[3] Sangnoi, Y.; Chankaew, S.; O-Thong, S. Indigenous *Halomonas* spp., the potential nitrifying bacteria for saline ammonium waste water treatment. *Pak. J. Biol. Sci*. 2017, *20*, 52–58.

[4] Bull, E. G.; Cunha, C. L. N.; Scudelari, A. C. Water quality impact from shrimp farming effluents in a tropical estuary. *Water Sci. Technol*. 2021, *83.1*, 123–136.

[5] Sanchez-Zazueta, E.; Martínez-Cordero, F. J.; Chávez-Sánchez, M. C.; Montoya-Rodríguez, L. Quantitative risk assessment of WSSV transmission through partial harvesting and transport practices for shrimp aquaculture in Mexico. *Prev. Vet. Med*. 2017, *146*, 27–33.

[6] John, E. M.; Krishnapriya, K.; Sankar, T. V. Treatment of ammonia and nitrite in aquaculture wastewater by an assembled bacterial consortium. *Aquaculture*. 2020, *56*, 735390.

[7] Yang, X.-P.; Wang, S.-M.; Zhang, D.-W.; Zhou, L.-X. Isolation and nitrogen removal characteristics of an aerobic heterotrophic nitrifying–denitrifying bacterium, *Bacillus subtilis* A1. *Bioresource Technol*. 2011, *102*, 854–862.

[8] Zhang, Q. L.; Liu, Y.; Ai, G. M.; Miao, L. L.; Zheng, H. Y.; Liu, Z. P. The characteristics of a novel heterotrophic nitrification–aerobic denitrification bacterium, *Bacillus methylotrophicus* strain L7. *Bioresource Technol*. 2012, *108*, 35-44.

[9] Chankaew, S.; O-Thong, S; Sangnoi, Y. Nitrogen removal efficiency of salt-tolerant heterotrophic nitrifying bacteria. *Chiang Mai J. Sci*. 2018, *45*, 11–20.

[10] Phatthongkleang, T., Sangnoi, Y.; O-Thong, S.; Uppabullung, A.; Keawtawee, T. The efficiency of *Bacillus* spp. to remove ammonia in shrimp aquaculture. *Wichcha J. NSTRU*. 2019, *38*, 1–15.

[11] Kawman, K.; Uppabullung, A.; Kaewtawee, T.; Sangnoi, Y. Effect of probiotic used on phytoplankton community structure in white shrimp (*Litopenaeus vannamei*) pond. *ASEAN J. Sci. Tech. Report*. 2022, *25*, 39–49.

[12] Olmos, J.; Acosta, M.; Mendoza, G.; Pitones, V. *Bacillus subtilis*, an ideal probiotic bacterium to shrimp and fish aquaculture that increase feed digestibility, prevent microbial diseases, and avoid water pollution. *Arch. Microbiol*. 2020, *202*, 427–435.

[13] Purivirojkul, W.; Maketon, M.; Areechon, N. Probiotic properties of *Bacillus sphaericus* and *Bacillus subtilis* in black tiger shrimp (*Penaeus monodon* Fabricius) culture. *Kasetsart J. (Nat. Sci.)* 2005, *39*, 262–273.

[14] Tamura, K.; Stecher, G.; Kumar, S. MEGA11: Molecular evolutionary genetics analysis version 11. *Mol. Biol. Evol.* 2021, *38*, 3022–3027.

[15] Strickland, J. D. H.; Parsons, T. R. *A Practical Handbook of Seawater Analysis*, 2nd ed.; The Alger Press Ltd.: Fishery Research Board, Canada, 1972; pp. 49–131.

[16] APHA. *Standard Methods for the Examination of Water and Wastewater*, 19th ed, American Public Health Association Inc.: New York, 1995.

[17] APHA. *Standard Methods for the Examination of Water and Wastewater, Part 3, Determination of Metals*, 17th ed, American Public Health Association Inc.: Washington DC, 1989.

[18] Boyd, C. E.; Tucker, C. S. *Water Quality and Pond Soil Analysis for Aquaculture*. Agricultural Experiment Station, Alabama, 1992.

[19] Kumar, P.; Kamle, M.; Borah, R.; Mahato, D. K.; Sharma, B. *Bacillus thuringiensis* as microbial biopesticide: uses and application for sustainable agriculture. *Egypt. J. Biol. Pest Control*. 2021, *31*, 95.

[20] Maeda, M.; Mizuki, E.; Nakamura, Y.; Hatano, T.; Ohba, M. Recovery of *Bacillus thuringiensis* from marine sediments of Japan. *Curr. Microbiol*. 2000, *40*, 418–422.

[21] Maeda, M.; Mizuki, E., Hara, M.; Tanaka, R.; Akao, T.; Yamashita, S.; Ohba, M. Isolation of *Bacillus thuringiensis* from intertidal brackish sediments in mangroves. *Microbiol. Res*. 2001, *156*, 195–198.

[22] Dash, H. R.; Mangwani, N.; Das, S. Characterization and potential application in mercury bioremediation of highly mercury-resistant marine bacterium *Bacillus thuringiensis* PW-05. *Environ. Sci. Pollut. Res*. 2014, *21*, 2642–2653.

[23] Anyanwu, N. G.; Ariole, C. N. Probiotic potential of an indigenous marine *Bacillus thuringiensis* on shrimp (*Penaeus monodon*) culture infected with *Vibrio mimicus*. *J. Applied Sci*. 2019, *19*, 173–179.

[24] Pang, S. T.; Ransangan, J.; Hatai, K. Isolation, identification and preliminary characterization of candidate probiotic bacteria from the intestine of domesticated goldfish (*Carassius auratus*). *J. Fish. Environ*. 2020, *44*, 39–52.

[25] Mendoza-Estrada, L. J.; Hernández-Velázquez, V. M.; Arenas-Sosa, I.; Flores-Pérez, F. I.; Morales-Montor, J.; Peña-Chora, G. Anthelmintic effect of *Bacillus thuringiensis* strains against the gill fish trematode *Centrocestus formosanus*. *Biomed Res. Int.* 2016, ID 8272407.

[26] Dawson, D.; Salice, C. J.; Subbiah, S. The efficacy of the *Bacillus thuringiensis israelensis* larvicide against *Culex tarsalis* in municipal wastewater and water from natural wetlands. *J. Am. Mosq. Control Assoc*. 2019, *35*, 97–106.

[27] Heyndrickx, M.; Lebbe, L.; Kersters, K.; De Vos, P.; Forsyth, G.; Logan, N. A. *Virgibacillus*: a new genus to accommodate *Bacillus pantothenticus* (Proom and Knight 1950). Emended description of *Virgibacillus pantothenticus*. *Int. J. Syst. Bacteriol.* 1998, *48*, 99–106.

[28] Seck, E.; Rathored, J.; Khelaifia1, S.; Croce, O.; Robert, C.; Couderc, C.; Di Pinto, F.; Sokhna, C.; Raoult, D.; Lagier, J.-C. *Virgibacillus senegalensis* sp. nov., a new moderately halophilic bacterium isolated from human gut. *New Microbes New Infect*. 2015, *8*, 116–126.

[29] Yin, X.; Yang, Y.; Wang, S.; Zhang, G. *Virgibacillus oceani* sp. nov. isolated from ocean sediment. *Int. J. Syst. Evol. Microbiol*. 2015, *65*, 159–164.

[30] Daroonpunt, R.; Tanasupawat, S.; Kudo, T.; Ohkuma, M.; Itoh, T. *Virgibacillus kapii* sp. nov., isolated from Thai shrimp paste (Ka-pi). *Int. J. Syst. Evol. Microbiol*. 2016, *66*, 1832–1837.

[31] Zhang, D.-C.; Schumann, P.; Wu, J.; Franca, L.; Neuner, K.; Margesin, R. *Virgibacillus flavescens* sp. nov., isolated from marine sediment. *Int. J. Syst. Evol. Microbiol*. 2016, *66*, 1138–1143.

[32] Agunbiade, M.; Oladipo, B.; Ademakinwa, A. N.; Awolusi, O.; Adesiyan, I. M.; Oyekola, O.; Ololade, O.; Ojo, A. Bioflocculant produced by *Bacillus velezensis* and its potential application in brewery wastewater treatment. *Sci. Rep*. 2022, *12*, 10945.

[33] Reddy, K. V.; Reddy, V. K.; Babu, B. S.; Lakshmi, T. V. Applications of *Bacillus* sp. in aquaculture waste water treatment. *Int J. S. Res. Sci. Tech*. 2018, *4*, 1806–1812.

[34] Lalloo, R.; Ramchuran, S.; Ramduth, D.; Go¨rgens, J.; Gardiner, N. Isolation and selection of *Bacillus* spp. as potential biological agents for enhancement of water quality in culture of ornamental fish. *J. Appl. Microbiol*. 2007, *103*, 1471–1479.

[35] Thurlow, C. M.; Williams, M. A.; Carrias, A; Ran, C.; Newman, M.; Tweedie, J.; Allison, E.; Jescovitch, L. N.; Wilson, A. E.; Terhune, J. S.; Liles, M. R. *Bacillus velezensis* AP193 exerts probiotic effects in channel catfish (*Ictalurus punctatus*) and reduces aquaculture pond eutrophication. *Aquaculture*. 2019, *503*, 347–356.

[36] Li, X.; Wang, T.; Fu, B.; Mu, X. Improvement of aquaculture water quality by mixed *Bacillus* and its effects on microbial community structure. *Environ. Sci. Pollut. Res*. 2022, *29*, 69731–69742.

[37] Karichappan, T.; Venkatachalam, S.; Jeganathan, P. M. Analysis of efficiency of *Bacillus subtilis* to treat bagasse based paper and pulp industry wastewater – a novel approach. *J. Korean Chem. Soc*. 2014, *58*, 198–204.

[38] Yan, L.; He, Y.; Kong, H.; Tanaka, S.; Lin, Y. Isolation of a new heterotrophic nitrifying *Bacillus* sp. strain. *J. Environ. Biol*. 2006, *27*, 323–326.

[39] Ren, W.; Wu, H.; Guo, C.; Xue, B.; Long, H.; Zhang, X.; Cai, X.; Huang, A.; Xie, Z. Multi-strain tropical *Bacillus* spp. as a potential probiotic biocontrol agent for large-scale enhancement of mariculture water quality. *Front. Microbiol*. 2021, *12*, 699378.

[40] Zokaeifar, H.; Babaei, N.; Saad, C. R.; Kamarudin, M. S.; Sijam, K.; Balcazar, J. L. Administration of *Bacillus subtilis* strains in the rearing water enhances the water quality, growth performance, immune response, and resistance against *Vibrio harveyi* infection in juvenile white shrimp, *Litopenaeus vannamei*. *Fish Shellfish Immunol*. 2014, *36*, 68–74.

JSTR
ASEAN Journal of Scientific and Technological Reports

Research article

Plasma Instability During ITBs Formation with Pellet Injection in Tokamak

Ponkris Klaywittaphat[1*], Thawatchai Onjun[2], Roppon Picha[3], Jiraporn Promping[4] and Boonyarit Chatthong[5]

[1] Faculty of Engineering, Thaksin University, Phatthalung, Thailand; ponkris@hotmai.com
[2] Thailand Institute of Nuclear Technology, Bangkok, Thailand; Thawatchi.onjun007@gmail.com
[3] Thailand Institute of Nuclear Technology, Bangkok, Thailand; aeroppon@gmail.ac.th
[4] Thailand Institute of Nuclear Technology, Bangkok, Thailand; ame026@gmail.ac.th
[5] Division of Physical Science, Faculty of Science, Prince of Songkla University, Songkhla, Thailand; boonyarit.ch@psu.ac.th
* Correspondence: ponkris@hotmail.com

Abstract: JET H-mode plasma discharge 53212 simulation during the pellet fueling operation in the presence of an internal transport barrier is carried out using the 1.5D BALDUR integrated predictive modelling code. The plasma instability during ITB formation with pellet injection in a tokamak is investigated. These simulations use a neoclassical transport model and an anomalous transport model (either multimode or mixed Bohm/gyro-Bohm core transport model). The boundary condition is described at the top of the pedestal, which is calculated theoretically based on a combination of magnetic and flow shear stabilization pedestal width scaling and an infinite-n ballooning pressure gradient model. The toroidal flow calculation is based on the neoclassical viscosity toroidal velocity model. It was found that the shallower pellet does not destroy the ITB, which locating mainly between r/a = 0.8 and 0.9. Moreover, in the plasma center region (0.4<r/a<0.6) the effective electron thermal diffusivities do not change during the ablation time. However, the effective electron thermal diffusivities decrease after pellet ablation, which means a shallower pellet can improve the internal transport barrier.

Keywords: Plasma, Fusion, Pellet, Transport, Micro-instability, ITB

Citation:
Klaywittaphat, P.; Onjun, T.; Picha, R.; Promping, J.; Chatthong, B. Plasma Instability During ITBs Formation with Pellet Injection in Tokamak *ASEAN J. Sci. Tech. Report.* **2022**, *25*(4), 11-20. https://doi.org/10.55164/ajstr.v25i4.247569.

Article history:
Received: October 14, 2022
Revised: October 26, 2022
Accepted: October 27, 2022
Available online: November 20, 2022

1. Introduction

The progress in understanding plasma instability in a tokamak has been discussed for several decades in fusion research and development. Various theoretical modeling and numerical codes have been developed as a tool for this study [1–3]. Transport analysis of plasma discharges from different tokamaks under several conditions has resulted in a better understanding of their behaviors. It was found that the ion and electron thermal transports agree with theoretical predictions for turbulent transport due to gradient-driven drift-type micro-instabilities [4–6]. J. Weiland reported that the anomalous heat transport in the plasma core is mainly driven by a combination of Ion Temperature Gradient (ITG) and Trapped Electron Mode (TEM) instabilities [1]. A comprehensive assessment of transport behaviors also requires further experimental studies in various scenarios and the inclusion of complicated non-linear effects in those numerical studies.

Nevertheless, the results from the linear analysis still survive for an overall understanding [4]. Many useful and quantitatively correct conclusions can be obtained from a study based on a simplified drift-fluid description. These purely fluid models [2,5], or models with elements of gyro-motion [3] incorporated, show reasonable agreement with experiments and can describe many diverse observations.

A recent analytic study of the dissipative trapped electron instability in steep density and temperature gradients, such as those found experimentally in internal transport barriers (ITBs) in the Mega Ampere Spherical Tokamak (MAST) [7], showed that the growth rate of long-wavelengths of TEM for $k_\theta \rho_i < 0.5$ has a non-trivial dependence on collisionality. In particular, the limit of low collisionality, $\nu_{eff}/\omega << 1$, the TEM is stabilized by increasing collisionality. The result of Ref. [7] also showed the role of collisionality on drift instabilities. The effect of the pellet with micro instability in MAST can be seen in [8].

This work investigates the impacts of pellets on the ITBs and micro-stability analysis of the drift electrostatic waves, specifically ITG and TEM modes. A self-consistent simulation of JET H-mode discharge 53212 is carried out using the 1.5D BALDUR integrated predictive modeling code. In this simulation, the pellet ablation described using the neutral gas shielding (NGS) model with grad-B drift effect is taken into account. The NGS pellet model is coupled with a plasma core transport model, a combination of a neoclassical transport model NCLASS and an anomalous transport model (either The Multimode model (MMM) or Mixed Bohm/gyro-Bohm core transport model). The evolution of growth rate due to ITG and TEM modes is analyzed during the pellet fueling operation. This can result in a better understanding of plasma behaviors during pellet injection and ITBs formation.

This paper is organized as follows. Section 2 describes the details of models used in this work, including core transport and pellet models. The simulation results and micro instability analysis is carried out in Section 3. The conclusions are shown in Section 4.

2. Description of Models

2.1 MMM 95 anomalous transport model

The Multimode model (MMM) [6] is a combination of three theoretical based models, including the Weiland model for ion temperature gradient (ITG) and trapped electron modes (TEM), the Guzdar-Drake model for drift-resistive ballooning modes (RB), and a model for kinetic ballooning modes (KB). The effect of plasma elongation is also included by multiplying all the anomalous transport contributions to the Multimode model with κ^{-4}, producing the observed asymptotic scaling of confinement time and the best overall match to experimental data. The description of the Weiland model for toroidal geometry and circular, concentric magnetic surfaces is given in Ref. [5]. In brief, the ITG mode is provided by

$$\omega_{ri} = \frac{k_\theta \rho_s}{2L_{ni} m_i^{1/2}} T_e^{1/2} \left[1 - \frac{2L_{ni}}{R}\left(1 + \frac{10}{9}\frac{T_i}{T_e}\right)\right] \tag{1}$$

and

$$\gamma_i = \frac{2^{1/2} k_\theta \rho_s}{R m_i^{1/2}} T_i^{1/2} \sqrt{\frac{R}{L_{Ti}} - \frac{R}{L_{Ti,th}}}. \tag{2}$$

The TEM is given by

$$\omega_{re} = \frac{k_\theta \rho_s}{2L_{ne} m_e^{1/2}} T_e^{1/2} \left[K_t \left(1 - \frac{2L_{ne}}{R}\right) - \frac{20}{3}\frac{L_{ne}}{R}\right] \tag{3}$$

and

$$\gamma_e = \left(\frac{2K_t}{m_i}\right)^{1/2} \frac{k_\theta \rho_s}{R} T_e^{1/2} \sqrt{\frac{R}{L_{Te}} - \frac{R}{L_{Te,th}}}\,. \tag{4}$$

The diffusion coefficient for the $E \times B$ *1993* drift-resistive ballooning mode model by Guzdar and Drake [9] is

$$D^{RB} = 94q^2 \rho_e v_{ei} (-R\hat{\chi} \cdot \nabla p/p)\kappa^{-4}, \tag{5}$$

Where p is the plasma pressure and$\rho_e = v_{the}/\Omega_e$. A soft beta limit is approximated by the ''kinetic ballooning mode'' model, with the particle diffusion coefficient given by

$$D^{KB} = c_s p_s^2 (-R\hat{\chi} \cdot \nabla p/p) exp\left[3.5\,\beta'/\beta'_{c_1} - 1\right]\kappa^{-4}, \tag{6}$$

where $\beta' \equiv d\beta/dr$, and $\beta'_{c1} = r(dq/dr)/(1.7q^3R)$ is an approximation to the first ballooning mode stability limit. Then the thermal and particle transport coefficients can be expressed as [6]:

$$\chi_i = 0.8\chi_{i,ITG\&TEM} + 1.0\chi_{i,RB} + 1.0\chi_{i,KB} \tag{7}$$

$$\chi_e = 0.8\chi_{e,ITG\&TEM} + 1.0\chi_{e,RB} + 1.0\chi_{e,KB} \tag{8}$$

$$D_H = 0.8D_{H,ITG\&TEM} + 1.0D_{H,RB} + 1.0D_{H,KB} \tag{9}$$

$$D_Z = 0.8D_{Z,ITG\&TEM} + 1.0D_{Z,RB} + 1.0D_{Z,KB} \tag{10}$$

where χ_i is the ion thermal diffusion coefficient in the unit of m²/s, χ_e is the electron thermal diffusion coefficient in the unit of m²/s, D_H is hydrogenic particle diffusion coefficient in the unit of m²/s and D_Z is impurity particle diffusion coefficient in the unit of m²/s.

2.2 Mixed Bohm/gyro-Bohm anomalous transport model

The Mixed Bohm/gyro-Bohm (Mixed B/gB) anomalous transport model [10-11] is semi-empirical. Both the electron and ion thermal diffusivities consist of two terms. The diffusivity of the Bohm term can be written as:

$$\chi_B = \alpha_B R \left|\frac{\nabla(n_e T_e)}{n_e B_\emptyset}\right| q^2 \tag{11}$$

With the constant α to be determined empirically. However, evidence from JET suggests that the Bohm term should also depend on the temperature gradient near the plasma edge. Consequently, Bohm scaling has a final form as follows:

$$\chi_B = 4 \times 10^{-5} R \left|\frac{\nabla(n_e T_e)}{n_e B_\emptyset}\right| q^2 \left(\frac{T_e(0.8\rho_{max}) - T_e(\rho_{max})}{T_e(\rho_{max})}\right), \tag{12}$$

The Gyro-Bohm term can be written as

$$\chi_{gB} = 5 \times 10^{-6} \sqrt{T_e} \left|\frac{\nabla(T_e)}{B_T^2}\right|. \tag{13}$$

The anomalous ion and electron thermal diffusivities are constructed from the sum of these Bohm and gyro-Bohm terms, with empirically determined coefficients:

$$\chi_i = 0.5\chi_{gB} + 4.0\chi_B, \tag{14}$$

$$\chi_e = 1.0\chi_{gB} + 2.0\chi_B. \quad (15)$$

The hydrogenic and impurity-charged particle diffusivity is given by

$$D_H = D_Z = (0.3 + 0.7\rho)\frac{\chi_e\chi_i}{\chi_e+\chi_i}. \quad (16)$$

2.3 NCLASS neoclassical transport model

Neoclassical ion thermal transport is computed using the NCLASS module [12]. The NCLASS module calculates the neoclassical transport properties of multi-species axisymmetric plasma of arbitrary aspect ratio, geometry, and collisionality, by solving the radial and parallel force balance equations for the flows within a flux surface using multiple species, reduced charge state approach given in Ref. [13]. The radial fluxes in the banana regime are related to these flows and the neoclassical viscosities. The bootstrap current and electrical resistivity are also derived from these flows. The classical and Pfirsch-Schlüter fluxes and those driven by a user-specified parallel force are also calculated. The viscosities are calculated by numerically integrating over velocity space and are continuous over all collisionality regimes and aspect ratios. In addition, other effects, including banana orbit squeezing, potato orbit effects, and additional force terms to accommodate neutral beam, charge exchange, toroidal field ripple, and anomalous toroidal drag forces, are included.

2.4 NGS ablation model and relocation model

Two simultaneous processes can occur during each pellet, including pellet ablation and mass relocation. The neutral gas shielding (NGS) model [2] is used, in which an ablation rate of this model can be expressed in terms of the power function as follows:

$$\frac{dN}{dt} = 5.2 \times 10^{16} n_e^{0.333} T_e^{1.64} r_p^{1.333} M_i^{-0.333} \quad (17)$$

Where N, n_e (m^{-3}), T_e (eV), r_p (m), and M_i (u) are the number of particles in a pellet, electron density, electron temperature, pellet radius, and pellet mass, respectively. For the mass relocation model, a scaling model of pellet drift displacement, based on the grad-B induced pellet drift [14, 15], has been considered. The developing of the scaling law for grad-B Drift [14], based on a set of ~800 simulations with varying injection and plasma target parameters in the vicinity of typical tokamak configurations (~ ±40% of standard parameter settings), least square fits have been carried out to determine the main parameter dependencies and to derive an equation for the rough calculation of the absolute average particle drift displacement in terms of the flux coordinate $(R_{max} - R_{min})/2$:

$$\Delta_{\text{Drift}} = C_1 \left(\frac{V_p}{100}\right)^{C2} r_p^{C_3} n_{e0}^{C_4} T_{e0}^{C_5} (\|\alpha| - C_6| + C_8)^{C_7} \times (1-\Lambda)^{C_9} a_0^{C_{10}} R_0^{C_{11}} B_0^{C_{12}} \kappa^{C_{13}} \quad (18)$$

With injection velocity V_p (m/s), pellet radius r_p (mm), axial density n_{e0} (10^{19} m^{-3}) and electron temperature T_{e0} (keV), injection angle $\alpha \in [-\pi, \pi]$, impact parameter of the pellet trajectory Λ (norm. minor radius), minor radius a_0 (m), major radius R_0 (m), toroidal field B_0 (T), and plasma elongation κ. To avoid statistical artifacts in the calculation coming from the rational q-surface effect on the drift-damping behavior, which cannot easily be described as part of a scaling fit formula, the q-profile was changed arbitrarily for each simulation run ($q_{edge} \in [3,9]$). Only pellets ablated before reaching the tangency point of the trajectory with the flux surfaces were considered. The results and root mean square (rms) errors obtained for the constants C_1-C_{13} for two different assumptions concerning the parameter space to be analyzed summarized in [14].

3. Simulation Results and Micro Instability Analysis

The summary of the basic plasma parameters and summary of the pellet injection parameters used in JET discharge 53212 a target, a plasma was chosen at I_p/B_t = 2.5 MA/2.4 T with $\delta \approx 0.34$ showing a confinement collapse when trying to raise the density beyond $n/n_{GW} = 0.8$ with strong gas puffing. In such a plasma solid 4 mm^3 deuterium cubes were launched at a speed of 160 m s^{-1} from the high field side downward at an angle of 44° with respect to the horizontal plane and with a tangency radius at a normalized minor radius $\rho \sim 0.6$–0.7. The optimization strategy translated into launching a first pellet string at 6 Hz to raise the density, followed by a pellet string at 2 Hz, which is sufficiently slow to allow confinement recovery after each pellet, shown in table 2 and table 3 of [25].

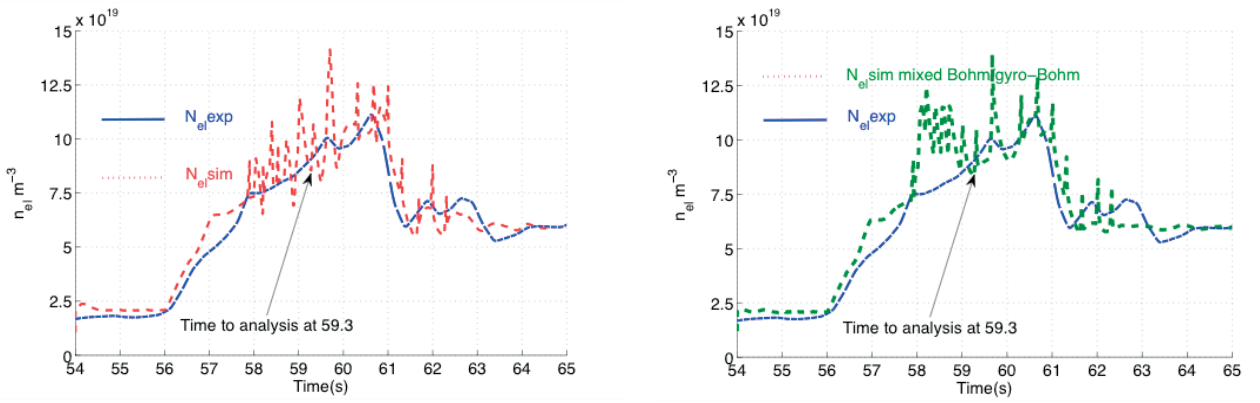

Figure 1. The time evolution of line average electron density is compared for experimental data and the simulations using either MMM95 (left) or Mixed Bohm/gyro-Bohm (right) [25].

Figure 1 compares an evolution of line average electron density obtained from the experiment and the simulations using the MMM95 transport model (left panel) and Mixed B/gB model (right panel). It can be seen in both panels that the line average electron density rises quickly after the pellet's launching. Both simulations tend to agree with experimental data, especially the simulation using the MMM95 transport model, which yields better agreement during the early period of pellet operation due to the off-diagonal elements of the transport matrix in the Weiland model, providing the convective flux adequate to reproduce the observed density profile peaking [22], which can be seen in Figure 1. At the later time of pellet operation, both simulations yield similar agreement with experimental data.

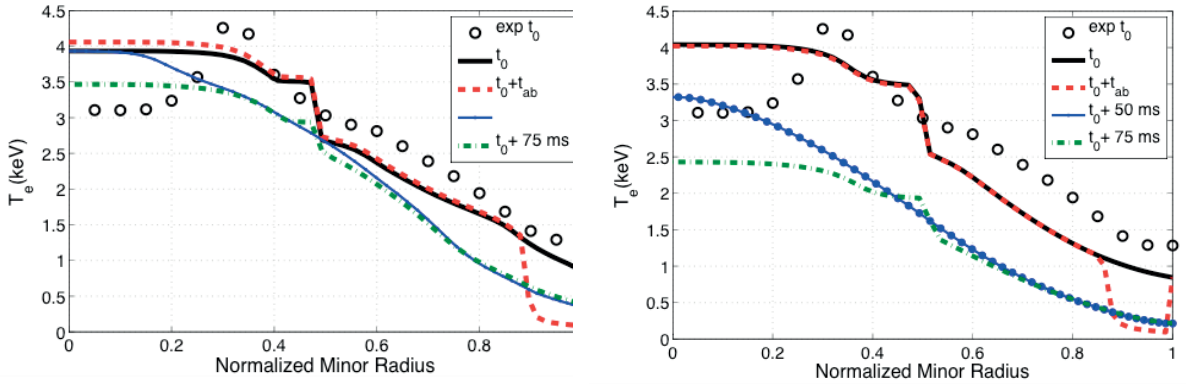

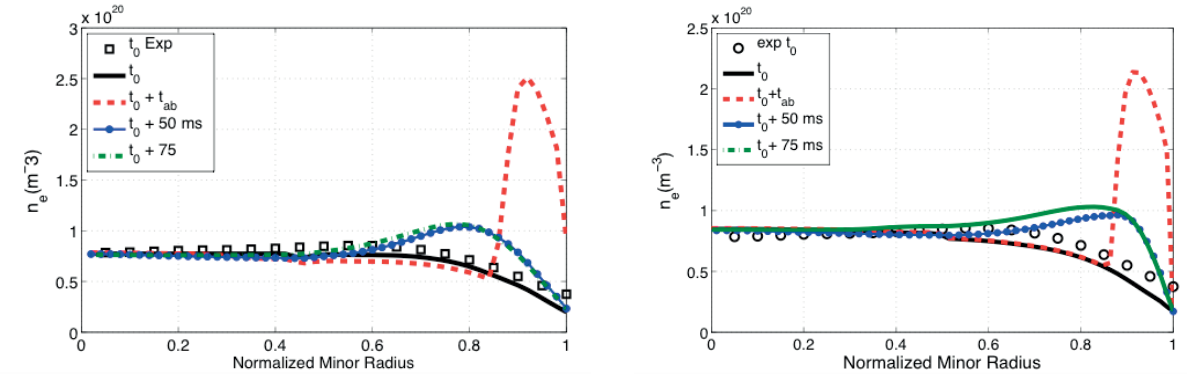

Figure 2. The electron temperature and density profiles during the pellet operation are plotted for the experimental data and the simulations using MMM95 (left) and Mixed Bohm/gyro-Bohm (right) [25].

Figure 2 shows the profile comparison between the experimental data and simulation using the MMM95 transport model (left panels) and Mixed B/gB model (right panels) for electron density and electron temperature at 59.3 sec. Note that this is during pellet operation. The first pellet is launched at a time of 57.87 sec. The simulations are shown at different times during the pellet perturbation, including time t_0 referring to the time before pellet injection, $t_0 + t_{ab}$ referring to the time during pellet ablation, t_0 + 50 ms referring to the time at 50 ms after pellet launching (during relaxation process), and t_0 + 75 ms referring to a time at 75 ms after pellet launching (at the end of the relaxation process). It can be seen at the time before pellet injection that both predicted electron density and temperature agree with experiment data. For the electron density, a new peak of electron density is formed after pellet injection. Consequently, plasma starts to relax by transporting density inwards and outward. It can also be seen the electron density relaxes faster at the plasma edge than at the plasma core because the electron transport density at the plasma edge region is increased. It is worth noting that there is an off-axis peak of the electron temperature profile at r/a = 0.35 in the experimental profile and a large gradient of the electron temperature profile at r/a =0.5 in both simulation results. It should be mentioned on the origin of these irregularities. These resulted from the off-axis and NBI heating used in the experiment and simulations.

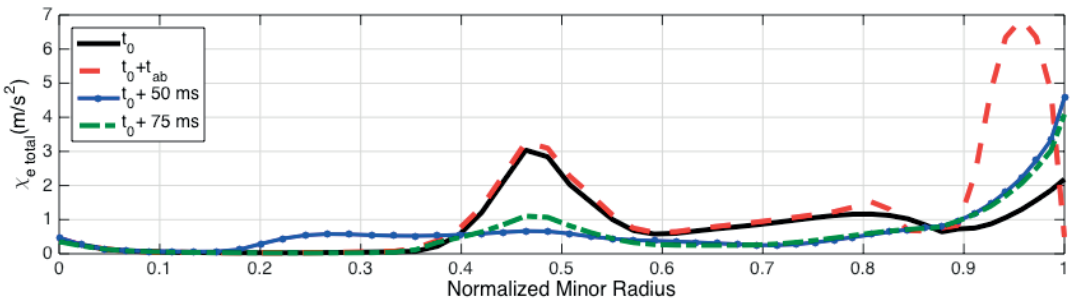

Figure 3. The profiles for total electron thermal diffusivity during the pellet operation are plotted for the simulations using MMM95.

Figure 3 shows the effective electron thermal diffusivities at different times during pellet operation. The panels show the results obtained from the simulation using the MMM95 transport model. It can be seen that the effective electron thermal diffusivities increase, especially in the region of pellet ablation ($0.8<r/a<1$). However, they decrease to levels similar to those before pellet injection in the plasma center region ($0.4<r/a<0.6$), and the effective electron thermal diffusivities do not change during the ablation time. However, the effective electron thermal diffusivities decrease after pellet ablation, which means a shallower pellet does not destroy the internal transport barrier because the electron thermal diffusivities in this area are not affected by a shallower pellet.

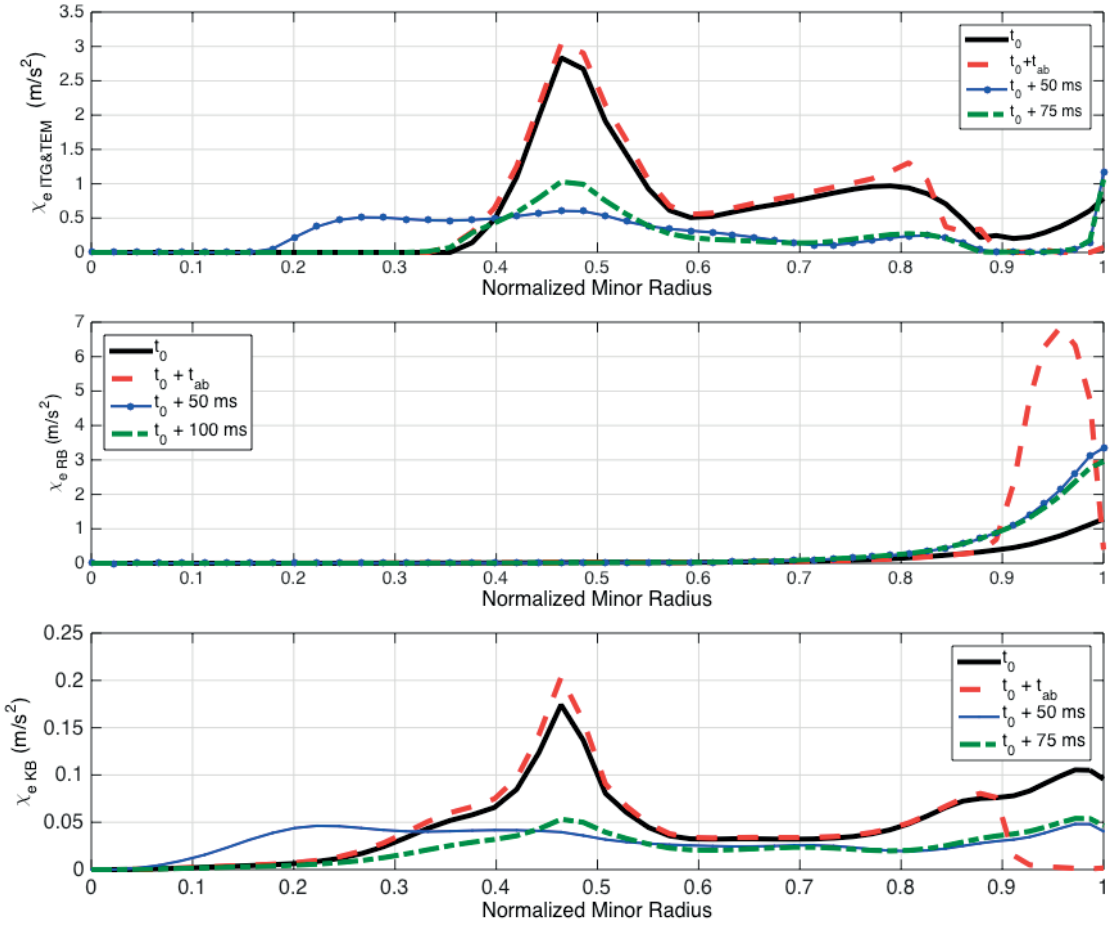

Figure 4. The components of electron thermal diffusivity profiles during the pellet injection obtained from the simulation using the MMM95 transport model are shown for the radius from ϱ = 0 to ϱ = 1.0. Those components are the drift wave (ITG&TE) (top panel), the drift-resistive ballooning (RB) modes (middle panel), and the kinetic ballooning (KB) modes (bottom panel).

Figure 4 shows the components of electron thermal diffusivities during the pellet injection obtained from the simulation using the MMM95 transport model. Those components are the drift wave (ITG&TEM), drift-resistive ballooning (RB) modes, and kinetic ballooning (KB) modes. It can be seen that the ITG&TEM component is dominant throughout the plasma, except near the plasma edge, in which the electron thermal diffusivities are dominated by both ITG&TEM and RB components. It can be noticed that right after a pellet enters the plasma, the ITG&TEM component remains almost the same, except for a reduction in the region near the plasma edge where another density peak is formed. Therefore, a reduction in the ITG&TEM component occurs throughout the plasma. This behavior also occurs for the KB component. For the RB component, right after a pellet enters the plasma, the RB component remains almost the same in the plasma core, except for a large increase near the plasma edge where another density peak is formed. This is caused by increased collisionality and resistivity near the plasma edge. Thus, it relaxes to the level before pellet injection.

Figure 5 shows the time evolution of electron density and temperature during pellet ablation. It can be seen that the electron density suddenly increases after pellet injection, but the electron temperatures rapidly drop. It is known that based on fluid concepts, an increase in the density gradient can stabilize the ion temperature gradient modes by decreasing the parameter $\eta_i = (\nabla T_i / T_i)/(\nabla n_i / n_i)$. However, in a gyrokinetic calculation for a density peaking case, it is found to be destabilizing [23]. Therefore, the stabilizing role of

density peaking depends on the actual fraction of trapped electrons and plasma collisionality. An increase of α ($\alpha = -q^2\beta R\nabla P/P$) can stabilize part of the microturbulence [24].

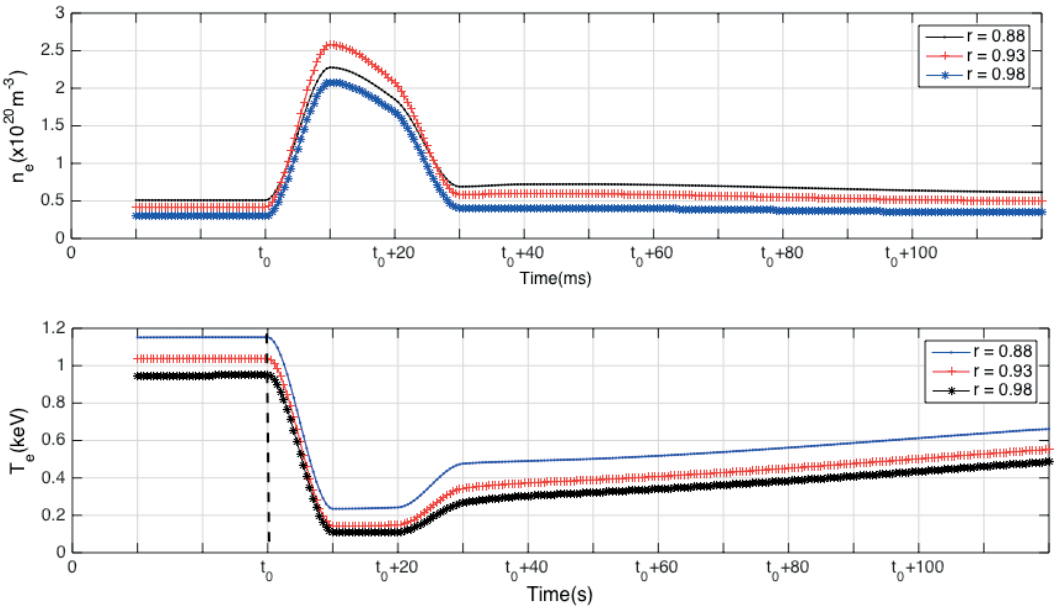

Figure 5. The time evolution of electron density, electron temperature, during pellet ablation.

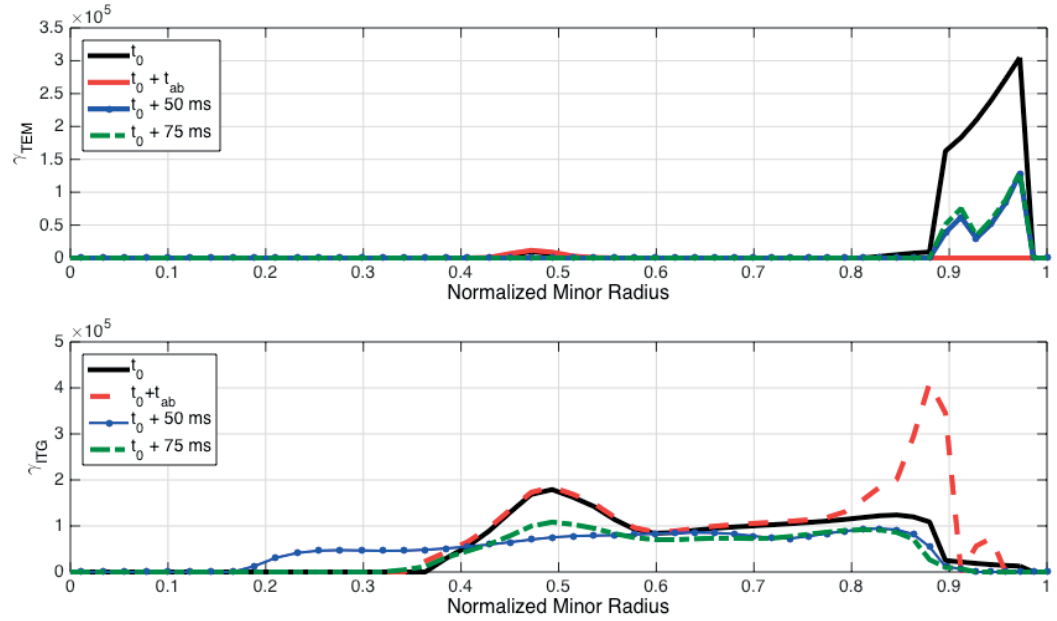

Figure 6. The profiles of the growth rate (s^{-1}) due to ITG and TEM during the pellet fueling operation are shown for the radius from ϱ = 0 to ϱ = 1.0.

Figure 6 shows the maximum growth rate for ITG and TEM modes during the pellet injection obtained from the simulation using the MMM95 transport code. At (r=0.88), the ITG growth rate increases immediately after pellet injection t_0+t_{abl}. The ITG modes can be stabilized by the increased density gradient and the decreased ion temperature gradient. However, the strong increase of ion temperature gradient at this time tends to destabilize the ITG growth rate. For the trapped electron modes (TEM) immediately after pellet

injection (t_0+t_{abl}). The TEM growth rate is decreased due to an increase in electron collisionality. Then, the growth rate recovers to the primary state at the middle location of the peak due to the pellet ablation profile, where (r=0.93). Immediately after pellet injection t_0+t_{abl}, we observe an initial decrease in the growth rate of TEM and a simultaneous increase in the growth rates of ITG. At this time, electron collisionality increases significantly, suppressing TEM growth rates. During the relaxation of the pellet deposition profile (t = t_0+50 ms), the growth rate based on TEM increases from the last time while the growth rate based on ITG mode drops at this time, and at t = t_0+50 ms, all profiles recover to the first state. At the outer surface (r=0.98), after the pellet ablation (at t = t_0 +50 ms), the growth rates and the complete stabilization of modes ITG and TEM are reduced. This suggests that in lower collisionality plasmas, the post-pellet may be unstable to TEM and ITG. It can also be seen that ITG modes dominate before pellet injection and are increased by the increased temperature gradient. TEM modes are stabilized by increased collisionality during pellet injection.

4. Conclusions

JET H-mode plasma discharge 53212 is carried out during the pellet fueling operation in the presence of an internal transport barrier (ITB) using the 1.5D BALDUR integrated predictive modelling code. It was found that the perturbation due to each pellet results in a change in thermal transport, especially in the resistive ballooning modes due to the increase of collisionality and resistivity near the plasma edge. It was found that the shallower pellet does not destroy the internal transport barrier, which locating mostly between r/a = 0.8 and 0.9. Moreover, in the plasma center region (0.4<r/a<0.6), the effective electron thermal diffusivities during the ablation time do not change. However, the effective electron thermal diffusivities decrease after pellet ablation, which means a shallower pellet can improve the internal transport barrier. A strong perturbation in the plasma causing a sudden change of thermal transport can be observed after each pellet enters the plasma. The results show that the micro-instability properties of the post-pellet profiles are highly sensitive to rapid and large excursions in the gradients, β_e and collisionality induced by the pellet injection. In particular, at a location corresponding to the part of the pellet deposition profile, ITG modes are destabilized by an increase in a temperature gradient, and TEM modes are stabilized by increased collisionality. The dominant mode in the simulation's pellet ablation region with the MMM95 core transport model is the resistive ballooning mode due to increased collisionality and resistivity near the plasma edge.

5. Acknowledgements

This work was partly supported by the International Atomic Energy Agency (IAEA) under contract No. 22785 and TSRI Fundamental Fund project number 91525. This work is a collaborative research project under the Center for Plasma and Nuclear Fusion Technology (CPaF).

References

[1] Manfredi, G.; Dendy, R.O. *Transport properties of energetic particles in a turbulent electrostatic field. Phys. Plasmas*, 1997, 4, 628.

[2] Parks, P. B.; Turnbull, R.J. *Effect of transonic flow in the ablation cloud on the lifetime of a solid hydrogen pellet in a plasma. Phys. Fluids*, 1978, 21, 1735.

[3] Singer, C.E. et al. .*Baldur: A one-dimensional plasma transport code.* Comput. Phys. Commun. 1988, 49 275

[4] Connor, J. W. et al. *Stability of the trapped electron mode in steep density and temperature gradients Plasma Phys. Controlled Fusion* ,2006, 48, 885.

[5] Weiland, J. *Collective modes in inhomogeneous plasma: kinetic and advanced fluid theory. Bristol: Institute of Physics Publishing,* 2000.

[6] Bateman, G. et al. *Predicting temperature and density profiles in tokamaks*. *Physics of Plasmas,* 1998, 5, 1793.

[7] Akers, R. J. et al *Transport and confinement in the Mega Ampère Spherical Tokamak (MAST) plasma. Plasma Phys. Control. Fusion,* 2003, 45, A175.

[8] Garzotti, L. et al. *Microstability analysis of pellet fuelled discharges in MAST Plasma Phys. Control. Fusion.*2014, 56, 035004.

[9] Guzdar, P. N. et al. *Shear flow generation by drift waves revisited. Physics of Fluids B*,1993, 5, 3712.
[10] M Erba et al. *Development of a non-local model for tokamak heat transport in L-mode, H-mode and transient regimes*, *Plasma Phys. Control. Fusion,* 1997, 39 261.
[11] Onjun, T. et al. *Comparison of low confinement mode transport simulations using the mixed Bohm/gyro-Bohm and the Multi-Mode-95 transport model. Physics of Plasmas*, 2001, 8, 975.
[12] Houlberg, W. A. et al. *Bootstrap current and neoclassical transport in tokamaks of arbitrary collisionality and aspect ratio*. *Phys. Plasma* , 1997 ,4, 3230.
[13] Hirshman, S. P. et al. *Neoclassical transport of impurities in tokamak plasmas. Nucl. Fusion,* 1981, 21, 1079
[14] Köchl, F. et al. *Pellet Drift Modelling – Validation and ITER Predictions, in Proc. 35th EPS Conf. Plasma Phys.* 32D P-4.099, 9–13 June 2008, Hersonissos, Greece.
[15] Pégourié, B. et al. *Homogenization of the pellet ablated material in tokamaks taking into account the ∇B-induced drif*. Nucl. Fusion, 2007, 47, 44.
[16] Parks, P. B. et al. *Effect of Parallel Flows and Toroidicity on Cross-Field Transport of Pellet Ablation Matter in Tokamak. Plasmas*,*Physical Rev Letters*, 2005, 94, 125002.
[17] Hannum, D. et al. *Comparison of high-mode predictive simulations using Mixed Bohm/gyro-Bohm and Multi-Mode (MMM95) transport models*. *Physics of Plasmas*,2001, 8, 965.
[18] Bateman, G. et al. *Integrated predictive modeling of high-mode tokamak plasmas using a combination of core and pedestal models. Physics of Plasmas,* 2003 ,10, 4358.
[19] Snyder, S. et al. *Effect of isotope mass on simulations of the high-mode pedestal and edge localized modes. Physics of Plasmas* 2005,12 112508
[20] Poolyarat, N. et al. *Simulation study of HL-2A-like plasma using integrated predictive modeling code. Plasma Physics Reports* ,2009,35,987.
[21] Chatthong, B. et al. *Model for toroidal velocity in H-mode plasmas in the presence of internal transport barriers. Nuclear Fusion*, 2010, 50(6), 064009.
[22] Garzotti, L. et al. *Particle transport and density profile analysis of different JET plasmas Nucl. Fusion.* 2003, 43, 1829.
[23] Romanelli, M. et al. *Effects of high density peaking and high collisionality on the stabilization of the electrostatic turbulence in the Frascati Tokamak Upgrade*. *Phys. Plasmas,* 2004 ,11 3845.
[24] Bourdelle, C. et al. *Impact of the α parameter on the micro stability of internal transport barriers*. *Nucl. Fusion,* 2005 ,45, 110.
[25] Klaywittaphat, P.; Onjun, T. *Transport and micro-instability analysis of JET H-mode plasma during pellet fueling*. *Nucl. Fusion,* 2017,57 022008.

JSTR
ASEAN Journal of Scientific and Technological Reports

Research article

Corrosion of Low Carbon Steel in Chloride Containing Environment

Tosapolporn Pornpibunsompob[1*], Sittha Saidarasamoot[2], Sawitri Phabjanda[3], Teeratas Pornyungyuen[4], Apirath Gositanon[5], Suradet Chalermboon[6] and Ploypilin Nakaracha[7]

[1] Metallurgical and Materials Engineering Laboratory, Research and Development Division, Defence Technology Institute, Nonthaburi, 11120, Thailand; tosapolporn.p@dti.or.th
[2] Metallurgical and Materials Engineering Laboratory, Research and Development Division, Defence Technology Institute, Nonthaburi, 11120, Thailand; sittha.s@dti.or.th
[3] Metallurgical and Materials Engineering Laboratory, Research and Development Division, Defence Technology Institute, Nonthaburi, 11120, Thailand; sawitri.p@dti.or.th
[4] Metallurgical and Materials Engineering Laboratory, Research and Development Division, Defence Technology Institute, Nonthaburi, 11120, Thailand; teeratas.p@dti.or.th
[5] Metallurgical and Materials Engineering Laboratory, Research and Development Division, Defence Technology Institute, Nonthaburi, 11120, Thailand; apirath.g@dti.or.th
[6] Metallurgical and Materials Engineering Laboratory, Research and Development Division, Defence Technology Institute, Nonthaburi, 11120, Thailand; suradet.c@dti.or.th
[7] Department of Materials Engineering, Faculty of Engineering, Kasetsart University, Bangkok 10900, Thailand; ploypailin.nak@ku.th
* Correspondence: E-mail: Tosapolporn.p@dti.or.th

Citation:
Pornpibunsompob, T.; Saidarasamoot, S.; Phabjanda, S.; Pornyungyuen, T.; Gositanon, A.; Chalermboon, S.; Nakaracha, P. Corrosion of Low Carbon Steel in Chloride Containing Environment. *ASEAN J. Sci. Tech. Report.* **2022**, *25*(4), 21-29. https://doi.org/10.55164/ajstr.v25i4.247174.

Article history:
Received: August 2, 2022
Revised: November 9, 2022
Accepted: November 13, 2022
Available online: November 20, 2022

Abstract: This research aims to investigate the corrosion of low-carbon steel in a chloride-containing environment. The investigation started by preparing and studying the surface condition of the specimens. The mechanical properties, microstructures and chemical compositions were also comparatively investigated between standard and corroded specimens. The results showed that the surface of the corroded samples was rough and peeling, different from the standard specimens, which were relatively smooth and non-corrosive. The average ultimate tensile strength and average yield strength of normal specimens were higher than those of corroded specimens at 5.39% and 2.32%, respectively. The corrosion products developed on the surface of corroded specimens caused a high-stress concentration area. The specimen is more prone to cracks and breaks when subjected to tensile stress. The surface of the normal specimen was composed of iron, oxygen, carbon, and silicon. In contrast, the surface of the corroded specimen contained the same elements as the normal specimen except chlorine which was detected. The film layer of the corroded specimen was cracked in contrast with the normal specimen, where the film still covered the metal substrate. The chemical composition analysis found that the corroded specimen's film layer contained chlorine, which is not detected in the film layer of the normal specimen. This is because the film layer of hot-rolled steel remains porous even passing the hot-rolling process. These pores allow chloride ions to diffuse and react with the film layer and the metal substrate. This makes the film layer of the corroded specimen thicker and initiates cracks. When stable alpha-iron-oxyhydroxide is formed on the steel surface, it can help to suppress corrosion.

Keywords: Corrosion, Low alloy steel, Chloride environment

1. Introduction

Low-carbon steels have many good properties in engineering applications, such as medium strength, malleability and ductility. It can be easily used in hot-rolled conditions and, after subsequent cold-rolling, annealing, and possibly coating. Modern processing provides a high degree of control of chemistry and processing to enable a wide range of grades with different combinations of strength and formability. Close control of gauge, width, shape, and flatness is also achieved[1]. Hot forming is one of the favorite processes in manufacturing low-carbon steel. As a result of the hot-forming process, the size and shape of the product are easily obtained. Furthermore, the parent material chemistry significantly influenced oxidation's kinetics and affected the oxide films' microstructure and composition [2]. This film is formed on the surface of the workpiece during hot rolling and is generally made up of Wustite (FeO), Magnetite (Fe_3O_4) and Hematite (Fe_2O_3) with positions arranged from the steel surface to the outer surface contacting environment, respectively. Wustite is developed from a eutectoid reaction and transforms to Magnetite, so the oxide film results in only Magnetite and Hematite layers[3]. Moreover, the oxide film on the surface is also porous. However, the film layer is deformed by a hot rolling process and extruded to the desired shape and thickness. The film has a certain density and is sufficient to provide effective corrosion protection in some normal atmospheres. Therefore, studying and analyzing the root causes of such occurrences is necessary.

The corrosion of hot-rolled low-carbon steel has been investigated for many years. However, the research on steel corrosion remains very interesting at present. Fundamentally, corrosion is due to moisture and dissolved oxygen but is accelerated by many contaminants, such as sulfur dioxide and chloride [4]. The corrosion products were quantitatively developed in a pollutant-free atmosphere depending on the exposure time and relative humidity. It had filiform corrosion characteristics. Meanwhile, cellular corrosion products grew on the filaments[5]. In the case of chloride environments, chloride plays an important role in accelerating corrosion reactions and rapid corrosion product formations. Various amounts of chloride depositions implied different accelerative corrosion mechanisms. The high amount of chloride over critical concentration is very significant for β-FeOOH formation. However, as to the low amount of chloride deposition, its effect was mainly conducive to transforming γ-FeOOH to α-FeOOH [6]. The corrosion will also deteriarate the mechanical properties of low alloy steel. A decrease in the sample cross-section governs the reduction of ductility. Additionally, the exfoliation was also a cause of degradation in terms of cracks. The random form of any pits on steel surface became progressively worse in the mechanical properties, related to mass loss and pit depth and extension[7-8].

In this study, some hot-rolled steel sheets showed many rusts on the surface of the storage area. Its quantity is larger than normal when observed visually. Moreover, when the rust was removed before being fabricated, it was deeper than usual. So, this research aims to analyze the cause of low-carbon hot-rolled steel corrosion by comparing normal and corrosion conditions. It will also introduce some suggestions for inhibiting and preventing corrosion.

2. Materials and Methods

Initially, two conditions of low-carbon hot-rolled steel specimens (normal specimens and corroded specimens) are received from a hot-rolled steel manufacturer in Thailand. The condition of the workpiece's surface was recorded after the visual inspection was examined. The three types of specimens were prepared: the three specimens for chemical composition testing (approximated to 50×50 mm), the three specimens for microstructural analysis (approximated to 10×15 mm), and the four specimens for mechanical properties testing (according to ASTM E8). To analyze microstructure and morphology, the specimens are performed by Carl Zeiss Sigma 500VP Field Emission Scanning Electron Microscope (FESEM). The microchemical analysis of both normal and corroded specimens was conducted by Oxford Aztec Ultim Max 60 Energy Dispersive Spectroscopy (EDS). The specimens for tensile testing were prepared by Wirecut & EDM machine and then mechanically tested by 100 kN Universal Tensile Testing Machine. Olympus DSX510 Digital Microscopes examined the fracture surface of two types of specimens. After analysis and testing, data collection and conclusion of the research results were collected. The process of analysis and testing is placed in Figure 1. The prepared specimen is shown in Figure 2. The chemical compositions were analyzed by BRUKER Q4 Optical Emission Spectroscopy (OES) and the results are shown in Table 1. They indicated that the specimen is low-carbon steel.

Table 1. Chemical composition of the specimens

Composition (%Wt.)	Conditions	Carbon	Silicon	Manganese	Phosphorous	Sulfur
Normal specimen	Specimen No.1	0.172	0.203	0.519	0.0035	< 0.005
	Specimen No.2	0.169	0.209	0.521	0.0029	< 0.005
	Specimen No.3	0.174	0.217	0.522	0.0029	< 0.005
	Average	**0.172**	**0.210**	**0.521**	**0.0031**	**< 0.005**
Corroded specimen	Specimen No.1	0.168	0.196	0.521	0.0019	< 0.005
	Specimen No.2	0.169	0.199	0.513	0.0019	< 0.005
	Specimen No.3	0.171	0.202	0.519	0.0017	< 0.005
	Average	**0.169**	**0.199**	**0.518**	**0.0018**	**< 0.005**

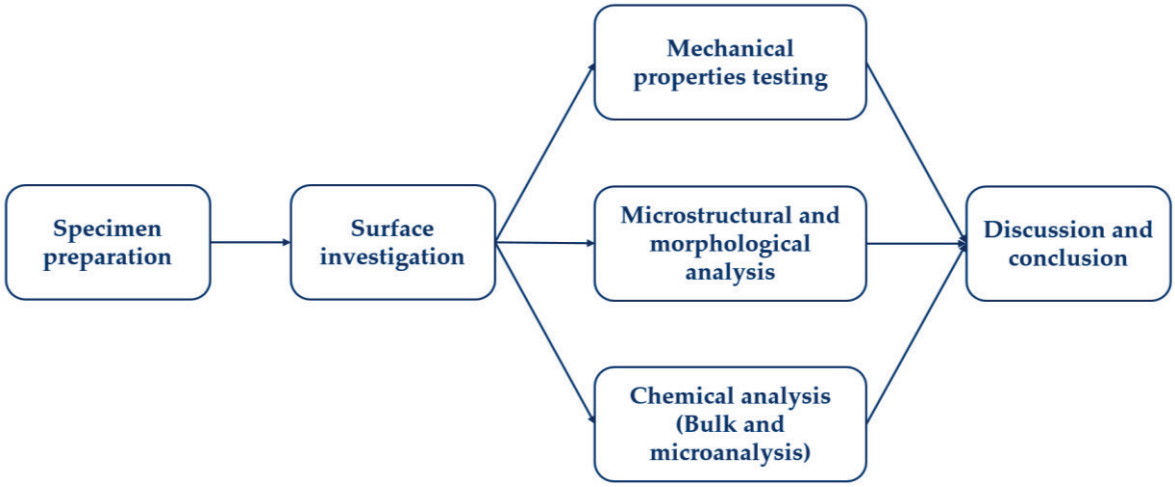

Figure 1. Specimen preparation and testing procedure

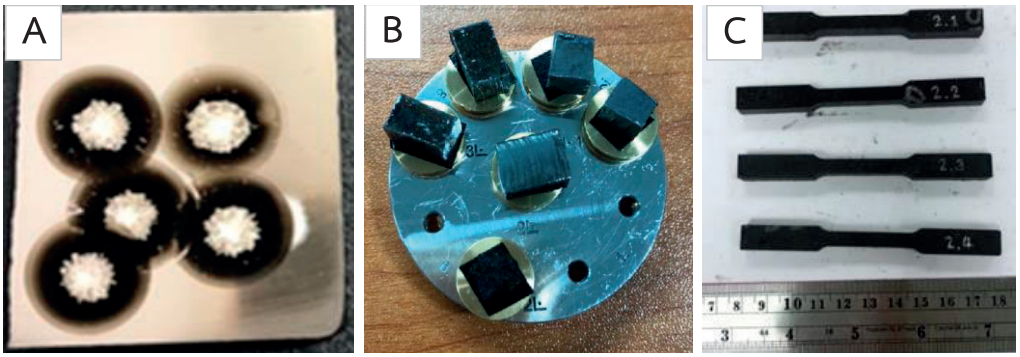

Figure 2. Testing and analysis specimen (A) chemical composition analysis specimen, (B) microstructure and morphology analysis specimen, and (C) specimen for tensile testing

3. Results and Discussion

The corrosion of low alloy steel in chloride containing atmosphere was studied in three approaches:

3.1 Mechanical properties approach

The tensile testing results of two types of specimens were placed in Table 2.

Table 2. Tensile testing results of normal and corroded specimens

Mechanical properties	Specimen type	Test results (MPa)				
		Specimen No.1	Specimen No.2	Specimen No.3	Specimen No.4	Average
Ultimate tensile strength	Normal	455.52	444.94	446.50	444.47	447.86
	Corrosion	423.80	429.25	421.88	424.85	424.95
Yield strength	Normal	295.19	286.99	282.08	291.36	288.91
	Corrosion	280.37	272.89	284.83	291.10	282.30

It was found that normal specimens have an average maximum tensile strength of 447.86 MPa, which is higher than that of corroded specimens with an average maximum tensile strength of 424.95 MPa. In the same way, the average yield strength of normal specimens is 288.91 MPa, while the average yield strength of corroded specimens is 282.30 MPa. Therefore, the average mechanical properties of normal specimens are higher than those of corroded specimens, as shown in Figure 3. If it is calculated as a percentage, it will be concluded that normal specimens have the average maximum tensile strength and the average yield strength higher than corroded specimens at 5.39% and 2.32%, respectively. Because the surface of corroded specimens is very rough due to corrosion products, tension loads acting on the corrosion pits will cause stress concentration and decrease the strength[8]. When the workpiece is subjected to tensile stress, it is easier to propagate some cracks. It can be noticed from the cracked surface, and it is a sharp tooth mark, as shown in Figure 4(A). When the tensile strength increases, the crack will propagate until the workpiece is completely fractured. While normal specimens do not have corrosion products on the surface, the fracture is caused by the ductile failure mechanism. The fracture surface is shown in Figure 4(B). Thus, it has a strength higher than the corroded workpiece.

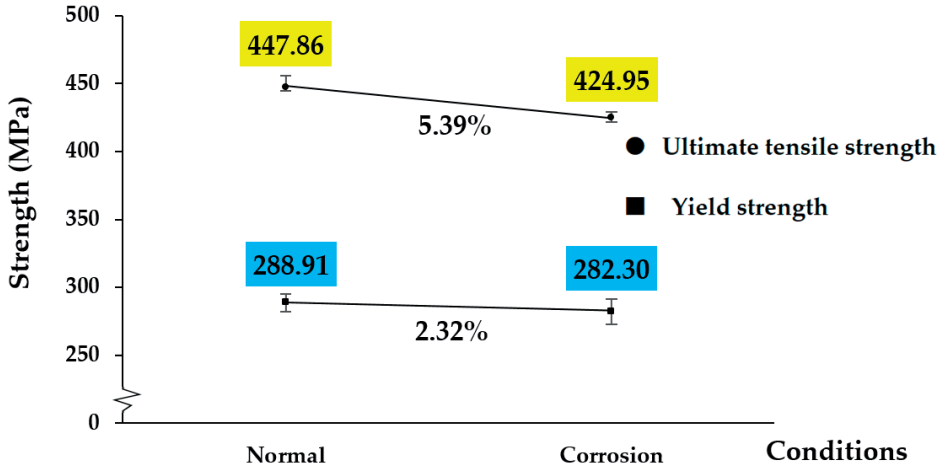

Figure 3. Average mechanical properties comparison between normal and corroded specimen

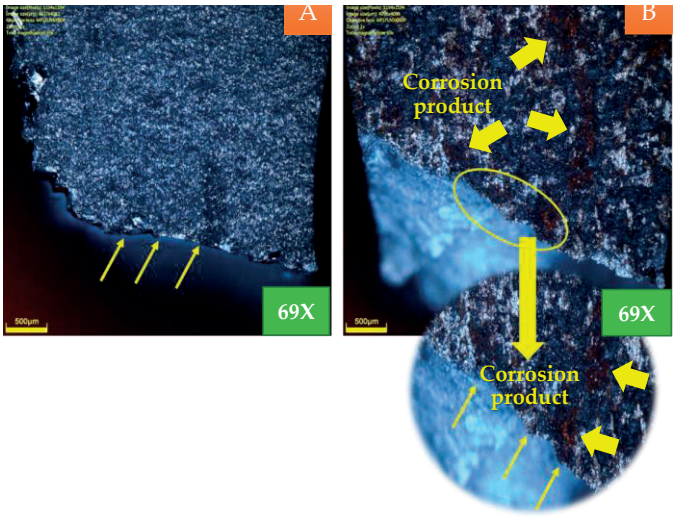

Figure 4. Fracture surface analyzed by optical microscope comparison between (A) Normal specimen and (B) Corroded specimen

3.2 Surface study approach

The surface condition of normal and corroded specimens, observed with visual and light microscopy, is shown in Figure 5. It can be seen that the normal specimens' surface is matte and does not peel off. As for the corroded workpiece, the surface of the workpiece is rough, and some area of the specimen's surface is peeled off. Also, it is found corrosion products when examined by scanning electron microscopy. As shown in Figure 6, it was found that the surface of the normal specimen is smooth and dull. Small scabs may be found on the surface in some places resulting from the hot rolling process. As for corroded parts, the workpiece's surface is rough and peeled off.

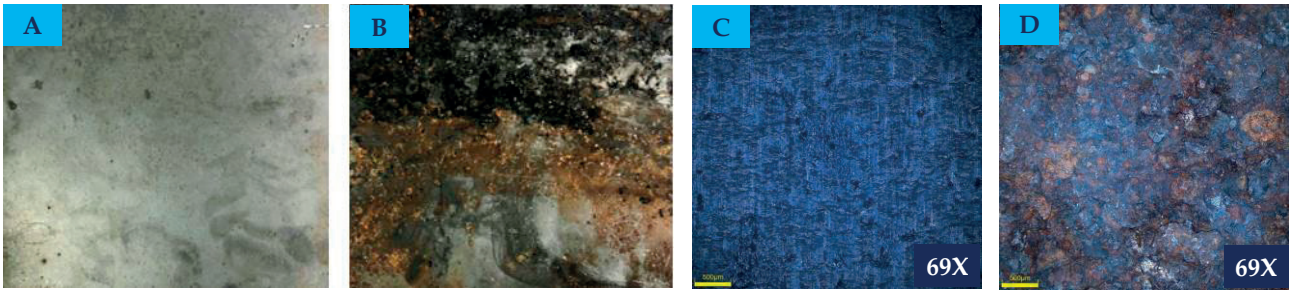

Figure 5. Surface investigation of specimens by visual examination (A) normal specimen, (B) corrosion specimen, and by optical microscope (C) normal specimen (D) corroded specimen

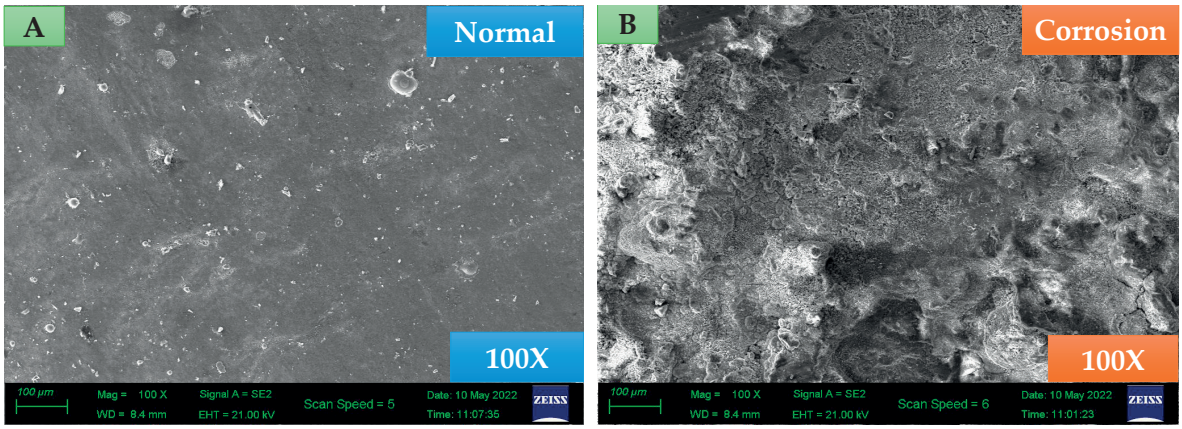

Figure 6. Surface morphology analyzed by FESEM (A) normal specimen (B) corroded specimen

The microchemical composition examined by EDS is depicted in Figure 7. It shows that the normal surface of the specimen is composed of iron, oxygen, carbon, and silicon, while the surface of the corroded specimen contains the same elements as the normal specimen except chlorine. It was detected on the surface of the specimen. Chlorine is one of the main elements that potentially cause corrosion in steel [6]. The effect of chlorine on corrosion is studied next.

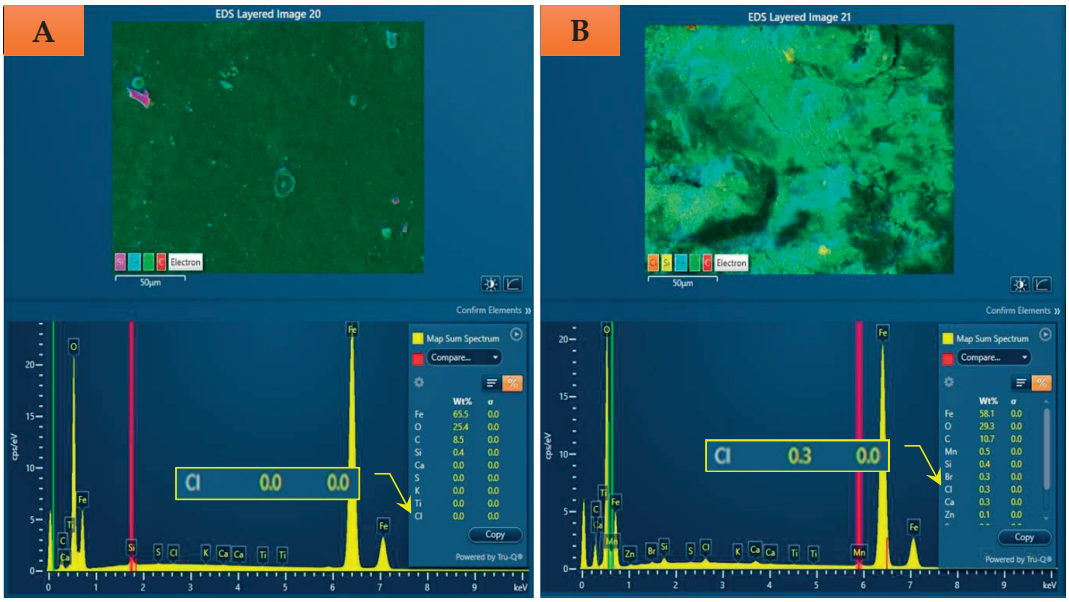

Figure 7. Microchemical composition of the specimen surface analyzed by EDS (A) Normal specimen (B) Corroded specimen

3.3 Protective film approach

A detailed investigation of the surface, especially at the protective film, was performed, as shown in Figure 8. It was found that normal specimens have a protective film coating on the surface. An oxidation reaction formed the film layer during the hot rolling process (Figure 8(A)). In contrast with corroded specimens, the protective film is destroyed. The film contains several cracks separating the protective film from each other. This phenomenon allows the metal surface to contact the corrosive environment directly. Therefore, oxidation reactions still occur continuously. So, the film layer of the corroded specimen is not only a result of the hot rolling process, but it is also caused by an oxidation reaction when the substrate is exposed to the corrosive environment. That explanation can also explain why the film thickness of the corroded workpiece is greater than the normal specimen.

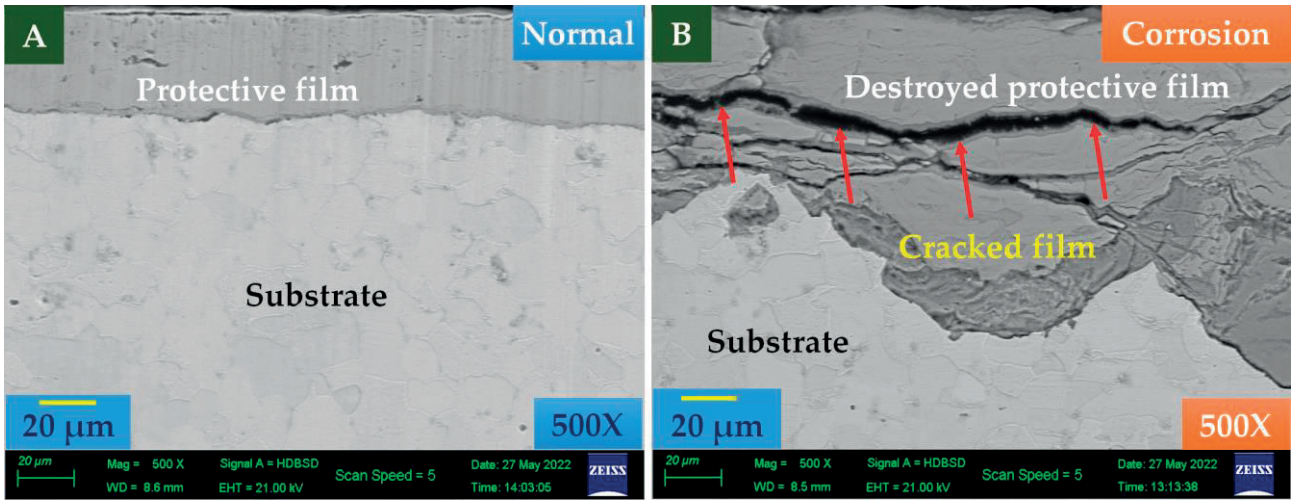

Figure 8. Morphology of protective film analyzed by FESEM (A) normal specimen (B) corroded specimen

The microchemical composition of normal specimens is shown in Figure 9. It was found that the protective film formed by the hot-rolling process was mainly composed of iron and oxygen. It is ferrous oxide. Moreover, it was observed that the iron content in the oxide film region was greater than that in the substrate. The substrate is composed of many elements within it. Therefore, as a proportion, the iron content is greater in the film layer area.

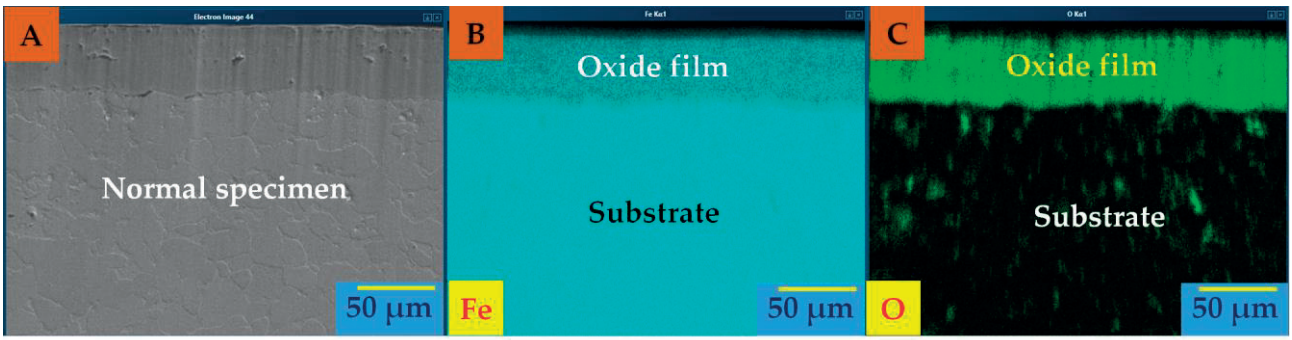

Figure 9. EDS mapping of cross-section's surface normal specimen (A) SEM micrograph (B) iron (C) oxygen

The oxide film layer is cracked in corroded specimens. However, the chemical composition is not quite similar to the normal specimens. Iron, oxygen, and chlorine are found in the oxide film. It remains similar to the composition of the corroded specimen's surface, as shown in Figure 10. Therefore, the oxidation of steel, despite the presence of chlorine, will continue to form compounds composed of iron and oxygen because the protective film is porous (Even though it has been hot rolled, making the film denser). This allows the chloride ions to easily pass through the film and react with the substrate resulting in a thicker and deeper oxidation film. However, if the oxidation layer is complete, it will inhibit chloride corrosion [6]. Chloride plays a vital role in catalyzing the oxidation of steel.

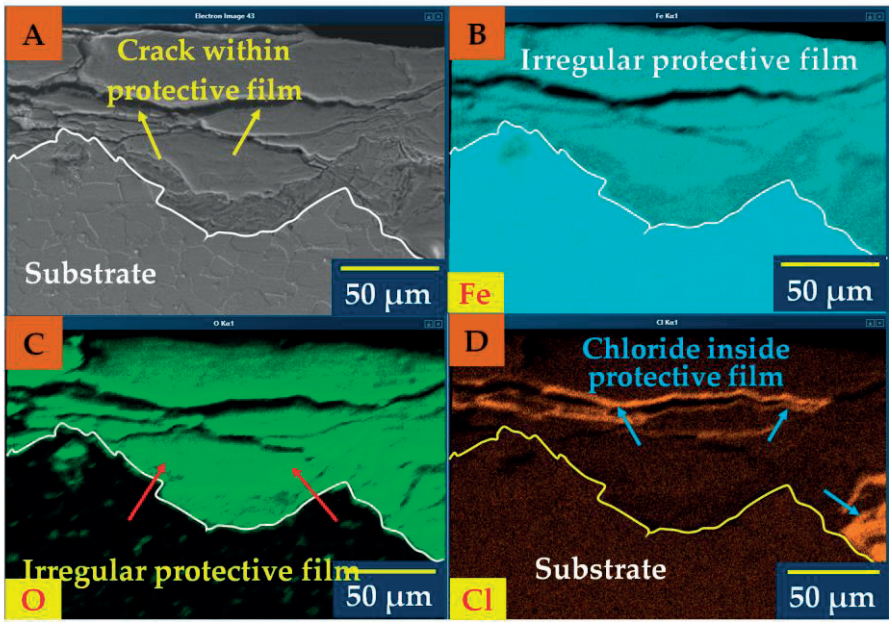

Figure 10. EDS mapping of cross-section's surface corroded specimen (A) SEM micrograph (B) Iron (C) Oxygen (D) Chlorine

Because the chloride ion catalyzes the oxidation reaction of steel, following Equations 1 – 2, resulting in an increment in both classification and quantity of corrosion product. This is consistent with the analysis results shown in Figure 10.

$$Fe \xrightarrow{\text{Anodic}} Fe^{2+} \xrightarrow{\text{Hydrolysis}} [FeOH]^{+} \xrightarrow{\text{Oxidation and precipitation}} \gamma\text{-FeOOH(s)} \quad (1)$$

In equation 1, Gamma-iron-oxyhydroxide (γ-FeOOH) is a corrosion product that develops earlier and then transforms to alpha-iron-oxyhydroxide (α-FeOOH) according to equation 2. Alpha-iron-oxyhydroxide is more stable and adheres to the surface than Gamma-iron-oxyhydroxide. So, this ferrous oxide helps suppress the corrosion process on steel specimens [9].

$$\gamma\text{-FeOOH(s)} \xrightarrow{\text{Chlorination}} FeO_x(OH)_{2-2x}Cl \xrightarrow{\text{Solid precipitation}} \alpha\text{-FeOOH(s)}+HCl(g) \quad (2)$$

The suggested methods for corrosion inhibition and protection are summarized below;

1. A suitable pre-treatment or surface coating on a bare carbon steel surface would help inhibit corrosion. It prevents the access of corrosive anions to the steel surface [10-12].
2. Avoiding direct exposure to chloride-containing atmospheres can suppress and prevent corrosion, even though low-carbon steel can be slightly corroded in the natural environment caused by humidity and dissolved oxygen [13-14].

4. Conclusions

Low-carbon hot-rolled steels were susceptible to corrosion under chloride-containing environments despite the protective film formed by the hot-rolling process. The phenomena caused the reduction of mechanical properties. The surface of the corroded specimen was rough and peeled off. Chloride ions penetrated the metal through the porous protective film and reacted with the substrate. It developed various compounds causing crack initiation and propagation in the film layer. When stable alpha-iron-oxyhydroxide was formed on the steel surface, it could help to suppress corrosion.

5. Acknowledgements

We would like to thank the Defence Technology Institute under the Ministry of Defence, Thailand, for supporting all expenses to attend the academic presentations.

Author Contributions: Sittha Saidarasamoot were the director of this project. Tosapolporn Pornpibunsompob wrote and submitted the article, coordinated with editor until the acticle had been accepted for publication. The specimens were prepared by Teeratas Pornyungyuen and Ploypilin Nakaracha. The tensile testing was performed by Suradet Chalermboon. Apirath Gositanon analyzed the specimen with Electron microscopy technique. Sawitri Phabjanda discussed and concluded the testing results.

Funding: This research was funded by Defence Technology Institute.

Conflicts of Interest: The authors declare that there is no conflict of interest regarding the publication of this article.

References

[1] Urabe, T. High Formability Steel In *Encyclopedia of Materials: Metals and Alloys, C. G. Francisca, M. Goro, 1st ed., Elsevier, Osaka, Japan*, 2021, 3-11.

[2] Ahmadi, D. *Oxide Scales Behaviour During Descaling and Hot Rolling*, Doctor of Philosophy in material science and engineering The University of Sheffield, England, June 2019, p. ii.

[3] Tanei, H.; Kondo, Y. Phase transformation of oxide scale and its control. *Nippon steel & Sumitomo metal technical report*, 2016, 111, March 2016.

[4] Fontana, M.G. *Corrosion engineering*, 3rd ed., McGraw-Hill, Singapore, 2001, 372-373.

[5] Lin, C.; Chen, S. Atmospheric corrosion behavior of mild steel in the initial stage under different relative humidity. *International journal of georesources and environment*, 2018, 4, 33-39.

[6] Ma, Y.; Li, Y.; Wang, F. Corrosion of low carbon steel in atmospheric environments of different chloride content. *Corrosion science*, 2009, 51, 997-1006.

[7] Martínez, C.; Briones, F.; Villarroel, M.; Vera, R. Effect of atmospheric corrosion on the mechanical properties of SAE 1020 Structural steel, *Materials.* 2018, 11, 1-17.

[8] Chen, Y. Y.; Tzeng, H. J.; Wei, L. I.; Shih, H. C. Mechanical properties and corrosion resistance of low-alloy steels in atmospheric conditions containing chloride. *Materials Science and Engineering A*, 2005, 398, 47-59.

[9] Tee, Ch. Atmospheric Corrosion of Steel: A Review and Case Study. *Journal of Science and Technology*, *Ubon Ratchathani University*, 2017, 19, 178-186.

[10] Etteyeb, N. et al, Corrosion inhibition of carbon steel in alkaline chloride media by Na_3PO_4. *Electrochimica acta*, 2007, 52, 7506-7512.

[11] Schuerz, S. et al. Corrosion behaviour of Zn–Al–Mg coated steel sheet in sodium chloride-containing environment. *Corrosion science*, 2009, 51, 2355-2363.

[12] Girciene, O. et al. The effect of phosphate coatings on carbon steel protection from corrosion in a chloride-contaminated alkaline solution. *Chemija*, 2013, 24, 251-259.

[13] Permsuwan, P. et al. Corrosion of different types of steel in atmospheric and tidal marine environment of Thailand. *Research and development journal*, 2011, 22, 17-24.

[14] Chowwanonthapunya, T. et al. A preliminary study of atmospheric corrosion performances of carbon steels in coastal and urban environments in Thailand, *Burapha university international conference* 2015, 10-12 July 2015, 625-632.

JSTR
ASEAN Journal of Scientific and Technological Reports

Research article

Water Quality Management Guidelines to Reduce Mortality Rate of Red Tilapia (*Oreochromis niloticus* x *Oreochromis mossambicus*) Fingerlings Raised in Outdoor Earthen Ponds with a Recirculating Aquaculture System Using Machine Learning Techniques

Putra Ali Syahbana Matondang[1], Wara Taparhudee[2*], Ruangvit Yoonpundh[3], and Roongparit Jongjaraunsuk[4]

[1] Fishery Science and Technology, Faculty of Fisheries, Kasetsart University, Bangkok, 10900, Thailand; putraalisyahbana.m@ku.th
[2] Department of Aquaculture, Faculty of Fisheries, Kasetsart University, Bangkok, 10900, Thailand; ffisrvy@ku.ac.th
[3] Department of Aquaculture, Faculty of Fisheries, Kasetsart University, Bangkok, 10900, Thailand; ffisrvy@ku.ac.th
[4] Department of Aquaculture, Faculty of Fisheries, Kasetsart University, Bangkok, 10900, Thailand; roongparit.jo@ku.th
[*] Correspondence: ffiswrt@ku.ac.th

Citation:
Matondang, P.A.S.; Taparhudee, W.; Yoonpundh, R.; Jongjaraunsuk, R. Water Quality Management Guidelines to reduce Mortality Rate of Red Tilapia *(Oreochromis niloticus x Oreochromis mossambicus)* Fingerlings Raised in Outdoor Earthen Ponds with a Recirculating Aquaculture System Using Machine Learning Techniques. *ASEAN J. Sci. Tech. Report.* **2022**, *25*(4), 30-41. https://doi.org/10.55164/ajstr.v25i4.247049.

Article history:
Received: July 5, 2022
Revised: October 26, 2022
Accepted: October 27, 2022
Available online: November 20, 2022

Abstract: Machine learning techniques have been widely adopted over the last few decades, especially in fisheries. This study aimed to determine the best practice of machine learning techniques with a decision tree algorithm in reducing the mortality rate of red tilapia (*Oreochromis niloticus* x *Oreochromis mossambicus*) fingerlings raised in outdoor earthen ponds with a recirculating aquaculture system. The study phase begins with collecting water quality parameters. The parameters were measured in the form of dissolved oxygen (mg L^{-1}), pH, temperature (˚C), total ammonia nitrogen (mg L^{-1}), nitrite-nitrogen (mg L^{-1}), alkalinity (mg L^{-1}), transparency (cm), and mortality rate (fish day^{-1}). Data Modelling was carried out using 10-fold cross-validation. The results of the performance measurement obtained an accuracy of 89.67% with ± 5.11% (micro average: 89.60%), a precision of 86.71% ± 18.02% (micro average: 80.00%), and recall of 72.50% ± 24.86% (micro average: 71.79%), with the most influential water quality parameter being nitrite-nitrogen (mg L^{-1}). Based on the results of this study show that data classification using a decision tree algorithm can be used as a reference to determine the decisions or actions of fish farmers in reducing the mortality rate of red tilapia fingerlings raised in outdoor earthen ponds with a recirculating aquaculture system.

Keywords: Machine learning, Decision tree algorithm, Red tilapia, Water quality, Mortality rate.

1. Introduction

Red tilapia does not have black pigment derived from hybridization between species in the genus, especially between *Oreochromis niloticus* and *Oreochromis mossambicus* [1]. This fish is still a superior commodity for freshwater aquaculture with important economic value throughout the world, including the whole world, especially Thailand. In Thailand, red tilapia farming is gaining popularity because the red color of the fish is like that of expensive marine fish species, and both domestic and international markets have shown an increasing demand for live fish and fish meat [2]. Based on data from the Food and Agriculture Organization of the United Nations, Tilapia is the third major species produced in world aquaculture after Grass carp (*Ctenopharyngodon idellus*) and Silver carp (*Hypophthalmichthys molitrix*), with a production contribution of 4.5 million tons in 2018 [3].

The increase in consumption of tilapia in the world illustrates that the pattern of fish consumption in the community is increasing and fish production needs to be increased to meet demand. However, the increase in tilapia production in meeting consumer needs will be limited by several factors, including a decrease in water quality due to nitrogen (N) waste originating from uneaten feed residue, feces, and excretory products on the gills. This waste will decompose, causing a decrease in water quality in the rearing system [4-5]. Although tilapia fingerlings reproduce freely in ponds, farmers must consider using properly produced fingerlings. Determination of optimal environmental conditions to achieve the best fingerlings growth performance is important to maximize and optimize production [6, 7]. The availability of good quality tilapia fingerlings at competitive prices is very important to maintain farm profitability [8]. Hence, water quality in the rearing system needs to be appropriately managed for the optimal life needs of red tilapia fingerlings. One way to overcome this problem is to use recirculating aquaculture system.

Recirculating aquaculture system (RAS) is an aquaculture system that implements efficient use of water to maximize the production of aquatic organisms by minimizing pollution and water costs [9-11]. RAS for tilapia cultivation has several advantages. Namely, it can be placed in areas that do not have sufficient water sources for cultivation [12] because this system can simultaneously increase water circulation and oxygenation in fish rearing [13]. RAS has a fish culture tank, a particulate filter to remove solids, a pump for water circulation, and an oxygenation device [14].

Automation and intelligence technology development has gradually influenced aquaculture towards the direction of intensive and intelligent aquaculture. This could significantly improve aquaculture efficiency worldwide [15-17]. They are combined with high-performance computers, namely machine learning technology that can mine information in data, thus offering solutions for smart aquaculture and introducing the fishing industry into a new era [17-19]. Machine learning algorithms and their applications in aquaculture have been widely applied, such as fish biomass estimation, fish identification and classification, fish behavioral analysis, and prediction of water quality in aquaculture activities [17].

In this study, data on the water quality parameters of red tilapia fingerlings raised in outdoor earthen ponds with a recirculating aquaculture system will be observed, which will then be analyzed for the effect of each measured water quality parameters on the mortality rate of red tilapia using a machine learning with decision tree algorithm. A decision tree algorithm is a popular machine learning tool. It is often used to identify possible consequences such as the outcome of chance events, investment risk, decision-making, and interest rates [20-22]. This classifier modeling method performs well even with complex data sets to identify pattern behavior [23]. On the other hand, the use of decision trees is very easy to understand and is similar to how humans make decisions [24]. In contrast to other models, such as the random forest, which is more complicated to interpret because it has many decision trees, naïve bayes, whose precision could decrease if the data used is few, and the neural network, which requires high processing time when the neural network is large.

The main aim of this study is to determine the best practice of machine learning techniques with a decision tree algorithm in reducing the mortality rate of red tilapia fingerlings raised in outdoor earthen ponds with a recirculating aquaculture system. By applying machine learning with a decision tree algorithm to water quality parameters data, we hope that the aquaculture management system will provide many recommendations and insights to support fish farmers' decisions and actions to reduce fish mortality of red tilapia fingerlings in outdoor earthen ponds with recirculating aquaculture system.

2. Materials and Methods

2.1 Study Area

This study was conducted at the Patthamarach Farm, Lam Plai Mat District, Buriram Province, Thailand, located at coordinates (15.067192, 102.788965) from November 2020-January 2021. The farm consists of a reservoir pond with a size of 9,210.18 m^2, 2 treatment ponds with a size of 3,609.86 m^2 and 4,593.06 m^2, 4 nursing ponds with a size of 1,600 m^2, 18 grow out/culture ponds with a size 1,600 m^2, 1 sedimentation pond with size 2,078.03 m^2, 1 biological treatment pond using water hyacinth with size 8,224.83 m^2, and 1 ready-to-use pond with size 7,183.4 m^2.

2.2 Data Collection

Red tilapia fingerlings were reared in the earthen ponds with Polyethylene (PE) using recirculating aquaculture system (RAS) with mono sex. Using 4 ponds with a size of 1,600 m^2 per each pond. The average initial weight of the fish was 50 g $fish^{-1}$, and the stocking density was 25 fish m^{-2}. Each pond was provided with 4 aerators in the form of a waterwheel which will be operated 24 hours a day to maintain the quality of dissolved oxygen during maintenance. Red tilapia fingerlings were fed a commercial diet (floating pellets) with 35% crude protein. Frequency of feeding 3 times a day at 08.00, 11.30, and 16.30 with ad satiation using the automatic feeder.

Water quality parameters were measured in the form of dissolved oxygen/DO (mg L^{-1}), temperature ($^{\circ}C$), pH, total ammonia nitrogen/TAN (mg L^{-1}), nitrite-nitrogen/NO_2-N (mg L^{-1}), alkalinity (mg L^{-1}), and transparency (cm) every day. Where dissolved oxygen, temperature, and pH were measured using YSI Professional Plus (Yellow Springs, OH, USA) twice daily in the morning and evening. The DO, pH, and temperature are divided into 2 parts: average and different. DO average, pH average, and average temperature state the central or typical value in water quality measurements carried out in the morning and evening. Meanwhile, DO, pH, and temperature are the different values of water quality measurements carried out in the morning and evening. Total ammonia nitrogen, nitrite-nitrogen, and alkalinity were measured following the American Public Health Association [25] once a day. And the water transparency in the maintenance pond was measured using a Secchi disk once a day.

Red tilapia fingerlings will be reared until they reach the average weight of 200 g $fish^{-1}$. The mortality rate of red tilapia fingerlings was measured during rearing by counting the number of fish that die per day. If the fish that died were less than 10, it was categorized as low mortality. If more than 10 fish died, it was categorized as high mortality.

2.3 Data Cleaning

Dataset obtained from a study object generally has imperfect entries, such as missing or unfilled data. In this study, the first step in managing missing values is understanding the reasons behind why they are missing by tracing the data lineage (origin) from the data source can lead to the identification of systemic problems during data retrieval or errors in data transformation. In the second step, knowing the source of the missing value will often guide which mitigation methodology to use. Missing values can be replaced with various artificial data to manage problems with little impact at the next step in the data science process. Missing values can be replaced with values that come from the data set (mean, minimum, or maximum values, depending on the characteristics of the attribute). This method is useful if the missing values occur randomly and the frequency of occurrence is quite rare. It is better to discard the irrelevant data because its existence can reduce the quality or accuracy of the expected data mining later [24].

2.4 Data Modelling

The dataset that has been cleaned using Microsoft Excel 365 will be imported into the RapidMiner studio version 9.10 software. Next, change the role in the outlook (mortality rate) column as a label. Then, store the dataset in the local repository or temporary repository. After that, input the cross-validation operator with 10 folds in the process page to get an accurate validation result. Choose stratified sampling with a split ratio of 90% of training data samples and 10% of testing data samples. Stratified sampling will ensure that training

and testing samples have the same distribution of class values. After that, input the decision tree model in the training subprocess with parameters are gain ratio as a criterion, 10 as maximal depth, 0.1 as confidence, 0.01 as minimal gain, 2 as minimal leaf size, 4 as minimal sizes for the split, and 3 as a number of pre pruning alternatives. The model is ready for the training subprocess. After that, input two more operators in the testing subprocess, and apply the model and performance consisting of accuracy, precision, and recall. The model is ready for the testing subprocess. Return to the main process and connect the output ports model. Finally, hit the run process locally in the dataset. The flowchart to determine the best water quality management practice to reduce the mortality rate of red tilapia fingerlings using the decision tree algorithm can be seen in figure 1. And the model configuration within cross-validation in RapidMiner Studio can be seen in figure 2.

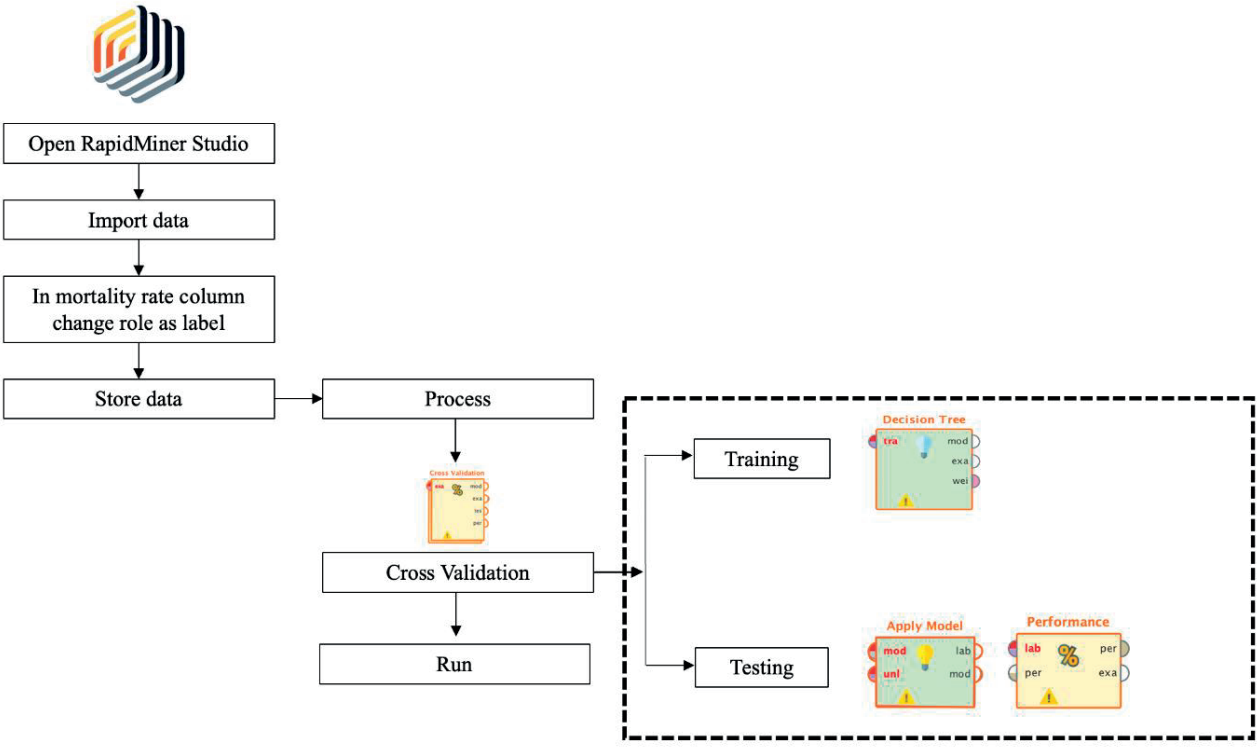

Figure 1. The flowchart to determine the best water quality management practice to reduce the mortality rate of red tilapia fingerlings using the decision tree algorithm

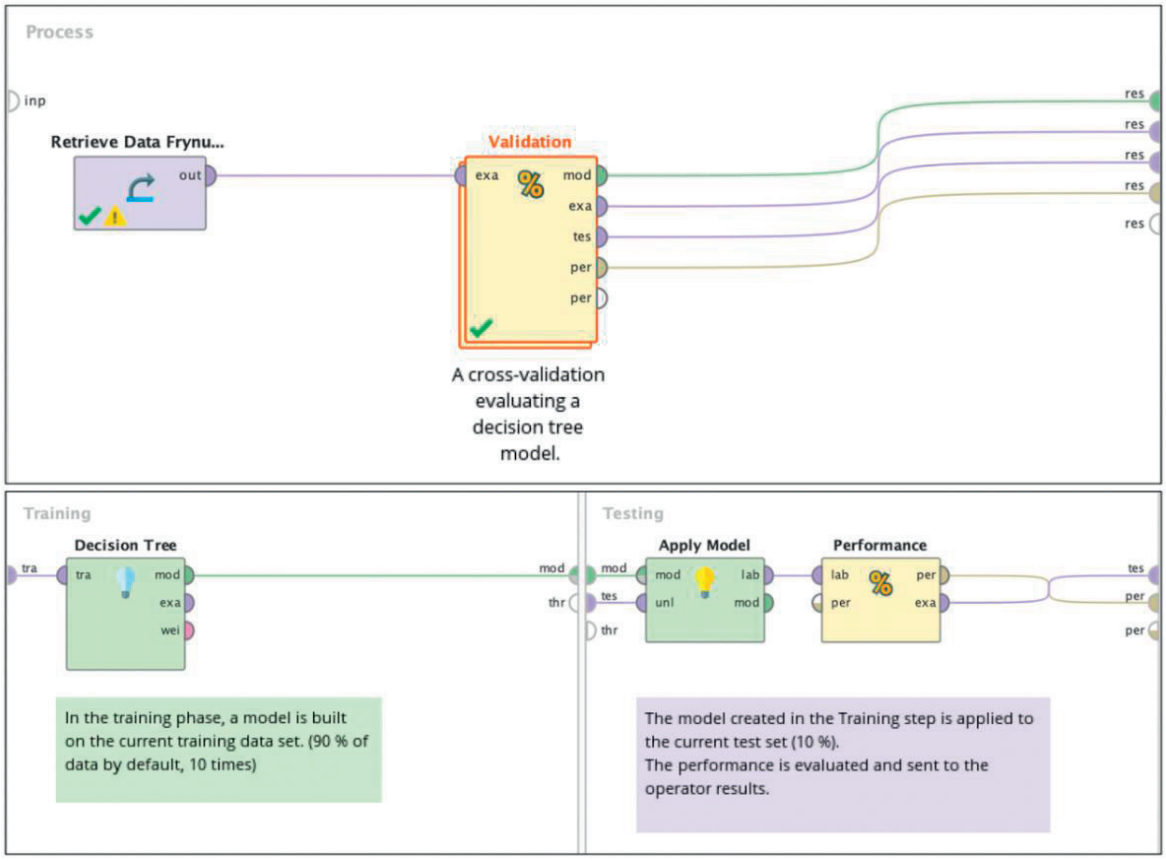

Figure 2. The model configuration within cross-validation in RapidMiner Studio

2.5 Performance Measurement

2.5.1 Confusion Matrix

The confusion matrix is a test method to minimize errors and ensure that the output is as desired. The confusion matrix describes the true and false results of a classification model. The value of the confusion matrix is usually shown in percent (%). The confusion matrix can be seen in figure 3.

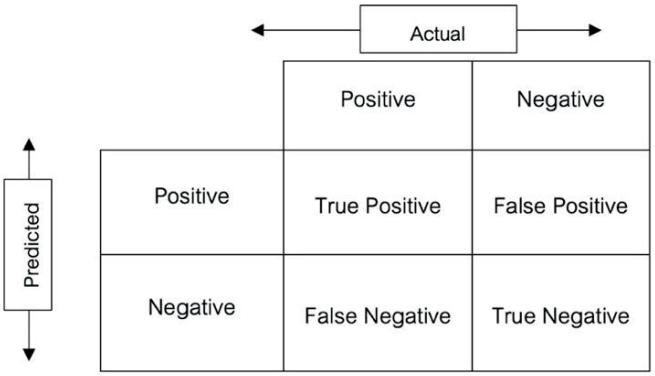

Figure 3. Confusion Matrix

2.5.2 Accuracy, Precision, and Recall

In performance measurement, there are three classification metrics: Accuracy, Precision, and Recall. Accuracy is how accurately the system can classify the data correctly. In other words, accuracy is a comparison between the data that is classified correctly and the whole data. Accuracy can be seen in equation 1. Precision

describes the number of positive data categories classified correctly divided by the total data classified as positive. Precision can be seen in equation 2. Meanwhile, recall shows how many the system correctly classifies percent of the positive category data. Recall can be seen in equation 3.

$$\text{Accuracy} = \frac{TP + TN}{TP + TN + FP + FN} \text{ x100\%} \quad (1)$$

$$\text{Precision} = \frac{TP}{TP + FP} \text{ x100\%} \quad (2)$$

$$\text{Recall} = \frac{TP}{TP + FN} \text{ x100\%} \quad (3)$$

True Positive (TP) was the number of positive data correctly classified by the system. True Negative (TN) was the number of negative data correctly classified by the system. False Positive (FP) was the number of positive data classified incorrectly by the system. False Negative (FN) was the number of negative data classified incorrectly by the system.

3. Results and Discussion

The best water quality management practice to reduce the mortality rate of red tilapia fingerlings was achieved under the decision tree algorithm; accuracy reached 89.67% with ± 5.11% (micro average: 89.60%), precision reached 86.71% ± 18.02% (micro average: 80.00%) and recall reached 72.50% ± 24.86% (micro average: 71.79%). Table 1. shows that the prediction of low with a true low of as many as 127 data and a true high of as many as 11 data with class precision reached 92.03%. The prediction of high with true low, as many as 7 data and for true high, as many as 28 data with class precision reached 80.00%. For class recall with a true low, it reached 94.78%. While for class recall with a true high, it reached 71.79%.

Table 1. Confusion Matrix with Decision Tree Algorithm

	True Low	True High	Class Precision
Pred. Low	127	11	92.03%
Pred. High	7	28	80.00%
Class Recall	94.78%	71.79%	

Table 2. The water quality parameters of red tilapia fingerlings are raised in outdoor earthen ponds with a recirculating aquaculture system.

Water Quality Parameter	Unit	Min	Max	Mean	Standard Deviation
DO average	mg L^{-1}	3.60	7.85	5.77	0.87
DO different	mg L^{-1}	0.00	3.90	1.54	0.94
pH average	-	5.15	7.60	7.29	0.23
pH different	-	0.00	0.90	0.19	0.19
Temperature average	˚C	18.50	27.00	22.67	1.92
Temperature different	˚C	0.00	4.00	1.79	0.84
Total ammonia nitrogen (TAN)	mg L^{-1}	0.00	3.00	1.11	0.73
Nitrite-nitrogen (NO_2-N)	mg L^{-1}	0.00	1.40	0.71	0.43
Alkalinity	mg L^{-1}	60.00	110.00	79.11	9.41
Transparency	cm	15.00	45.00	33.78	8.22

The water quality management practice to reduce the mortality rate of red tilapia fingerlings raised in outdoor earthen ponds with a recirculating aquaculture system shows that the most influential factor in the mortality rate of red tilapia fingerlings was NO_2-N (Figure 4). In the implementation stage using a decision tree algorithm using RapidMiner 9.10, a decision tree algorithm with 12 terminal nodes was obtained to

determine the mortality rate of red tilapia fingerlings raised in outdoor earthen ponds with a recirculating aquaculture system.

Terminal node number 1 states that if the NO_2-N is more than 1.275 mg L^{-1}, the mortality rate for red tilapia fingerlings is high. Terminal node number 2 states that if NO_2-N is less than or equal to 1.275 mg L^{-1}, the DO average is more significant than 7.475 mg L^{-1}, then the mortality rate for red tilapia fingerlings is high. Terminal node number 3 has the NO_2-N is less than or equal to 1.275 mg L^{-1}, DO average is less than or equal to 7.475 mg L^{-1}, alkalinity is greater than 71.250 mg L^{-1}, transparency is greater than 44.869 cm, temperature average is greater than 22.250 ˚C, then the mortality rate for red tilapia fingerlings is high. Terminal node number 4 has NO_2-N is less than or equal to 1.275 mg L^{-1}, DO average is less than or equal to 7.475 mg L^{-1}, alkalinity is greater than 71.250 mg L^{-1}, transparency is greater than 44.869 cm, temperature average is less than or equal to 22.250 ˚C, then mortality rate for red tilapia fingerlings is low. Terminal node 5 has NO_2-N is less than or equal to 1.275 mg L^{-1}, DO average is less than or equal to 7.475 mg L^{-1}, alkalinity is greater than 71.250 mg L^{-1}, transparency is less than or equal to 44.869 cm. The mortality rate for red tilapia fingerlings is low.

Terminal node number 6 has NO_2-N is less than or equal to 1.275 mg L^{-1}, DO average is less than or equal to 7.475 mg L^{-1}, alkalinity less than or equal to 71.250 mg L^{-1}, transparency is greater than 33.766 cm, DO different is greater than 0.450 mg L^{-1}, alkalinity is greater than 61.250 mg L^{-1}, the month is greater than 1.5. The mortality rate for red tilapia fingerlings is low. Terminal node number 7 has NO_2-N is less than or equal to 1.275 mg L^{-1}, DO average is less than or equal to 7.475 mg L^{-1}, alkalinity is less than or equal to 71.250 mg L^{-1}, transparency is greater than 33.766 cm, DO different is greater than 0.450 mg L^{-1}, alkalinity is greater than 61.250 mg L^{-1}, the month is less than or equal to 1.5, NO_2-N is greater than 0.013 mg L^{-1}. The mortality rate for red tilapia fingerlings is high. Terminal node number 8 has NO_2-N is less than or equal to 1.275 mg L^{-1}, DO average is less than or equal to 7.475 mg L^{-1}, alkalinity is less than or equal to 71.250 mg L^{-1}, transparency is greater than 33.766 cm, DO different is greater than 0.450 mg L^{-1}, alkalinity is greater than 61.250 mg L^{-1}, the month is less than or equal to 1.5, NO_2-N is less than or equal to 0.013 mg L^{-1}, temperature average is greater than 22.750 ˚C, then mortality rate for red tilapia fingerlings is low.

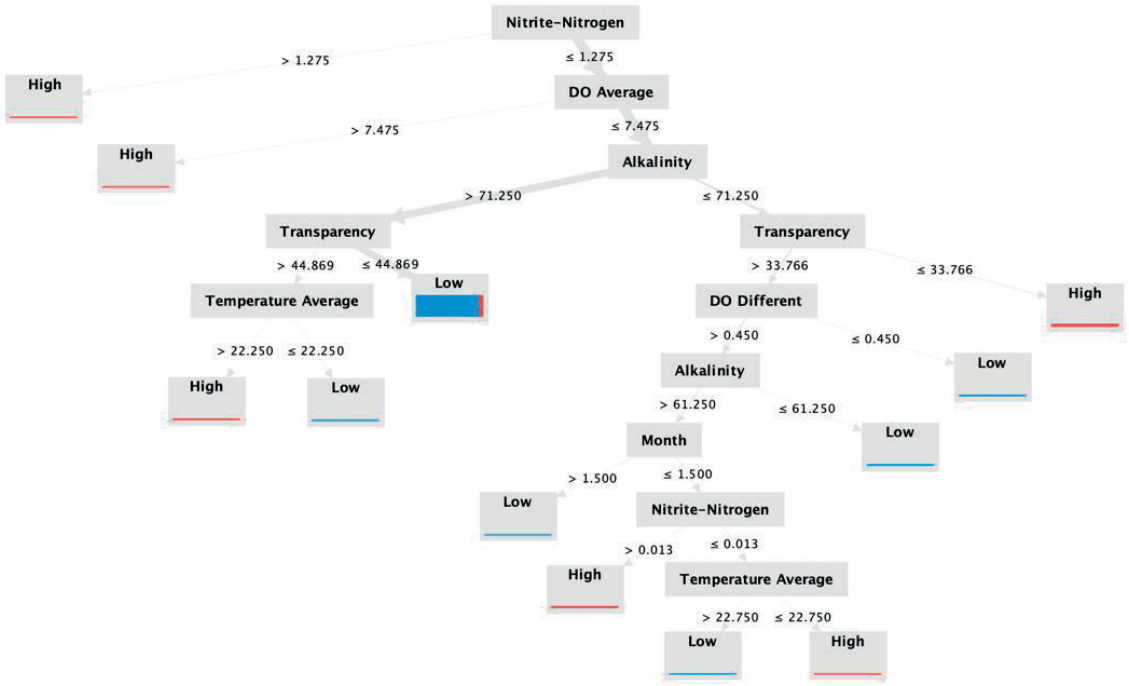

Figure 4. Decision tree of water quality management practice to reduce the mortality rate of red tilapia fingerlings raised in outdoor earthen ponds with a recirculating aquaculture system.

Terminal node number 9 has NO_2-N is less than or equal to 1.275 mg L^{-1}, DO average is less than or equal to 7.475 mg L^{-1}, alkalinity is less than or equal to 71.250 mg L^{-1}, transparency is greater than 33.766 cm, DO different is greater than 0.450 mg L^{-1}, alkalinity is greater than 61.250 mg L^{-1}, the month is less than or equal to 1.5, NO_2-N is less than or equal to 0.013 mg L^{-1}, temperature average is less than or equal to 22.750 ˚C, then mortality rate for red tilapia fingerlings is high. Terminal node number 10 has NO_2-N is less than or equal to 1.275 mg L^{-1}, DO average is less than or equal to 7.475 mg L^{-1}, alkalinity is less than or equal to 71.250 mg L^{-1}, transparency is greater than 33.766 cm, DO different is greater than 0.450 mg L^{-1}, alkalinity is less than or equal to 61.250 mg L^{-1}. The mortality rate for red tilapia fingerlings is low. Terminal node number 11 states that, If NO_2-N is less than or equal to 1.275 mg L^{-1}, DO average is less than or equal to 7.475 mg L^{-1}, alkalinity is less than or equal to 71.250 mg L^{-1}, transparency is greater than 33.766 cm, DO different is less than or equal to 0.450 mg L^{-1}. The mortality rate for red tilapia fingerlings is low. And terminal node 12 has NO_2-N is less than or equal to 1.275 mg L^{-1}, DO average is less than or equal to 7.475 mg L^{-1}, alkalinity is less than or equal to 71.250 mg L^{-1}, transparency is less than or equal to 33.766 cm. The mortality rate for red tilapia fingerlings is high.

The results of measurements of DO, pH, and temperature during the rearing of red tilapia were 3.60-7.85 mg L^{-1}, 5.15-7.60, and 18.5-27 ˚C with the average of DO, pH, and temperature being 5.77 ± 0.87 mg L^{-1}, 7.29 ± 0.22 and 22.6 ± 1.92 ˚C, respectively (Table 2). These results were classified as appropriate growth for the red tilapia fingerlings in outdoor earthen ponds with RAS. The optimal DO for rearing tilapia fingerlings ranges from 6-6.5 mg L^{-1} [26] or is not less than 3 mg L^{-1} [27]. Tilapia is also known to be resistant to very low DO. Most tilapia can tolerate DO in the range of 0.1-0.5 mg L^{-1} for various periods [28]. The optimal DO will produce the best fish performance, while low DO will limit respiration, growth, and metabolic activity in fish [28-29]. On the other hand, low DO can also cause fish fingerlings to be susceptible to disease [28, 30]. Stable pH values for rearing tilapia range from 7-8. In this range, fish do not need the energy to adapt [27, 31]. According to Boyd [32], a suitable pH value for fish growth ranges from 6.5-9. Although fish can survive at pH values of 4-6 and 9-10, the production is poor. And at a pH of less than 4 and more than 11, it can cause mortality in fish. The temperature range for normal development, reproduction, and growth of tilapia fingerlings are about 20-34 ˚C depending on the fish species [33-34] with an optimum range of about 25-30 ˚C [34-35]. Tilapia can also tolerate temperatures as low as 7.4-11 ˚C, but only for short periods [36]. Prolonged exposure to tilapia at this low temperature will certainly cause mass mortality. Feeding of tilapia was reduced sharply below 20 ˚C and they stopped feeding at about 16 ˚C, while severe mortality occurred at 12 ˚C [37].

The results of measurements of TAN and NO_2-N during the rearing of red tilapia fingerlings ranged from 0-3 mg L^{-1} and 0-1.4 mg $L^{-1,}$ with the average of TAN and NO_2-N being 1.10 ± 0.73 mg L^{-1} and 0.70 ± 0.43 mg L^{-1} , respectively (Table 2). These results were inappropriate for rearing red tilapia fingerlings in outdoor earthen ponds with RAS. TAN is a combination of two forms, Unionized ammonia (NH_3), which is toxic to fish, and ammonium ion (NH_4^+), which is non-toxic [30]. The optimal TAN for tilapia growth is less than 0.01 mg L^{-1} [28], or less than 0.5 mg L^{-1} [30, 38-39]. Research from Benli and Köksal [40] found that the median lethal concentration (48 h, LC_{50}) of unionized ammonia (NH_3) tilapia fingerlings exposed to varying levels of ammonia was 1.0 and 7.40 mg L^{-1}. When the fingerlings were exposed to ammonia concentrations, they showed increased movement, ventilation, convulsions, and spiral swimming. They also had excessive mucous secretion on the gills and body surface, bleeding on the gills, and darkening of the eyes and skin.

In this study, the most influential factor in the mortality of red tilapia fingerlings was NO_2-N. This is because red tilapia fingerlings can still tolerate the toxicity of TAN during rearing. After all, it has the appropriate DO and pH values. TAN toxicity will increase if DO decreases and the toxicity of TAN will decrease if pH decreases [41-42]. This concurs with Redner and Stickney (1979), who found that the 48 h LC_{50} for *Oreochromis aureus* was 2.46 mg L^{-1}. When the fish were acclimatized to the sublethal concentration of 0.43-0.53 mg L^{-1} for 35 days, they could withstand a concentration of 3.4 mg L^{-1} NH_3 without any mortality for 48 h [43]. In eutrophic fish ponds, the concentration of NH_3 fluctuates daily due to photosynthesis and respiration. In the morning, pH is minimum, and TAN is in the form of NH_4^+. Whereas in the afternoon, when the pH is maximum (around 9.0-9.5), the TAN balance shifts towards an increase in the amount of NH_3. Therefore, in the afternoon in eutrophic ponds, fish can experience temporary poisoning because an increased environmental pH increases the NH_3 component [42].

NO_2-N is a toxic nitrogen compound in freshwater fish commodities that can affect fish culture and effectiveness [44]. The concentration of NO_2-N in fish rearing should not exceed 0.5 mg L^{-1} [45]. The high concentration of NO_2-N during the treatment period was probably caused by excessive high protein feed, the use of nitrogen fertilizers, high stocking density, and the less-than-optimal performance of the biofilter in absorbing nitrogen compounds in the pond. Frequent aeration or the action of strong winds can also increase nitrite levels due to the increased mixing of nitrite produced by ponds in the oxygen-starved bottom mud. During bacterial nitrification, ammonia is first oxidized to nitrite by ammonia-oxidizing bacteria (*Nitrosomonas* spp. or *Nitrosospira* spp.) and then to less toxic nitrate via bacterial nitrite-oxidizing (*Nitrobacter* spp., *Nitrospira* spp.). Therefore, nitrite remains available in water as an intermediate in the bacterial oxidation of ammonia to nitrate, a product of fish nitrogen excretion. Thus, an imbalance in the nitrification process of bacteria can also increase nitrite concentration in water [46, 47].

When fish absorb NO_2-N, the mechanisms of nitrite toxicity include its competition with chloride (Cl^-) for uptake in the gill epithelium, increased levels of extracellular K^+ that affect skeletal muscle contraction and membrane potential, and impaired binding of oxygen to hemoglobin due to the oxidation of Fe^{2+} to Fe^{3+}, results in the production of methemoglobin (MetHb), and causes hypoxia due to a decrease in the oxygen-carrying capacity of the blood [28, 48]. Blood containing methemoglobin is brown, so nitrite poisoning in fish is often called brown blood disease [49]. A study by Atwood et al. [50] found that small tilapia (4.4 g) was more nitrite tolerant than large fish (90.7 g). The 96-hour NO_2-N LC_{50} was 81 and 8 mg L^{-1} in small and large fish, respectively. Adding a chloride source (500 mg L^{-1} $CaCl_2$ or NaCl) to culture water can protect small and large fish from nitrite toxicity. The protection achieved in chloride: nitrite ratio of 1.5:1 for culture water can protect tilapia from nitrite toxicity [50].

The alkalinity and transparency during the rearing of red tilapia were 60-110 mg L^{-1} and 15-45 cm, with the average of alkalinity and transparency being 79.19 ± 9.41 mg L^{-1} and 33.78 ± 8.22 cm, respectively (Table 2). These results were classified as appropriate for rearing red tilapia fingerlings in outdoor earthen ponds with RAS. Alkaline water generally has a relatively high pH and concentration of bicarbonate (HCO_3^-) and carbon dioxide (CO_2) [28]. FAO [27] reported that at an alkalinity range of 80-150 mg L^{-1}, it could maintain carbon dioxide levels in the waters even when it rains. On the other hand, alkalinity of more than 50 mg L^{-1} can increase the growth of tilapia fingerlings [51]. Lack of carbon dioxide in the water can cause mortality in phytoplankton, depleting the DO in the water. A sign of oxygen depletion and overall deterioration of pool water is the color of the water changing from green to light green to brown. This can lead to mass mortality in fish kept [27]. Transparency is closely related to light penetration and attenuation of underwater ecosystems [52]. It plays an important role in understanding variations in aquatic ecological environments, such as the photosynthesis of phytoplankton and their growth [53]. The ideal water transparency in fish rearing is between 30-40 cm [54], and low transparency can affect the visual impairment of fish [35].

4. Conclusions

The results of this study indicate that machine learning techniques with a decision tree algorithm can be applied in determining the best water quality management practice to reduce the mortality rate of red tilapia fingerlings. The decisions and actions of fish farmers in preventing water quality factors can cause the aquaculture system to experience mass mortality and increase the productivity of red tilapia fingerlings raised in outdoor earthen ponds with a recirculating aquaculture system.

5. Acknowledgments

The authors are grateful to the Graduate School and Faculty of Fisheries, Kasetsart University, for the financing of the study. The first author received a scholarship to obtain a master's degree. We also thank the Patthamarach Farm, Lam Plai Mat District, Buriram Province, Thailand, for providing research data.

Author Contributions: Conceptualization, P.A.S.M., W.T. and R.J.; methodology, P.A.S.M., W.T., R.Y. and R.J.; validation, P.A.S.M., W.T. and R.J.; writing—original draft preparation, P.A.S.M.; writing—review and editing, P.A.S.M., W.T., R.Y. and R.J. All authors have read and agreed to the published version of the manuscript. .

Funding: This research was funded by the Graduate School and Faculty of Fisheries, Kasetsart University.

Conflicts of Interest: The authors declare no conflicts of interest.

References

[1] Fang, W.; Huang, J.; Li, S.; Lu, J. Identification of pigment genes (melanin, carotenoid and pteridine) associated with skin color variant in red tilapia using transcriptome analysis. *Aquaculture*. 2022, *547*, 737429.

[2] Jongjaraunsuk, R.; Taparhudee, W. Weight estimation model for red tilapia (*Oreochromis niloticus* Linn.) from images. *Agriculture and Natural Resources*. 2022, *56(1)*, 215-224.

[3] FAO. *The State of World Fisheries and Aquaculture 2020*. FAO: Rome, Italy, 2020; 244.

[4] Brune, D.E.; Schwartz, G.; Eversole, A.G.; Collier, J.A.; Schwedler, T.E. Intensification of pond aquaculture and high rate photosynthetic systems. *Aquacultural Engineering*. 2003, *28(1-2)*, 65-86.

[5] Putra, I.; Effendi, I.; Lukistyowati, I.; Tang, U.M. Growth and survival rate of red tilapia (*Oreochromis* Sp.) cultivated in the brackish water tank under biofloc system. *Advances in Engineering Research*. 2019, *190*, 96-99.

[6] Azaza, M.S.; Dhraïef, M.N.; Kraïem, M.M. Effects of water temperature on growth and sex ratio of juvenile Nile tilapia *Oreochromis niloticus* (Linnaeus) reared in geothermal waters in Southern Tunisia. *Journal of Thermal Biology*. 2008, *33(2)*, 98-105.

[7] Ekasari, J.; Rivandi, D.R.; Firdausi, A.P.; Surawidjaja, E.H.; Zairin, M.; Bossier, P.; De Schryver, P. Biofloc technology positively affects Nile tilapia (*Oreochromis niloticus*) larvae performance. *Aquaculture*. 2015, *441*, 72-77.

[8] García-Ríos, L.; Miranda-Baeza, A.; Coelho-Emerenciano, M.G.; Huerta-Rábago, J.A.; Osuna-Amarillas, P. Biofloc technology (BFT) applied to tilapia fingerlings production using different carbon sources: Emphasis on commercial applications. *Aquaculture*. 2019, *502*, 26-31.

[9] Lekang, O.I. *Aquaculture Engineering*. Blackwell Publishing: United Kingdom, 2007; 354.

[10] Dalsgaard, J.; Lund, I.; Thorarinsdottir, R.; Drengstig, A.; Arvonen, K.; Pedersen, P.B. Farming different species in RAS in Nordic countries: Current status and future perspectives. *Aquacultural Engineering*. 2013, *53*, 2-13.

[11] Wambua, D.M.; Home, P.G.; Raude, J.M.; Ondimu, S. Environmental and energy requirements for different production biomass of Nile tilapia (*Oreochromis niloticus*) in recirculating aquaculture systems (RAS) in Kenya. *Aquaculture and Fisheries*. 2021, *6(6)*, 593-600.

[12] Delong, D.P.; Losordo, T.M.; Rakocy, J.E. *Tank Culture of Tilapia*. SRAC Publication, 2009; 8.

[13] Xiao, G.; Cheng, X.; Xie, J.; Zhu, D. Assessment of aeration plug-flow devices used with recirculating aquaculture systems on the growth of tilapia *Oreochromis niloticus. Aquacultural Engineering*. 2020, *91*, 102116.

[14] Srithong, C.; Musig, Y.; Areechon, N.; Taparhudee, W. Water quality and growth performance of hybrid catfish (*Clarias macrocephalus* x *C. gariepinus*) comparison in two type of water recirculating system and a water exchange system. *Kasetsart University Fisheries Research Bulletin*. 2015, *39(3)*, 57-69.

[15] Avnimelech, Y. *Biofloc Technology: A Practical Guide Book*, 3rd ed.; World Aquaculture Society: Baton Rouge, United States of America, 2014; 258.

[16] FAO. *The State of World Fisheries and Aquaculture*. FAO: Rome, Italy, 2018; 227.

[17] Zhao, S.; Zhang, S.; Liu, J.; Wang, H.; Zhu, J.; Li, D.; Zhao, R. Application of machine learning in intelligent fish aquaculture: A review. *Aquaculture*. 2021, *540*, 736724.

[18] Samuel Some studies in machine learning using the game of checker. *IBM Journal of Research and Development*. 2000, *44(1/2)*, 206-226.

[19] Liakos, K.G.; Busato, P.; Moshou, D.; Pearson, S.; Bochtis, D. Machine learning in agriculture: A review. *Sensors (Basel)*. 2018, *18(8)*, 2674.

[20] Azad, M.; Moshkov, M. Multi-stage optimization of decision and inhibitory trees for decision tables with many-valued decisions. *European Journal of Operational Research*. 2017, *263(3)*, 910-921.

[21] Khosravi, K.; Pham, B.T.; Chapi, K.; Shirzadi, A.; Shahabi, H.; Revhaug, I.; Prakash, I.; Tien Bui, D. A comparative assessment of decision trees algorithms for flash flood susceptibility modeling at Haraz watershed, Northern Iran. *Sci Total Environ*. 2018, *627*, 744-755.

[22] Ho, J.Y.; Afan, H.A.; El-Shafie, A.H.; Koting, S.B.; Mohd, N.S.; Jaafar, W.Z.B.; Lai Sai, H.; Malek, M.A.; Ahmed, A.N.; Mohtar, W.H.M.W.; Elshorbagy, A.; El-Shafie, A. Towards a time and cost effective approach to water quality index class prediction. *Journal of Hydrology*. 2019, *575*, 148-165.

[23] Everaert, G.; Bennetsen, E.; Goethals, P.L.M. An applicability index for reliable and applicable decision trees in water quality modelling. *Ecological Informatics*. 2016, *32*, 1-6.

[24] Kotu, V.; Deshpande, B. *Getting Started with RapidMiner*, 2nd ed., 2019; 15

[25] APHA. *Standard Methods*, 23rd ed.; American Public Health Association: Washington DC, United States of America, 2017; 545

[26] Abdel-Tawwab, M.; Hagras, A.E.; Elbaghdady, H.A.M.; Monier, M.N. Dissolved oxygen level and stocking density effects on growth, feed utilization, physiology, and innate immunity of nile tilapia, *Oreochromis niloticus. Journal of Applied Aquaculture*. 2014, *26(4)*, 340-355.

[27] FAO. *Handbook on Enhancing the Entrepreneurial Capability of Farmers*. FAO: Bangkok, Thailand, 2021; 72.

[28] El-Sayed, A.F.M. Environmental requirements. In *Tilapia Culture*, Academic Press: Alexandria, Egypt, 2020, 47-67.

[29] Tsadik. G, G.; Kutty. M, N. Influence of ambient oxygen on feeding and growth of the tilapia, *Oreochromis niloticus* (Linnaeus). *African Regional Aquaculture Centre*. 1987, 13.

[30] Li, D.; Liu, S. Water quality monitoring in aquaculture. In *Water Quality Monitoring and Management*, Academic Press: India, 2019, 303-328.

[31] El-Sherif, M.S.; El-Feky, A.M.I. Performance of nile tilapia (*Oreochromis niloticus*) fingerlings. I. Effect of pH. *International Journal of Agriculture and Biology*. 2009, *11*, 297-300.

[32] Boyd, C.E.; Pillai, V.K. *Water Quality Management for Pond Fish Culture*, 22nd ed.; CMFRI Special Publication: Alabama, United States, 1984; 96.

[33] El-Sherif, M.S.; El-Feky, A.M.I. Performance of nile tilapia (*Oreochromis niloticus*) fingerlings. II. Influence of different water temperatures. *International Journal of Agriculture and Biology*. 2009, *11*, 301-305.

[34] Xie, S.; Zheng, K.; Chen, J.; Zhang, Z.; Zhu, X.; Yang, Y. Effect of water temperature on energy budget of Nile tilapia, *Oreochromis niloticus. Aquaculture Nutrition*. 2011, *17(3)*, e683-e690.

[35] El-Sayed, A.-F.M.; Kawanna, M. Optimum water temperature boosts the growth performance of Nile tilapia (*Oreochromis niloticus*) fry reared in a recycling system. *Aquaculture Research*. 2008, *39(6)*, 670-672.

[36] Sifa, L.; Chenhong, L.; Dey, M.; Gagalac, F.; Dunham, R. Cold tolerance of three strains of nile tilapia, *Oreochromis niloticus*, in China. *Aquaculture*. 2002, *213(1-4)*, 123-129.

[37] Balarin, J.D.; Haller, R.D. The intensive culture of tilapia in tanks, raceways and cages. In *Recent Advances in Aquaculture*, Croom Helm: London, United Kingdom, 1982, 266-355.

[38] Hargreaves, J.A.; Tucker, C.S. *Managing Ammonia in Fish Ponds*. SRAC Publication: United States of America, 2004; 8.

[39] Jongjaraunsuk, R.; Is-haak, J.; Taparhudee, W. Feeding rate of red tilapia (*Oreochromis niloticus mossambicus*) and correlation between feed intake and water quality. *RMUTSB Academic Journal*. 2019, *7*, 166-180.

[40] Benli, A.Ç.K.; Köksal, G. The acute toxicity of ammonia on tilapia (*Oreochromis niloticus* L.) larvae and fingerlings. *Turkish Journal of Veterinary and Animal Sciences*. 2005, *29(2)*, 339-344.

[41] Chervinski, J. *The Biology and Culture of Tilapias : Environmental physiology of tilapias*. in *ICLARM Conference Proceedings*. 1982. Manila, Philippines: ICLARM.

[42] Hargreaves, J.A.; Kucuk, S. Effects of diel un-ionized ammonia fluctuation on juvenile hybrid striped bass, channel catfish, and blue tilapia. *Aquaculture*. 2001, *195(1-2)*, 163-181.

[43] Redner, B.D.; Stickney, R.R. Acclimation to Ammonia by Tilapia aurea. *Transactions of the American Fisheries Society*. 1979, *108(4)*, 383-388.

[44] Sikora, M.; Nowosad, J.; Kucharczyk, D. Nitrogen compound oxidation rate in recirculation systems using three biological filter medias in rearing common carp (*Cyprinus carpio* L.) juveniles. *Aquaculture*. 2022, *547*, 737532.

[45] Ebeling, J.; Jensen, G.; Losordo, T.; Masser, M.; McMullen, J.; Pfeiffer, L.; Rakocy, J. *Model Aquaculture Recirculation System (MARS)*. National Council for Agricultural Education: Lowa State University, United States, 1995; 51.

[46] Deane, E.E.; Woo, N.Y. Impact of nitrite exposure on endocrine, osmoregulatory and cytoprotective functions in the marine teleost *Sparus sarba. Aquat Toxicol*. 2007, *82(2)*, 85-93.

[47] Ciji, A.; Akhtar, M.S. Nitrite implications and its management strategies in aquaculture: A review. *Reviews in Aquaculture*. 2019, *12(2)*, 878-908.

[48] Jensen, F.B. Nitrite disrupts multiple physiological functions in aquatic animals. *Comparative Biochemistry and Physiology Part A: Molecular & Integrative Physiology*. 2003, *135(1)*, 9-24.

[49] Boyd, C.E.; Tucker, C.S. *Pond Aquaculture Water Quality Management*, 1 ed.; Kluwer Academic Publisher: Boston, 1998; 634.

[50] Atwood, H.L.; Fontenot, Q.C.; Tomasso, J.R.; Isely, J.J. Toxicity of nitrite to nile tilapia: Effect of fish size and environmental chloride. *North American Journal of Aquaculture*. 2001, *63(1)*, 49-51.

[51] Cavalcante, D.D.H.; Poliato, A.D.S.; Ribeiro, D.C.; Magalhães, F.B.; Carmo-e-Sá, M.V. Effects of CaCO3 liming on water quality and growth performance of fingerlings of nile tilapia, *Oreochromis niloticus*. *Acta Scientiarum. Animal Sciences*. 2009, *31(3)*, 327-333.

[52] Feng, L.; Hou, X.; Zheng, Y. Monitoring and understanding the water transparency changes of fifty large lakes on the Yangtze Plain based on long-term MODIS observations. *Remote Sensing of Environment*. 2019, *221*, 675-686.

[53] Bai, S.; Gao, J.; Sun, D.; Tian, M. Monitoring water transparency in shallow and eutrophic lake waters based on GOCI observations. *Remote Sensing*. 2020, *12(1)*, 163.

[54] Ghosh, S.; Sarita; Senthamilan, S.; Chatterjee, S. Optimum condition of water for aquaculture. *Agriallis*. 2019, *1(4)*, 18-22.

JSTR
ASEAN Journal of Scientific and Technological Reports

Research article

An Experimental Set for Studying the Changing State of Matter with Smart Learning Media Displayed Through the IoT System for Smart-Lab

Jiraporn Chomanee[1], Nisagorn Nakarang[2], Sek Handee[3], Patchara Choksuriwong[4], Supagorn Katathikarnkul[5], and Tanchanok Poonsin[6*]

[1] Department of Basic Science and Mathematics, Faculty of Science, Thaksin University, Songkhla, 90000, Thailand; jiraporn.ch@tsu.ac.th
[2] Chemistry Program, Faculty of Education, Thaksin University, Songkhla, 90000, Thailand;
[3] Chemistry Program, Faculty of Education, Thaksin University, Songkhla, 90000, Thailand;
[4] Chemistry Program, Faculty of Education, Thaksin University, Songkhla, 90000, Thailand; Pang.nisakorn13@gmail.com
[5] Department of Basic Science and Mathematics, Faculty of Science, Thaksin University, Songkhla, 90000, Thailand
[6] Department of Teaching Science and Mathematics, Faculty of Education, Thaksin University, Songkla, 90000, Thailand; tanchanok.p@tsu.ac.th
* Correspondence: tanchanok.p@tsu.ac.th

Citation:
Chomanee, J.; Nakarang, N.; Handee, S.; Choksuriwong, P.; Katathikarnkul, S.; Poonsin, T. An Experimental Set for Studying the Changing State of Matter with Smart Leaning Media Displayed Through the IoT System for Samart-Lab. *ASEAN J. Sci. Tech. Report.* **2022**, *25*(4), 42-49. https://doi.org/10.55164/ajstr.v25i4.247317.

Article history:
Received: September 1, 2022
Revised: November 12, 2022
Accepted: November 14, 2022
Available online: November 20, 2022

Abstract: The purposes of this research were to develop and find the quality of the experimental set for studying the changing state of matter with smart learning media displayed through the IoT system. The data collection tools used in this research were 1) the accuracy percentage, 2) a suitability assessment form 3) a learning achievement test in "changing state of matter" and 4) satisfaction questionnaires. The statistics for analyzing the collected data were mean ($\bar{X}$), percentage, standard deviation (S.D.), and t-test dependent. The result showed that the Digital Thermo Sensor had 98.5% accuracy in 30℃ -100℃ compared with the standard thermometer. The experimental set was used to determine the melting points of pure substances, Naphthalene, Biphenyl, and water's boiling point. The result found that the accuracy of melting point of Naphthalene and Biphenyl and the boiling point of water was 99.87, 99.75, and 99.99, respectively. The quality of the experimental set was also studied. Three experts evaluated the developed experiment set at a very good level. The experimental set successfully developed students' understanding of a change of state concept. About 80% of students scored above the prescribed criterion of 70% of the total score. After learning, the scores of the students were higher than those before learning at a confidence level of 0.01. 30 grade-10 students evaluated the satisfaction evaluation at an excellent level. Therefore, the experimental set developed suitable for student learning in the topic of change of state effectively.

Keywords: Thermal analysis; Changing state of matter; Smart lab

1. Introduction

Chemistry phenomena are explained in terms of atoms and molecules. It is critical for chemistry students to correctly understand and apply the

concepts of the particulate nature of matter (PNM). Nevertheless, changing the state of matter is one of the most challenging topics due to the abstract nature of atoms and molecules, which requires students' ability to logically operate on information and symbols beyond personal experience and concrete cases in the real world [1,2]. Students have difficulty learning chemistry at the particulate level, like atoms and molecules that cannot be observed or experienced directly. In particular, many of these students have misconceptions about the structures and behaviors of submicroscopic particles due to the obstacle of building appropriate mental models [3]. To help students comprehend the change of state concepts, chemistry educators have developed various visual representations and are trying to bridge concrete phenomena and abstract concepts. An experimental set and learning media can visually represent particulate structures and processes that may help students build mental models or imaginations [4].

Science experiments often rely on sensors to collect data. Digital sensors allow people to gather a large quantity of raw data. Traditionally, these data are kept as original records to support scientific claims. In many cases, the data are used only by the experimenters themselves and may be forgotten or discarded after some time [5]. Technological advancements inspired our Internet of Things (IoT) research. The Internet of Things (IoT) is a system of interrelated computing devices, mechanical and digital machines, objects, animals, or people that are provided with unique identifiers and the ability to transfer data over a network without requiring human-to-human or human-to-computer interaction [6]. The Internet of Things is vital in the Fourth Industrial Revolution, or Industry 4.0 [7]. Likewise, they can also be used to transform school labs. Their applications have been demonstrated in engineering education [8] but seem underexplored in chemistry education. This study aimed to introduce a low-cost instrument developed by Arduino board with Digital Thermo Sensor illustrating smartphone results via the Blynk application through the Internet of Things. This research develops an experimental set based on Arduino and its technology to help students learn the change of state concepts and improve their chemistry comprehension.

2. Materials and Methods

2.1 NodeMCU V3 ESP8266

NodeMCU V3 ESP8266 is a microcontroller based on an ESP8266 Arduino board connected to a wifi signal. The main parts are nine digital input/output pins, one analog input pin, a USB connection, the power jack, and a reset button. The NodeMCU V3 ESP8266 can be programmed with the Arduino Software (IDE) and powered by an AC to DC adapter (or battery) to start [9]. NodeMCU V3 ESP8266 in this research is shown in Figure 1A.

2.2 DS18B20 temperature sensor

DS18B20 is a digital temperature sensor providing -55 °C to 125 °C measurable temperature ranges. It is one of the most popular temperature sensors on the market. It can be used as the temperature monitor tool in a smart farm, house, water station, etc. It is similar to DHT11/DHT22 temperature and humidity sensor. The DS18B20 temperature sensor has many formats, including IC and waterproof sensors. This study uses the NodeMCU ESP8266 board, reads data from a sensor, and displays results on a serial monitor [5]. Figure 1B shows the temperature sensor developed in this research.

2.3 Blynk application

Blynk is a free platform with iOS and Android applications to control Arduino. It is easy to program, use in real-time, and connect with Arduino, ESP8266, ESP32, NodeMCU, Rasberry pi [5].

2.4 The changing state of matter

Detecting a changing state of matter is not always straightforward as seeing a kettle boil, so special techniques have been developed. One technique is Thermal analysis, which takes advantage of the effect of the enthalpy change during a changing state of matter. This work studied the changing state of matter such as Naphthalene and Biphenyl. The change of state was examined by incubating Naphthalene and Biphenyl over its melting point. Then, a sample was allowed to cool, and its temperature was monitored. The heat evolved at a changing state of matter, and the cooling stopped until the transition was complete. The cooling curve

along the isobar (1 atm). The transition temperature was obvious and was used to mark as freezing point ($liquid \rightarrow solid$). The diagram of an experimental set and the experimental set are depicted in Figure 2 and Figure 3, respectively. The thermal analysis graph for changing state of matter with smart learning media displayed through the IoT system display with the Blynk application on a smart device is shown in Figure 4

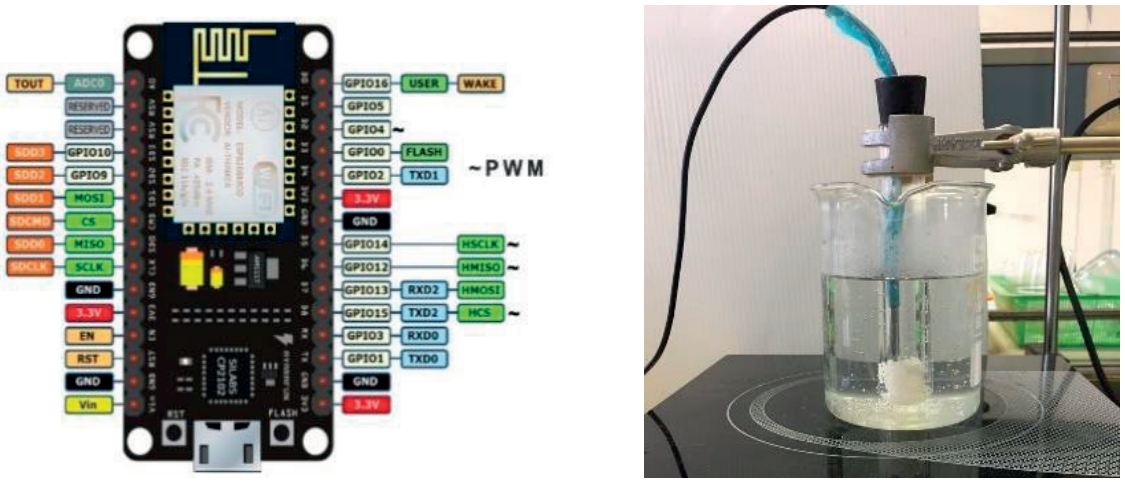

(A) (B)

Figure 1. (A) diagram of NodeMCU V3 ESP8266, (B) temperature sensor used in this study

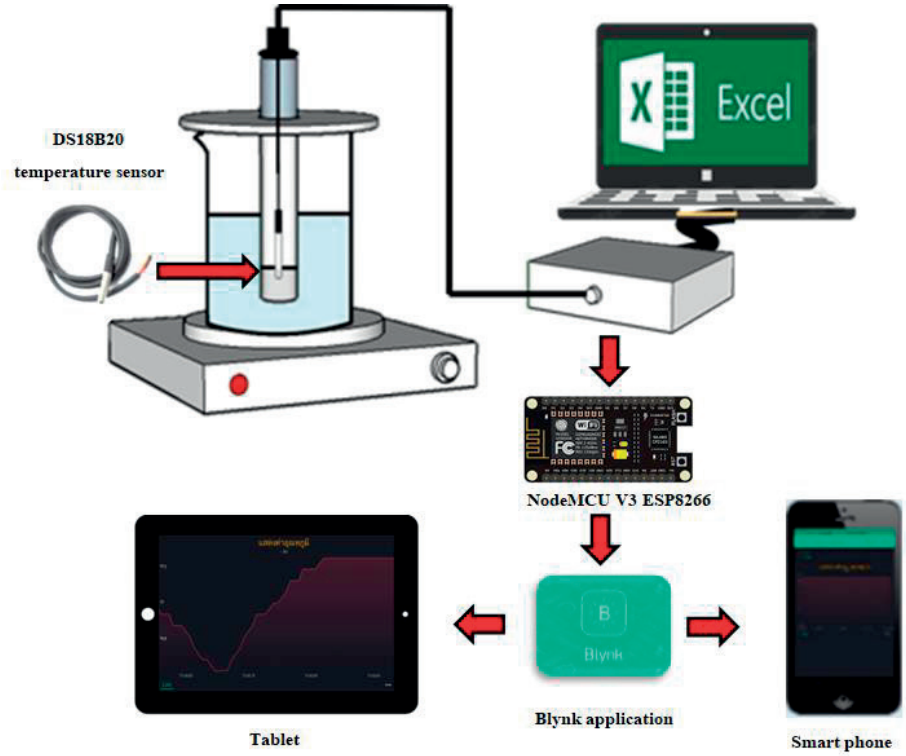

Figure 2. Diagram of an experimental set

Figure 3. An experimental set for studying the changing state of matter with smart learning media displayed through the IoT system for smart-lab

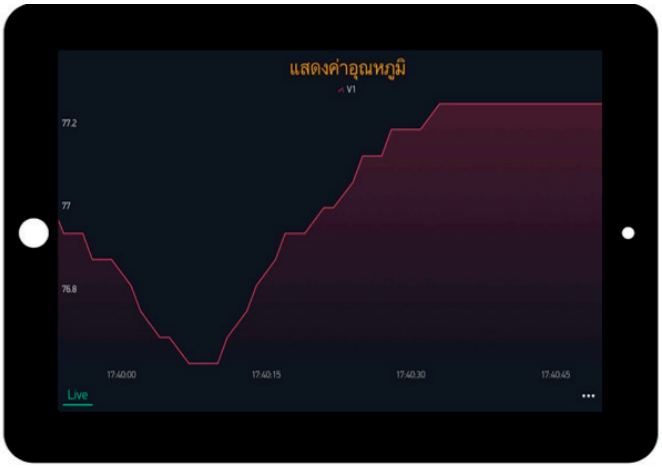

Figure 4. Thermal analysis graph for changing state of matter with smart learning media displayed through the IoT system displayed with the Blynk application on a smart device

2.5 The efficiency of an experimental set

To ensure that the experimental set is suitable, we invited the experts, who are university professors in chemistry, to measure the quality of the experimental set by using questionnaires. We modified the experimental set based on their suggestions. Finally, the experimental set was administered to students. Then, the learning achievement of students and satisfaction were also evaluated.

2.6 Research participant

The research participants included 30 science students in grade 10 in the second semester of the 2021 academic year. Three science educators checked the pre- and post-test in change of state concept and ensured content validity and understandability of questions. A T-test was used for paired comparison [10]. Statistical analysis was performed using the Statistical Package for Social Science.

3. Results and Discussion

The results of this research are presented in the following sections.

3.1 The accuracy of Digital Thermo Sensor (DTS) detection

The accuracy of DTS detection was studied. The increasing rate of water temperature was detected at room temperature (30℃) until boiling water (100℃). They measured the temperature of 200 mL water in a breaker at room temperature (30 ℃) initial temperature and increased the temperature to 100 ℃. The temperature was recorded every 10 seconds until it reached 100°C. The accuracy of DTS compared with a standard thermometer is shown in Figure 5. The accuracy percentage of DTS was calculated. It was defined as:

$$\% \text{ error} = \left|\frac{X_{mea} - X_i}{X_i}\right| \times 100$$

$$\% \text{ accuracy} = 100 - \% \text{ error}$$

where X_{mea} is the measured value by DTS and X_i is the true value of a standard thermometer. The result found that DTS had 98.5% accuracy in 30℃ -100℃.

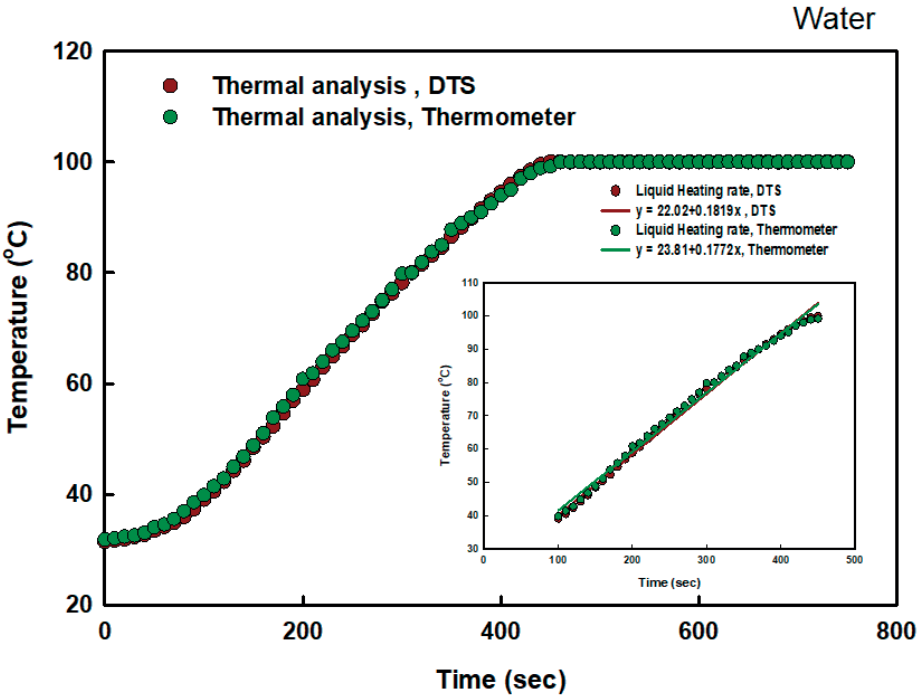

Figure 5. The accuracy of DTS compared with a standard thermometer for 200 mL water measured at 30℃ initial temperature and 100℃

3.2 Determination of changing state of matter by using an experimental set

Changing states of matter such as Naphthalene, Biphenyl, and water were determined using an experimental set. The result revealed that the boiling point of water and melting point of Naphthalene and Biphenyl was 100.01, 80.05, and 69.03, respectively.

The thermal analysis behavior of pure Naphthalene is shown in Figure 6. A continuous decrease in temperature was observed when Naphthalene was cooled up to 1000 sec (liquid cooling period). In this stage, the liquid of Naphthalene releases heat into the environment. The temperature decreased as the entropy of the Naphthalene molecules decreased. Then, the temperature remained steady at 80℃. At this stage, the liquid was converted into a solid state. The freezing of Naphthalene began at 1000 sec (80℃), and the freezing was complete at 1300 sec (80 ℃). Therefore, the local solidification time was 1000-1300 sec. After that, the temperature decreased due to the thermal exchange between Naphthalene in solid form and the surroundings (solid cooling period).

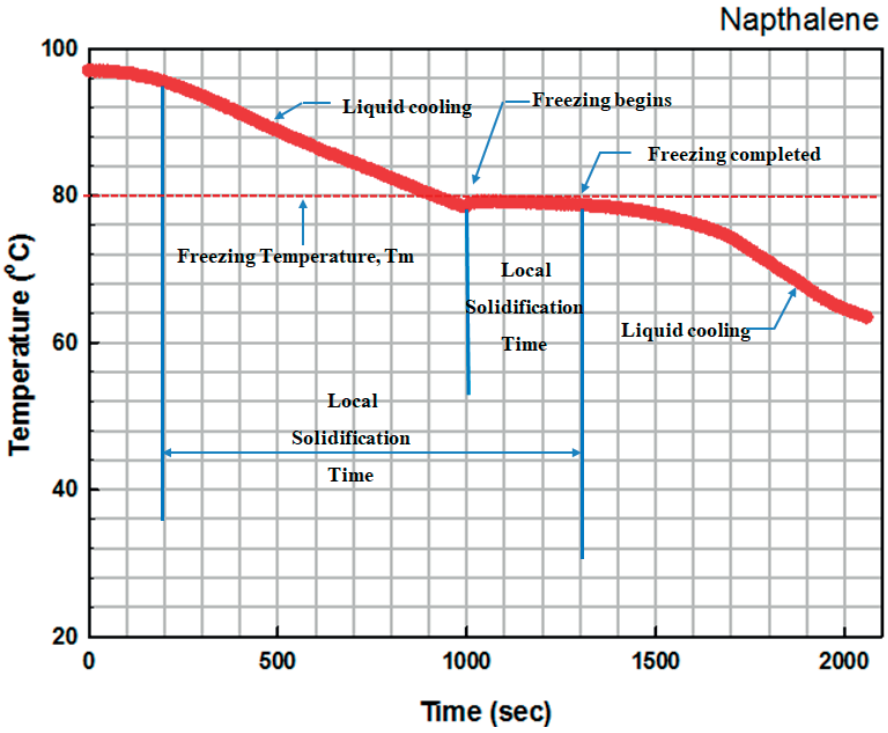

Figure 6. The cooling curve for pure Naphthalene

Table 1 shows the accuracy of the melting point and boiling point of substances by using an experimental set compared with the theory value. The result found 99.87%, 99.75%, and 99.99% accuracy for the experimental set.

Table 1. Comparison of melting and boiling point of substance by using an experimental set compared with theory value

Substance	Melting point from experimental set (°C)*	Boiling point from experimental set (°C)*	Melting point/boiling point from theory (°C)	Accuracy percentage (%)
Naphthalene	80.50 ± 0.06	-	80.60	99.87
Biphenyl	69.03 ± 0.04	-	69.20	99.75
Water	-	100.01 ± 0.01	100	99.99

The melting and boiling point of substances was measured using the experimental set at standard atmospheric pressure (1 atm)
The melting and boiling point of substances from theory was measured at standard atmospheric pressure (1 atm)
*Value are mean ± standard deviation (n=3)

3.3 The efficiency of an experimental set

The experimental set for studying the changing state of matter with smart learning media displayed through the IoT system for the smart lab was evaluated quality by using a suitability assessment form for 3 experts who are chemistry instructors in Thai Universities with more than ten years of experience in teaching and doing research in chemistry. The result revealed that the use of the experiment set for studying the changing state of matter with smart learning media displayed through the smart lab IoT system had a very good quality.

To examine the pre- and post-test in a change of state concept results of the students using an experimental set, a dependent Sample t-test (Paired Samples t-test) was conducted. The mean scores, standard deviations, and t-tests are presented in Table 2.

Table 2. Mean scores and standard deviations of the pre- and post-test in a change of state concept of 30 students

Pre-test					**Post-test**						
Number of students					Number of students						
N	n	n/N (%)	Mean	S.D.	N	n	n/N (%)	Mean	S.D.	t	Sig
30	0	0	3.57	1.591	30	23	77	7.33	1.446	-7.571	.000

N = The number of students who scored above the prescribed criterion of 70%. N = The number of participants.

The criterion of 70% of the full score 10 points, 7 points, was used for passing the test. It was shown that everyone had a pre-test score lower than 7 points. No one passed the pre-test in a change of state concept (n=0). The mean pre-test score of 30 research students was 3.57 (out of 10), which indicated that students had little knowledge and understanding of changing state of matter. After experiencing the new learning via an experimental set for studying the changing state of matter with smart learning media displayed through the IoT system for a smart lab, students achieved much higher scores, around two times higher. Besides, 23 out of 30 students (77%) passed the prescribed criterion, getting scores higher than 70%. The post-test scores were statistically significantly higher than the pre-test scores at the significant level of 0.01, as seen in Table 3. Therefore, an experimental set for studying the changing state of matter with smart learning media displayed through the IoT system for smart lab positively impacts students' understanding of the change of state topic. It can be used as an alternative teaching strategy in school.

3.4 The results from the satisfaction questionnaire

We evaluated students' satisfaction with the learning modules using the satisfaction questionnaire. The questionnaire was composed of 5 items with 5 levels of the Likert scale. The Likert scales were divided as 1 (very poor), 2 (poor), 3 (average), 4 (good), and 5 (excellent). Students were free to select a scale for an item. Students took around 5-10 minutes to fill out this document after finishing the class. The items of the satisfaction questionnaire were analyzed to find what students thought about our learning modules, as shown in Table 3.

Table 3. The satisfaction of students with the learning modules

Items	$\bar{X}$	**S.D.**	**Level**
1. Time	4.61	0.57	excellent
2. Atmosphere	4.45	0.59	good
3. Useful in learning	4.53	0.61	excellent
4. Benefit in learning	4.50	0.60	excellent
Total	4.52	0.59	excellent

The result exposed that students were satisfied with this experimental set at an excellent level because it shows accurate values and is easy to connect via wifi internet to the other components. In addition, most students preferred the demonstrations of the experimental set and agreed that the experimental set helped them to learn the change of state concept**.**

4. Conclusions

An experimental set for studying the changing state of matter with smart learning media displayed through the IoT system for the smart lab was developed in this study to work well in finding the changing

state of Naphthalene, Biphenyl, and water. The IoT technology in the experimental set has provided intuitive user interfaces for remotely accessing science laboratories during the COVID-19 pandemic, resulting in improved student engagement and learning in online environments. Furthermore, the advantages of the experimental set are low cost, high accuracy, and ease of linking via wifi to free platforms with iOS and Android applications or other devices. After the instruction, students' learning and satisfaction were evaluated. The finding revealed that the instruction using a learning module, in particular, change of state, facilitated students' learning to a higher level. Most students agree that this learning module helps them to learn about the change of state concept. This study suggests that an experimental set for studying the changing state of matter with smart learning media displayed through the IoT system for smart-lab improves student learning and enjoyment of chemistry, especially the change of state topic

5. Acknowledgements

The success of this study was due to the support and cooperation of many people and organizations. The authors thank all participants. Thaksin university was also acknowledged.

Author Contributions: Conceptualization, T.P. and J.C.; designed the experiments, T.P., J.C. and S.K.; performed the experiments, N.N. and S.H.; analysis and investigation, N.N., S.H., T.P. and J.C.; writing-review and editing, T.P. and J.C.

Funding: This research received no external funding

Conflicts of Interest: The authors declare no conflict of interest

References

[1] Pinarbasi, T.; Canpolat, N. Students' understanding of solution chemistry concepts. *J Chem Educ* 2003, *80*(11), 1328-1332.

[2] Cole, R.S.; Todd, J.B. Effect of web-based multimedia homework with immediate rich feedback on student learning in general chemistry. *J Chem Educ* 2003, *80*(11), 1338-1343.

[3] Gabel, D.L. Use of the Particle nature of matter in developing conceptual understanding. *J Chem Educ* 1993, *70*(3), 193-194. 1993

[4] Tang, H.; Abraham, A.R. Effect of computer simulations at the particulate and macroscopic levels on students' understanding of the particulate nature of matter. *J Chem Educ* 2016, *93*, 31-38.

[5] Xie, C.; Li, C.; Ding, X.; Jiang, R; Sung, S. Chemistry on the cloud: From wet labs to web labs. *J Chem Educ* 2021, *98*, 2840-2847.

[6] Chomanee, J.; Wuttisamai, P.; Puntong, P.; Suakaew, P.; Katathikarnkul, S. Development of an apparatus for educational heat of reaction in chemical laboratory with digital thermal sensor and IoT on smartphone. *TSU J* 2020, *23*(3), 70-78.

[7] Tao, F.; Zhang, H.; Liu, A.; Nee, A.Y.C. Digital twin in industry: State-of-the-art. *IEEE Trans Industr Inform* 2019, *15*(4), 2405-2415.

[8] Sepasgozar, S.M.E. Digital twin and web-based virtual gaming technologies for online education: A Case of construction management and engineering. *Appl Sci* 2020, *10*(13), 4678.

[9] Chanthamanee, P.; Jinda, P.; Prasitpong, S. Newton's law of cooling experiment set using Arduino temperature sensor. *J Phy: Conf Ser* 2022

[10] Steel, R.G.D.; Torrie, J.H. Principles and procedures of statistics: A biometrical approach; McGraw-Hill, New York, 1980.

JSTR
ASEAN Journal of Scientific and Technological Reports

Research article

The Effect of *Acacia mangium* Leaf Feed on Apparent Metabolizable Energy, Growth Performance, and Carcass Composition of Broiler Chickens

Saichon Lerdsuwan[1*], Warrapong Nalinanon[2], Duangjai Pisuttharachai[3]

[1] Animal Science, Disciplines of Technology Agriculture, King Mongkut's Institute of Technology Ladkrabang, Prince of Chumphon Campus, Chumphon, 86160, Thailand; e-mail: saichon.le@kmitl.ac.th.

[2] Fishery Science and Aquatic Resources, Disciplines of Technology Agriculture, King Mongkut's Institute of Technology Ladkrabang, Prince of Chumphon Campus, Chumphon, 86160, Thailand; e-mail: warrapong.na@kmitl.ac.th

[3] Fishery Science and Aquatic Resources, Disciplines of Technology Agriculture, King Mongkut's Institute of Technology Ladkrabang, Prince of Chumphon Campus, Chumphon, 86160, Thailand; e-mail: duangjai.pi@kmitl.ac.th

* Correspondence: saichon.le@kmitl.ac.th.

Abstract: The experiments were conducted to determine the apparent metabolizable energy of *Acacia mangium* leaf meal (AMLM) and the effect on growth performance and carcass composition of broiler chickens (*Arbor acres*). Twenty-four broiler chickens at the age of 24 days were divided into 2 groups with four replications of two chickens raised individually in a cage. The apparent metabolizable energy of AMLM-feeding chicken was 2,359.90 kcal/kg. Experimental diets consisted of AMLM 0%, 2.5%, 5%, 7.5%, and 10% feeding for 161 one-day-old unsexed broiler chickens and were randomly assigned to five groups with four replications of eight chickens in a completely randomized design. Feed and water were offered *ad-libitum* throughout the experimental period. At the age of 45 days, 2 broilers per replicate were slaughtered, and the carcass was determined. The results indicated that broiler chickens fed AMLM diets were not significantly different in weight gain, average daily gain and feed intake compared to the control diet ($P>0.05$). But chickens fed AMLM had decreased feed conversion ratio than the control ($P<0.05$). In addition, broiler chickens fed AMLM diets were not significantly different in all carcass composition parameters compared to the control diet ($P>0.05$). It is concluded that the AMLM contained 10% in diets does not affect broiler chickens' growth performance and carcass composition.

Keywords: *Acacia mangium* leaf meal, Metabolizable energy, Growth performance, Carcass composition, Broiler chicken.

Citation:
Lerdsuwan, S.; Nalinanon, W.; Pisuttharachai, D. The Effect of *Acacia mangium* Leaf Feed on Apparent Metabolizable Energy, Growth Performance, and Carcass Composition of Broiler Chickens . *ASEAN J. Sci. Tech. Report.* **2022**, *25*(4), 50-58. https://doi.org/10.55164/ajstr.v25i4.247587

Article history:
Received: October 19, 2022
Revised: November 28, 2022
Accepted: December 1, 2022
Available online: December 22,2022

1. Introduction

The global poultry sector is characterized by faster growth in consumption and trade than any other major agricultural sector. In 2020 poultry meat production was 132 million tonnes, growing from 2020 to about 3 million tonnes [1].

Poultry feedstuffs are expensive, limiting the growth of poultry production in tropical areas. The cost of feeding has been put at 60-80% of

poultry production. There is a constant need to look for locally available and cheaper feed ingredients that do not attract competition between humans and livestock.

The largest area of plantation of *Acacia mangium* (AM) is in South East Asia, where planting covers about 2 Mha [2]. In the 2000s, Malaysia and Indonesia had nearly 850,000 ha of commercial plantations of AM [3]. In Thailand, commercial plantations of AM had about 1,000,000 Rai [4]. As an exotic and fast-growing tree, AM can be used in a wide range, such as furniture, sawn wood, pulp, and paper [5]. Logging operations in plantation forests usually generate abundant waste, such as residual wood, branches/twigs, leaves, and bark. The waste accounts for more than 60% of the total biomass [6]. The AMLM contained 14% crude protein, 2.15% crude fat, 39.81% NFE, and 26.4% crude fiber [7], which could be used as feed alternatives in commercial livestock. The fresh *Acacia mangium* leaf can be used for ruminant animals [8-9]. However, there is a lack of direct information on the usefulness of AMLM in poultry diets. Other results were obtained the *Leucaena leucocephala* leaf meal (25% crude fiber) could be an acceptable use of resources up to 10% in laying hen diets [10]. Therefore, the objective of this study was to determine the effect of *AMLM* on metabolizable energy, growth performance, and carcass quality of broiler chickens.

2. Materials and Methods

2.1 Study chemical composition and metabolizable energy

2.1.1. Chemical composition

Fresh acacia mangium leaves (AML) were harvested from 2-4-year-old *acacia mangium* tree stands in the KMITL PCC forest in Chumphon province, Thailand. The leaves were cut and spread out on a clean concrete floor of a well-ventilated room for 3-4 days until they became crispy [11]. Dried AML were grinding through a 3-horse-power locally built hammermill (Thais, Thailand) equipped with a 2 mm screen. Sample AMLM were taken and analyzed for proximate analysis [12], tannin [13], and gross energy [12] according to analytical methods for oxygen bombs.

2.1.2 Metabolizable energy

Twenty-four broiler chickens (*Arbor acres*), 24 days of age, were used to test the metabolizable energy value of AMLM. The chickens (1 female and one male) were assigned to 45 x 30 x 35 cm individual cages and allotted to 2 groups with 6 replicates. Dextrose and soybean meal was used as a basal diet to calculate the metabolizable energy, which was determined using the substitution method according to Hill and Anderson [14]. Dextrose in the basal diet was replaced by 30% AMLM to make up experimental diets (Table 1). After 7 days adaptation period, 7 day collection period was started by adding 1% chromium oxide to the experimental diet as an initial marker. As a finishing marker, 1% chromium oxide was added to each experimental diet on the 8th day of collection. A collection of excreta (mixed fecal and urine) was started when the chromium oxide appeared in the excreta and kept until the appearance of chromium oxide in the excreta. Every day, the excreta samples were dried in a drying oven at 60 °C for 72 h. Finally, the total excreta was grounded to 1 mm in the blender mill grinder. Diet and excreta samples were analyzed for chemical analysis, protein [12], and gross energy (Oxygen bomb calorimeter, Parr model 6050) to determine the metabolizable energy (ME). The ME content of AMLM was calculated according to the equation developed by Hill and Anderson [14] as follows:
ME per gm diet = Energy per gm diet – (excreta energy per gm diet + 8.22 x gm N retained per gm diet)
To compute the ME of material substituted for glucose, the following equation applies:

$$\text{ME per gm substitute} = 3.64 - \left[\frac{\text{ME per gm referent diet} - \text{ME per gm diet with substitute}}{\text{Proportion of substitute}}\right]$$

(3.64 = experimentally established ME per gm of glucose dry matter)

Table 1. Ingredient composition of experimental diets

Ingredients (%) as fed basis	Reference diet	Test diet
Dextrose	45.81	15.81
Soybean meal (48% CP)	53.00	53.00
AMLM	-	30.00
DCP (P 18)	0.50	0.50
Salt	0.19	0.19
Vitamins & trace minerals [1/]	0.50	0.50
total	100.00	100.00

[1/] This premix provided the following microelements (μg/kg): vitamin A, 4,500,000 IU; vitamin D, 750,000 IU; vitamin E, 10,000; vitamin K3, 750; vitamin B1, 1,100; vitamin B2, 3,000; vitamin B3, 10,000; vitamin B6, 2,000; vitamin B12, 12.5; pantothenic acid, 7,000; folic acid, 425; biotin, 100; Cu, 5,000; Fe, 4,800; I, 500; Mn, 30,000; Se,100; Zn, 50,000.

2.2 Study growth performance and carcass quality

2.2.1. Growth performance

A total of 160 one-day-old broiler chicks (CP 707) were allocated to 5 dietary treatments and 4 replicates of 8 chickens (4 male and 4 female) in a completely randomized design for 1 to 45 days. The chickens were housed in a 1.35 x 1.50 m. pen in an open-air facility. Feed and water were provided *ad libitum* throughout the trial. Dietary treatments were 1) control group (0% AMLM), 2) to 5) equipped with a diet containing 2.5%, 5.0%, 7.5%, and 10.0% AMLM. All diets were fed in mash form, using the ME for formulating dietary treatments. The birds were fed a common corn-cassava-soybean-based diet formulated as-fed to meet [15] requirement for a starter diet (3,100 kcal of ME/kg; 23% CP) from 1 to 17 d of age, a grower diet (3,150 kcal of ME/kg; 20% CP) from 18 to 31 d of age and a finisher diet (3,200 kcal of ME/kg; 18% CP) from 32 to 45 d of age (Table 2). The chickens weight and feed consumption were measured on days 1 and 45.

2.2.2. Carcass composition

At the end of the experiment (45 d), 2 chickens per replicate (1 male and 1 Female) were individually weighed and slaughtered. The chickens were defeathered and weighed. Abdominal fat, neck, head, shanks, and edible offal (gizzard, liver, and heart) were excised and finally calculated as a percentage of live body weight. Cold carcass (pre-chilling in water at 20 ^{0}C for 20 min, chilling at 4 ^{0}C for 25 min, and dripping for 3 min) was cut into wings, thighs, drumsticks, breasts, and backbone. The yields of the various cuts are calculated as a percentage of cold carcass weight. Moreover, to evaluate the digestive organs (with digesta), proportions of the crop, spleen, small intestine (duodenum, jejunum, and ileum), cecum, and large intestine to live body weight were calculated. The length of intestinal segments, including the duodenum, jejunum, ileum, cecum, and large intestine, was measured according to Mossami [16]. In addition, the thickness of the muscular layer of the gizzard wall was measured at the maximum width by vernier calipers [17].

2.2.3. Statistical analysis

All data growth performance and carcass composition were subjected to analysis of variance procedures suitable for a completely randomized design using the GLM procedure [18]. Means were compared using Duncan. Statements of statistical significance were based on $P<0.05$.

Table 2. Ingredient composition and nutrient content of experiment diets (as fed basis)

Ingredients (%)	Starter Diets					Grower Diet					Finisher Diet				
	Acacia mangium leaf meal level (%)					*Acacia mangium* leaf meal level (%)					*Acacia mangium* leaf meal level (%)				
	0	2.5	5.0	7.5	10	0	2.5	5.0	7.5	10	0	2.5	5.0	7.5	10
Corn meal	30.00	30.00	28.00	27.45	23.50	34.00	32.00	30.00	30.00	30.00	36.56	33.61	30.76	27.80	25.00
Cassava chip	24.00	21.47	20.52	18.40	19.37	27.21	26.58	25.68	23.08	20.48	30.00	30.00	30.00	30.00	30.00
Soybean meal (45%CP)	30.28	29.85	29.60	29.23	29.18	25.00	24.68	24.45	24.02	23.58	20.15	20.00	19.80	19.70	19.44
Fish meal (60% CP)	9.50	9.50	9.50	9.50	9.50	8.00	8.00	8.00	8.00	8.00	8.00	8.00	8.00	8.00	8.00
A. Mangium leaf meal	0.00	2.50	5.00	7.50	10.00	0.00	2.50	5.00	7.50	10.00	0.00	2.50	5.00	7.50	10.00
DCP (18%P)[1]	2.30	2.30	2.40	2.40	2.40	2.40	2.40	2.45	2.45	2.45	2.20	2.20	2.25	2.27	2.27
Salt	0.19	0.19	0.19	0.19	0.19	0.19	0.19	0.19	0.19	0.19	0.19	0.19	0.19	0.19	0.19
Vitamin-mineral premix[2]	0.33	0.33	0.33	0.33	0.33	0.20	0.20	0.20	0.20	0.20	0.20	0.20	0.20	0.20	0.20
Palm oil	3.40	3.85	4.46	5.00	5.53	3.00	3.45	4.03	4.56	5.10	2.70	3.30	3.80	4.34	4.90
Total	100	100	100	100	100	100	100	100	100	100	100	100	100	100	100
Chemical composition, analysis (% DM basis)															
Dry matter (%)	90.62	90.53	90.62	91.22	90.54	90.36	90.37	90.55	90.33	90.33	90.30	90.34	90.09	90.34	90.65
Ash (%)	7.92	7.76	8.03	8.18	8.35	7.49	7.81	8.24	8.50	8.04	8.09	7.93	8.25	8.41	8.01
Crude protein (%)	21.18	22.32	22.44	21.77	22.93	18.31	18.32	18.74	18.91	18.97	16.37	17.04	16.58	16.91	17.33
Crude fat (%)	4.13	4.34	4.92	5.58	5.48	3.49	4.43	4.84	5.14	3.71	4.50	4.81	4.40	4.78	3.62
Crude fiber (%)	3.73	3.91	4.42	4.70	4.81	2.80	3.02	3.78	4.62	5.25	2.84	3.36	4.19	4.89	5.05
Gross energy (Kcal/ kg)	4,735	4,595	4,646	4,558	4,603	4,294	4,393	4,509	4,845	4,525	4,670	4,430	4,305	4,600	4,571

[1] DCP = Dicalcium phosphate. , [2] Vitamin-mineral premix provides per kg of diet: vitamin A 15,000 IU; vitamin D_3 3,000 IU; vitamin E 25 IU; vitamin K_3 0.5 g; vitamin B_1 2.5 mg; vitamin B_2 7 mg; vitamin B_6 4.5 mg; vitamin B_{12} 0.025 mg; pantothenic acid 35 mg; nicotinic acid 35 mg; chorine chloride 0.25 g; biotin 0.025 mg; Cu 1.6 mg; folic acid 0.5 mg; Mn 0.06 g; Se 0.15 mg; Fe 0.08 g; I 0.4 mg; Zn 0.045 g

3. Results and Discussion

3.1. Study chemical composition and metabolizable energy

Results of the proximate analysis of AMLM are presented in Table 3. It reveals that it is high in crude fiber (25.92%), tannin (13.28%), and gross energy (5,200.29 Kcal/kg). The crude protein content was lower than those (15.2% and 15.6 %) obtained respectfully by Van et al. and Keir et al. [19-20]. The composition of leaves is generally affected by various factors such as plant age, soil fertility, and preparation method [10]. The metabolizable energy content for broiler chicken of AMLM was analyzed to be 2,359.90 Kcal/kg. This value was similar to the ME of *the L. leeucocephala* leaf meal (2,377 Kcal/kg) obtained by Hien et al. [21].

Table 3. The **c**hemical composition and metabolizable energy of AMLM (% dry matter)

Items	***Acacia mangium* leaf meal**
Moisture, %	13.58
Crude protein, %	11.62
Crude fat, %	2.99
Crude fiber, %	25.92
Crude ash, %	4.09
Nitrogen-free extract, %	41.80
Calcium, %	1.00
Phosphorus, %	0.04
Tannin, %	13.28
Gross energy, Kcal/kg	5,200.29
Metabolizable energy, Kcal/kg	2,359.90

3.2. Study growth performance and carcass composition

3.2.1. Growth performance

Broiler chicken performance from one to forty-five days of age is shown in Table 4. There were no significant differences in final body weight, weight gain, ADG, and DFI among dietary treatments. This result agreed with Eichie et al. [22], who reported that broilers fed with leucaena leaf meal lower than 12.16% in diets had feed intake and body weight gain different from the control diet. However, other studies have reported negative responses in growth performance to fed acacia leaf meal and leucaena leaf meal by broilers [11, 23-24].

However, broiler chickens fed the AMLM diet had a higher ($P<0.05$) FCR than those fed the control diet. The results in the negative response of FCR generally agreed with earlier reports [23-24]. The higher FCR due to feeding leaf meals compared to feeding the control diet may also be attributed to increased levels of dietary fibers and tannin, which could impair dietary nutrient utilization [10, 25]. The possible effect of the anti-nutritional compounds (fibers and tannin) has a limited capacity to digest high-fibrous ingredients efficiently, and the chickens lack the enzymes necessary for utilizing high-fibrous ingredients [26-27]. Therefore, using the highest dietary level of the AMLM could result in inadequate nutrient availability for the birds, which could negatively affect the FCR.

Table 4. Effect of AMLM on broiler chickens performance during ages of 1 to 45 days

Items	*Acacia mangium* leaf meal level (%)					*SEM*	*P-value*
	0	**2.5**	**5**	**7.5**	**10**		
Initial BW (g/chick)	42.19	41.88	42.19	42.19	42.19	0.131	0.941
Final BW (g/chick)	2095.00	1934.69	1989.00	1990.58	1913.44	25.238	0.177
WG (g/chick)	2052.81	1892.81	1946.82	1948.39	1871.25	25.246	0.178
ADG (g/day/chick)	45.62	42.06	43.26	43.30	41.58	0.561	0.178
DFI (g/day/chick)	102.33	103.87	103.87	108.86	104.63	0.796	0.083
FCR	2.25[b]	2.48[a]	2.41[a]	2.52[a]	2.52[a]	0.030	0.006

SEM, standard error of the mean.

[a,b] Mean in the same row with different superscripts differ significantly (P<0.05).

BW = Body weight; WG = Weight gain; ADG = Average daily gain;

DFI = Daily feed intake; FCR = Feed conversion ratio

3.2.2. Carcass composition

The carcass composition of forty-five days of age broiler chickens is shown in Table 5. Carcass parts were not significantly (P>0.05) affected by dietary AMLM. The relative weights of the carcass cut were similarities suggest that the control and the test diets (leaf meal-based diets) promoted similar carcass quality. This result was in agreement with Eichie et al. and Onibi et al. [22-23], who reported that broilers fed with a leucaena leaf meal in diets had carcass characteristics not different from the control diet.

The effect of diets supplemented with AMLM on digest organ size is shown in Tables 6 and 7. The visceral organ size was not significant (P>0.05) affected by dietary AMLM. No significant differences in the length of the duodenum, cecum, and large intestine were observed among the treatments. But chicken fed with AMLM diets had ilium longer (P<0.05) than those fed with a control diet (0% AMLM). Besides that, chicken fed with more than 5% AMLM diet tended to have a higher small intestine length (P=0.09), jejunum length (P=0.06), and gizzard wall thickness. The increase in the size of the intestinal segments is a physical adaptation to the presence of the AMLM. This represents an enhanced development of the intestinal segment [28-29]. An increase in the intestinal length could also result from an increase in gastro-duodenal refluxes as triggered by the high fiber content in the leaf meal feed base diet [29-31]. In this study, chicken fed with more than 5% AMLM diet tended to have higher gizzard wall thickness. One possible explanation for the higher relative gizzard wall thickness at a higher level of inclusion of leaf meals in the diet. The gizzard breaks down ingested feed by muscular action, and higher dietary fiber promotes more increased thickening of the muscles [23].

Table 5. The effects of AMLM on carcass composition of broiler chickens

Items	*Acacia mangium* leaf meal level (%)					*SEM*	*p-value*
	0	**2.5**	**5**	**7.5**	**10**		
Live weight (kg)	2.11	2.01	2.11	2.05	2.07	0.018	0.328
Dressed weight (%)[1/]	69.06	70.63	70.84	70.53	69.83	0.253	0.149
Edible offal (%)[1/]							
Gizzard	1.84	1.68	1.79	1.85	1.97	0.041	0.253
Liver	2.15	2.13	2.07	2.22	2.27	0.056	0.835
Heart	0.52	0.52	0.52	0.55	0.55	0.012	0.922
Abdominal fat (%)[1/]	2.33	2.31	2.04	2.13	2.07	0.069	0.585
Blood and feather (%)[1/]	7.95	7.11	7.56	7.93	8.34	0.244	0.594
Neck and head (%)[1/]	7.05	7.47	6.66	7.10	7.43	0.134	0.296
Shanks (%)[1/]	3.26	3.43	3.35	3.72	3.75	0.084	0.254

Table 5. The effects of AMLM on carcass composition of broiler chickens (Continued)

Items	*Acacia mangium* leaf meal level (%)					SEM	p-value
	0	2.5	5	7.5	10		
Cold Carcass (kg)	1.46	1.42	1.50	1.45	1.44	0.013	0.486
Wings (%)[2/]	11.77	11.94	11.36	11.43	12.82	0.203	0.151
Thighs (%)[2/]	19.57	18.87	19.50	19.48	20.02	0.337	0.892
Drumsticks (%)[2/]	15.21	15.22	14.54	14.81	15.34	0.138	0.322
Breasts (%)[2/]	28.83	28.62	29.37	29.50	28.60	0.400	0.934
Backbone (%)[2/]	22.79	22.96	23.90	24.47	24.69	0.312	0.191

SEM, standard error of the mean.
[1/]percentage of live weight, [2/]percentage of cold carcass weight.

Table 6. The effects of AMLM on the relative weight of visceral organs [3/] (Percentage of live weight).

Organ size (%)	*Acacia mangium* leaf meal level (%)					SEM	p-value
	0	2.5	5	7.5	10		
crop	0.34	0.40	0.36	0.32	0.30	0.017	0.360
Spleen	0.18	0.29	0.21	0.23	0.26	0.019	0.421
Small intestine	2.81	2.92	2.81	2.98	2.78	0.045	0.631
Duodenum	0.73	0.72	0.68	0.74	0.68	0.010	0.184
Jejunum	1.11	1.10	1.08	1.17	1.07	0.022	0.672
Ileum	0.97	1.10	1.05	1.07	1.03	0.024	0.580
Cecum	0.33	0.30	0.27	0.34	0.33	0.009	0.112
Large intestine	0.15	0.14	0.12	0.14	0.14	0.008	0.844

SEM, standard error of the mean.
[3/] Visceral organs weight considered with digesta.

Table 7. The effects of AMLM on intestinal and gizzard length of broiler chickens.

Organ size (cm)	*Acacia mangium* leaf meal level (%)					SEM	p-value
	0	2.5	5	7.5	10		
Small intestine	197.13	195.56	206.44	211.88	210.63	2.512	0.115
Duodenum	30.50	29.13	29.81	33.19	28.88	1.056	0.727
Jejunum	69.49	68.44	71.44	72.94	75.13	0.802	0.052
Ileum	70.13^{c}	71.31^{bc}	77.44^{ab}	80.06^{a}	78.63^{a}	1.134	0.007
Cecum	17.56	16.81	18.00	17.06	18.63	0.236	0.100
Large intestine	9.50	9.88	9.75	8.63	9.38	0.319	0.777
Gizzard wall thickness (mm)	17.85	19.25	19.20	20.11	22.79	0.820	0.382

SEM, standard error of the mean.
[a,b,c] Mean in the same row with different superscripts differ significantly ($P<0.01$).

4. Conclusions

Under the condition described in this study, We found that the apparent metabolizable energy in broiler-fed AMLM was 2,359.90 kcal/kg. Broiler chickens fed up to 10% AMLM in diets do not affect broiler chickens' growth performance and carcass composition.

5. Acknowledgements

The author would like to thank all members of the overall project, especially KMITL Prince of Chumphon farm, who gave facilitated research equipment. The undergraduate student from the animal science program KMITL PCC to participate in the project.

Author Contributions: Conceptualization, S.L. and W.N.; performed the experiments, S.L., D.P. and W.N.; formal analysis, S.L.; data collection, S. L., D. P. and W. N.; writing—original draft preparation, S.L.; writing—review and editing, S.L.; supervision, S.L.; project administration, S.L.; funding acquisition, S.L., and W.N.. All authors have read and agreed to the published version of the manuscript.

Funding: This research was funded by KMITL Research and Innovation Services (KRIS), Bangkok, Thailand,

Conflicts of Interest: The authors declare that there is no conflict of interest regarding the publication of this article.

References

[1] Brice, Y. *AVEC working group on turkey. Annual report, Association of poultry processors and poultry treade in the EU countries ASBL. Belgium*, 2022.
[2] Midgley, S.J.; Turnbull, J.W. Domestication and use of Australian acacia: case studies of five important species. *Aust. Syst. Bot.* 2003; 16, 89-102.
[3] Kull, C.A.; Rangan, H. Acacia exchanges: wattles, thorn trees, and the study of plant movements. *Geoforum*. 2008; *39*(3), 1258-1272.
[4] Visuthitepkul, S. Quality of sawntimber *acacia mangium willd.* From planting by agro-forestry practices. *Thai J. For.* 1998; 17, 61-74.
[5] Maelim, S.; Khlangsap, N.; Thaiutsa, B. Provenance trials of 1-year old *Acacia mangium* Willd. at wang nam khiew forestry research and training station, nakhon ratchasima province. *Thai J. For.* 2017; *36*(2), 35-45.
[6] Jarwanto, D.; Tachibana, S. Decomposition of lignin and holocellulose on *Acacia mangium* leaves and twings by six fungal isolates from nature. *Pak. J. Biol. Sci.* 2010; *13*(12), 604-610.
[7] Lerdsuwan, S.; Nalinanon, W. Reduction of fiber content in *Acacia mangium* leaves meal by commercial enzyme. *J. Sci. Technol. MSU. Univ*. 2016; (Suppl.1), 647-652.
[8] Sruamsiri, S. The use of acacia (*Acacia mangium*) as protein source in dairy ration. *J. Agric. Sci.* 2001; *17*(1), 82-91.
[9] Clavero, T.; Razz, R. Utilization of *Acacia mangium* as supplement for growing sheep. *Revista Cientifica*. 1999; *9*(4), 311-313.
[10] Abou-Elezz, F.M.K.; Sarmiento-Franco, L.; Santos-Ricalde, R.; Solorio-Sanchez, F. Nutritional effects of dietary inclusion of Leucaena leucocephala and Moringa oleifera leaf meal on Rhode Island Red hens' performance. *Cuba. J. Agric. Sci.* 2011; *45*(2), 163-169.
[11] Zanu, H. K.; Mustapha, M.; Addo Nartey, M. Response of broiler chickens to diets containing varying levels of leucaena (*leucaena leucocephpla*) leaf meal. *Online J. Anim. Feed. Res*. 2012; *2*(2), 108-112.
[12] A.O.A.C. *Official Methods for Analysis*, 5th ed. *Association of Official Analytical Chemists, Washington DC*, 1990.
[13] Burns, R. E. Method for estimate of tannin in grain sorghum. *Agron. J.* 1971; 63, 511.
[14] Hill, F.M.; Anderson, D.L. Comparisn of metabolizable energy and productive energy determinations with growing chicks. *J. Nutr.* 1958; *64*(4), 587-603. https://doi.org/10.1093/jn/64.4.587.
[15] NRC. *Nutrient requirement of poultry*, 9th ed. *National Academy Press, Washington D.C.,* 1994.
[16] Mossami, A. *Effects of different inclusions of oat hulls on performance, carcass yield and gut development in broiler chickens*. Thesis, Agricultural Science, Swedish University, 2011.
[17] Amerah, A.M.; Lentle, R.G.; Ravindran, V. Influence of feed form on gizzard morphology and particle size spectra of duodenal digesta in broiler chickens. *J. Poult. Sci.* 2007; *44*(2), 175-181.
[18] SAS. *SAS/SAT Guide for Personal Computers. Version SAS University*. SAS inst., INC., Cary, NC., 2003.
[19] Van, D.T.T.; Mui, N.T.; ledin, I. Effect of method of processing foliage of Acacia mangium and inclusion of bamboo charcoal in the diet on performance of growing goats. *Anim. Feed Sci. Technol*. 2006; *130*(3-4), 242-256.
[20] Keir, B.; Lai, N.V.; Preston, T.R.; Orskov, E.R. Nutritive value of leaves from tropical trees and shrubs: 1. *In vitro* gas production and *in sacco* rumen degradability. *Livest. Res. Rural. Dev*. 1997; *9*(4), 1-5.

[21] Hien, T.Q.; Trung, T.Q.; Ha, T.V. Determination of the metabolic energy value of leucaena leucocephala leaf meal on luong Phuong broiler chicken. Vietnam. *J. Sci. Technol.* 2016; *2*(9), 23-26.
[22] Eichie, F.O.; Akinyemi, D.E.; Adegbenro, M. Effect of replacement of soybean meal with *leucaena leucocephala* leaf meal on performance, haematology, carcass measures and organ weight in broiler chickens. *Am. J. Exp. Agric.* 2015; *8*(5), 327-334.
[23] Onibi, G.E.; Folorunso, O.R.; Elumelu, C. Assessment of partial equi-protein replacement of soyabean meal with cassava and leucaena leaf meals in the diets of broiler chicken finishers. *Int. J. Poult. Sci.* 2008, *7*(4), 408-413.
[24] Ncube, S.; Halinami, T.E.; Chikosi, E.V.I.; Saidi, P.T. Effect of *Acacia angustissima* leaf meal on performance, yield of carcass components and meat quality of broilers. *S. Afr. J. Anim. Sci.* 2018; *48*(2), 271-283.
[25] Nwokolo, E.N.; Akpapunam, M.; Ogunjimi, T. Effect of vary level of dietary fibre on mineral availability in poultry diet. *Nig. J. Anim. Prod*. 1985, 12, 129-133.
[26] Son, J.H.; Ragland, D; Adeola, O. Quantification of digesta flow into de caeca. Br. Poult. Sci. 2002; *43*(2), 322-324, https://doi.org/10.1080/00071660120121562.
[27] Ige, A.O.; Odunsi, A.A.; Akinlade, J.A.; Ojedapo, L.O.; Ameen, S.A.; Aderinola, O.A.; Rafiu,T.A. Gliricidia leaf meal in layer's diet effect on performance, nutrient digestibility and economy of production. *J. Anim. Vet.* 2006; *5*(6), 483-486.
[28] Jiang, J.F.; Sang, X.M.; Huang, X.; Zhou, W.D.; Wu, J.L.; Zhu, H.C.; Jiang, Y.Q. Effects of Alfalfa meal on growth performance and gastrointestinal tract development of growing ducks. *Asian-Australas* J Anim Sci. 2012*; 25*(10), 1445-1450.
[29] Ncube, S.; Halinami, T.E.; Mwale, M.; Saidi, P.T. Effect of *acacia angustissima* leaf meal on the physiology of broiler intestines. *J. Agric. Sci.* 2017; *9*(2), 53-62.
[30] Mateos, G.G.; Jimenez-Monero, E.; Serrano, M.P.; Lazaro, R.P. Poultry responses to high levels of dietary fiber sources varying in physical and chemical characteristics. J. *Appl. Poult. Sci.* 2012; *21*(1), 156-174.
[31] Martens, S.D.; Tiemann, T.T.; Bendelle, J.; Peters, M.; Lascano, C.E. Alternative plant protein sources for pigs and chickens in the tropics: Nutritional value and constraints: A review paper. *J. Agr. Rural. Dev. Trop.* 2012; *113*(12), 101-123.

JSTR
ASEAN Journal of Scientific and Technological Reports

Research article

Effects of Different Potting Media on the Growth of Commercial Cacti

Kittiphan Ritthidechrat[1] and Chamaiporn Anuwong[1*]

[1] Department of Plant Production Technology, Faculty of Agricultural Technology, King Mongkut's Institute of Technology Ladkrabang, Bangkok, Thailand; 65046007@kmitl.ac.th
[1] Department of Plant Production Technology, Faculty of Agricultural Technology, King Mongkut's Institute of Technology Ladkrabang, Bangkok, Thailand; chamaiporn.an@kmitl.ac.th
* Correspondence: chamaiporn.an@kmitl.ac.th

Abstract: This research aims to study the appropriate growing media for the growth of cacti that can reduce production costs and promote cacti's growth. The research used four genera of cacti, i.e., *Gymnocalycium*, *Astrophytum*, *Mammillaria*, and *Echinopsis*, which were famous in the commercial market in Thailand. The experimental design was completely randomized designs (CRD) with four different growing media and three replications; T1) fermented rain tree leaves (FRTL): perlite: vermiculite: pumice: vermicompost as a control, T2) FRTL: rice husk: coconut coir: charcoal: vermicompost, T3) FRTL: rice husk ash: coconut husks chips: expanded clay: vermicompost and T4) rice husk ash: vermicompost. The plant was cultivated the plastic pot 2-inches and collected the growth for six months. The result showed that *Mammillaria* was planted in Treatment 3 gave the greatest stem diameter and the number of roots. A similar increase in stem diameter of *Echinopsis* and *Gymnocalycium* had the newest areoles. While planted in T4, as a result, the genus *Astrophytum* has increased in stem diameter, the number of new areoles, and the number of roots. In the *Gymnocalycium* also found an increase in stem diameter. Therefore, the use of cacti growing media in T3 as an appropriate for the growth of cacti. Furthermore, it can reduce the production cost of growing media about 0.72 baht per pot (33%) when compared with the commercial media (T1) in a 2-inches plastic pot.

Keywords: Cacti; Growing media; Plant growth

Citation:
Ritthidechrat, K.; Anuwong, C. Effects of Different Potting Media on the Growth of Commercial Cacti. *ASEAN J. Sci. Tech. Report.* **2022**, *25*(4), 59-67. https://doi.org/10.55164/ajstr.v25i4.247560

Article history:
Received: October 14, 2022
Revised: November 28, 2022
Accepted: December 1, 2022
Available online: December 22, 2022

1. Introduction

The cactus is a plant belonging to the family Cactaceae [1]. It is a plant that is native to the desert [2]. Cacti are slow-growing plants. The stems are succulent. Therefore, it can grow in arid places and is commonly grown as an ornamental plant. Because there flowers, stems and spines. They are unique, such as arborescent, shrubby, or creeping with a woody or succulent stem. The latter may be globular, cylindrical, or columnar [3]. Cactus spines produce by specialized structures called areoles. Areoles are an identifying feature of cacti. In addition to spines, areoles produce new flowers. Cactus flowers are beautiful and, depending on the species, are diverse in size, number, form, and color[4-6]. Thailand began to cultivate before the year 1954 with imports from abroad. Later, Thailand developed a species. Therefore, cultivation is increasingly popular [7].

Cactus needs a suitable rooting atmosphere for better growth. While traditional soils are often the problem, especially producing cacti of poor aeration and drainage. Cactus growers must find growing media suitable for

growing cacti. The optimal growing media used to produce cacti should have four basic functions: air space and water, which affect root growth and the integrity of the stem and create adequate nutrient reservoirs [8]. Now various organic ingredients like coconut coir, coconut husks chips, vermicompost, rice husk ash, rice husk are being utilized for the cactus grower and commercial purposes. Similarly the mineral potting substrates/ inorganic such as vermiculite, expanded clay, and pumice. Several studies support that soilless media management affects plant's growth and development [9]. In this case, the cactus should be grown in porous media, so that the plant media's aeration, drainage, and water-holding capacity ensure proper growth [10]. The epidemic situation of COVID-19 causing people to work from home and have more free time, so people are interested in growing more cacti [11], At the same time, cactus also has the shape, size, and ease of cactus cultivation. As a result, people are interested in growing cacti. [12]. The popular genus of cacti are *Gymnocalycium*, *Astrophytum*, *Mammillaria*, and *Echinopsis* [13].

Nowadays, there are many people who are interested in growing cacti. But the planting materials that farmers use are expensive. Causing cactus growers to find alternative materials to reduce production costs. By choosing materials that have similar properties to the materials used and that there are enough nutrients to meet the needs of the cactus. To be suitable for the growth of cacti and reduce the cost of cactus production.

2. Materials and Methods

2.1 Study area and media preparation

All experiments were actualized under plastic greenhouse conditions with 50% net shading with a temperature of 30 °C, and a light intensity of 11,530 LUX in Chonburi, Thailand. Plants were cultivated between March 2022 to September 2022. The experiment was arranged in a completely randomized design (CRD) and replicated three times with four pots per replication. The growing media included four treatments as follows: T1) fermented rain tree leave (FRTL): perlite: vermiculite: pumice: vermicompost (1: 1: 1: 1: 1) as a control, T2) FRTL: rice husk: coconut coir: charcoal: vermicompost (1: 1: 1: 1: 1), T3) FRTL: rice husk ash: coconut husks chips: expanded clay: vermicompost (1: 1: 1: 1: 1), T4) rice husk ash: vermicompost (1: 2). The planting materials in each treatment were mixed by volume. During the experiment, the cacti were not fertilized.

2.2 Plant preparation

The 6-month-old cacti seedlings were used in the experiment. The diameter size of the cacti were as follows: *Gymnocalycium* was in the size range of 1.13 – 1.93 cm and *Astrophytum* was in the size range of 0.96 – 1.55 cm, *Echinopsis* was in the size range of 1.71 – 2.94 cm, and *Mammillaria* was in the size range of 1.13 – 1.83 cm. These were planted in 2-inch plastic pots using different growing media. During the experiment, 40 ml of water was watered every 3 days and no cactus fertilization was performed during the whole experiment.

2.3 Growing media analysis

The chemical and physical properties of growing media were analyzed before and after at 6 months of planting in 4 genera of cacti. A 250 g of growing media was saturated with distilled water and stood for an hour before measured pH and electrical conductivity. The saturation extract's electrical conductivity (EC) was measured using a portable electrical conductivity meter (220 pH/EC meter). The pH of growing media was recorded by Orion research digital pH/millivolt meter with a glass electrode using buffers of pH 4.0 and 9.0 for standardizing the instrument. Growing media on physical properties were analyzed followed by the methods of Spomer [14]. The total porosity, bulk density and growing media moisture were calculated by the formula: Bulk density (g/cm^3) = (weight of pot and growing media – weight of pot)/pot volume. Total porosity (%) = {(weight of pot and growing media saturated with water – weight of pot and growing media) × 100}/pot volume. Growing media moisture (%) = (weight of water/weight of dry growing media) × 100.

2.4 Plant growth analysis and Statistical analysis

All growth parameters of the four genera of cacti were determined at 6 months after planting and were as follows: stem diameter, number of new areoles, number of roots, and root length. The collected data

were analyzed according to the completely randomized designs by Statistix 8 program, and the mean was compared by the Least Significant Difference Test (LSD) at 95%.

3. Results and Discussion

3.1 Results

3.1.1 Properties of planting material and production costs

pH value: The pH value of the growing media before planting was statistically significant difference. The mixed material in T2 had the highest pH at 7.85, while T1 had the lowest pH (7.55). After six months of planting, it was found that in the genus *Gymnocalycium*, pH values were statistically different. It was found T2 had the highest pH values at 7.85 (Table 2), while T1 had the lowest pH (7.53). In the genus *Astrophytum*, the pH of all growing media decreased when compared with before planting and was statistically different. T3 had the highest pH at 7.38, while T4 had the lowest pH (6.84). In the genus *Echinopsis*, the pH was statistically different. T3 had the highest pH at 7.63, while T4 had the lowest pH (7.19). However, the pH value was not statistically different in the genus *Mammillaria* (7.64-7.78).

Electrical Conductivity: EC (mS/cm): EC of the growing media before planting was a statistically significant difference (Table 1). The mixed material in T2 was the highest (1.02 mS/cm), while T3 had the lowest (0.54 mS/cm). After six months of planting, it was found that EC in growing media of all four genera of cacti decreased when compared with before planting. However, it showed no statistically different results. In the genus *Gymnocalycium*, the EC value was the phase of 0.51 - 0.69 mS/cm, and 0.45 - 0.54 mS/cm in the genus *Astrophytum.* The EC was in the range of 0.44 - 0.71 mS/cm in the genus *Mammillaria*, and 0.51 - 0.64 mS/cm in the genus *Echinopsis* (Table 2).

Growing media Moisture (percentage by weight): Growing media moisture of planting material before planting found that T1 and T4 had the lowest moisture content at 39.41 and 40.62 %, respectively (Table 1). After six months of planting, it was found that in the genus *Gymnocalycium*, the growing media moisture was statistically different. T4 had the lowest growing media moisture (34.65%). In the genus *Astrophytum* also was significantly different but T2 had the lowest growing media moisture (38.92%). Whereas, in the genus *Mammillaria*, there was not statistically different (37.94 - 41.63%). The genus *Echinopsis* was statistically variant. The T2 had the lowest growing media moisture (32.29%) (Table 2).

Bulk density (grams/cubic centimeter): Bulk density of growing media before planting was a statistical difference. The T2 had the lowest density at 0.46 g/cm^3 (Table 1). After six months of planting, the four treatments were not statistically different in all 4 genera of cacti. There were in ranged of 48.41 - 64.75, 55.21 - 60.71, 38.89 - 45.45, and 48.41 - 64.74 g/cm^3, respectively (Table 2).

Total porosity (%): The total porosity of the growing media before planting was significantly different. The T2 was the highest at 58.73%, but not different from T3 and T1 (54.03 and 51.73%, respectively) (Table 1). After six months of planting cacti, it was not statistically different in all 4 genera. There were in range of 48.41 - 64.75, 55.21 - 60.71, 38.89 - 45.45, and 48.41 - 64.74%, respectively (Table 2).

Table 1. Properties of growing media before planting cacti and planting a cactus and cost of growing media

Treatment	pH	EC (mS/cm)	Growing media Moisture (%)	Bulk Density (g/cm³)	Total porosity (%)	Cost (bath/2″ pot)
1	7.55[b]	0.73[b]	39.41[b]	0.57[b]	51.75[a]	2.20
2	7.85[a]	1.02[a]	55.84[a]	0.46[c]	58.73[a]	1.18
3	7.77[a]	0.54[c]	46.18[ab]	0.58[b]	54.03[a]	1.48
4	7.77[a]	0.81[b]	40.62[b]	0.70[a]	34.84[b]	2.86
%CV	0.92	8.31	17.22	8.31	10.26	
LSD$_{0.05}$	0.13	0.12	14.75	0.09	9.62	

[a, b, c] different characters in the same column are statistically different at 95% confidence level ($P \leq 0.05$)

Table 2. Properties of growing media at after 6 months of planting of all 4 genera of cacti.

Treatment	pH	EC (mS/cm)	Growing media Moisture (%)	Bulk Density (g/cm³)	Total porosity (%)
			Gymnocalycium		
1	7.53[b]	0.55	57.61[a]	0.77	53.19
2	7.85[a]	0.69	49.18[a]	0.79	48.41
3	7.83[a]	0.51	50.07[a]	0.81	64.75
4	7.79[a]	0.61	34.65[b]	0.80	58.30
%CV	1.42	15.93	12.93	16.22	17.64
LSD$_{0.05}$	0.21	ns	11.66	ns	ns
			Astrophytum		
1	7.13[a]	0.54	44.47[b]	0.71	55.21
2	7.33[a]	0.48	38.92[c]	0.74	60.71
3	7.38[a]	0.45	52.61[a]	0.80	59.49
4	6.84[b]	0.49	39.77[bc]	0.77	55.56
%CV	1.92	14.73	5.82	7.72	9.40
LSD$_{0.05}$	0.26	ns	4.82	ns	ns
			Mammillaria		
1	7.65	0.58	40.25	0.94[a]	43.11
2	7.64	0.58	37.94	0.83[ab]	45.45
3	7.66	0.44	41.63	0.93[ab]	43.18
4	7.78	0.71	40.09	0.69[b]	38.89
%CV	1.23	25.80	13.89	12.94	12.84
LSD$_{0.05}$	ns	ns	ns	0.21	ns
			Echinopsis		
1	7.29[bc]	0.53	49.83[a]	0.67[b]	53.19
2	7.45[ab]	0.51	41.45[ab]	0.66[b]	48.41
3	7.63[a]	0.55	43.88[ab]	0.82[a]	64.74
4	7.19[c]	0.64	32.29[c]	0.90[a]	58.30
%CV	1.55	15.96	8.34	8.19	17.64
LSD$_{0.05}$	0.22	ns	6.57	0.12	ns

[a, b, c] different characters in the same column are statistically different at 95% confidence level ($P \leq 0.05$)
ns = not statistically different
note: treatment 1 = FRTL: perlite: vermiculite: pumice: vermicompost (1: 1: 1: 1: 1)
treatment 2 = FRTL: rice husk: coconut coir: charcoal: vermicompost (1: 1: 1: 1: 1)
treatment 3 = FRTL: rice husk ash: coconut husks chips: expanded clay: vermicompost (1: 1: 1: 1: 1)
treatment 4 = rice husk ash: vermicompost (1: 2)

Production costs (bath/ 2 inches pot): The cost of each growing media in 2-inch pots was found that in T1 was 2.20 bath/ 2 inches pot. However, in T2 was lowest (1.18 bath), and in T3 was lower than T1 (1.48 bath). The highest cost was found in T4 that 2.86 bath (Table 1).

3.1.3 Plant growth

The experimental planting of cacti in 4 different growing media for six months showed that there was a statistically significant difference. In the genus, *Gymnocalycium* grew on T4 was the highest stem diameter (3.87 cm) while T2 had a minimum diameter (3.53 cm) (Table 3; Figure 1). In the *Astrophytum*, T4 had the largest diameter (3.05 cm) while T1 had the lowest diameter (2.65 cm). In the genus *Mammillaria*, T3 had a maximum diameter (4.33 cm), while T4 had the lowest diameter (3.88 cm). In the genus, *Echinopsis* grown on T3 was not different from growing on T1 and T4 had the largest stem diameter (4.52, 4.50, and 4.50 cm) while growing on T2 has the minimum stem diameter (3.98 cm).

Table 3. The stem diameters of all 4 genera of cacti after planting in different growing media for 6 months.

Treatment	Stem diameter (cm)			
	Gymnocalycium	*Astrophytum*	*Mammillaria*	*Echinopsis*
1	3.73^{ab}	2.65^{b}	4.17^{ab}	4.50^{a}
2	3.53^{b}	2.76^{ab}	4.01^{ab}	3.98^{b}
3	3.74^{ab}	2.87^{ab}	4.33^{a}	4.52^{a}
4	3.87^{a}	3.05^{a}	3.88^{b}	4.50^{a}
C.V.%	10.54	14.25	10.92	4.28
LSD$_{0.05}$	0.32	0.33	0.37	0.15

$^{a, b}$ different characters in the same column are statistically different at 95% confidence level ($P \leq 0.05$)

The number of new areoles of the genus *Gymnocalycium* and *Astrophytum* were significantly different. In genus *Gymnocalycium* grown on T2 was not different from growing on T3. And it had the highest number of new areoles (4.67 areoles) while planting on T4 had the lowest number of new areoles (3.67 areoles) (Table 4). The *Astrophytum* grown in T4 had the highest number of new areoles (3.58 areoles) while those grown on T2 had the lowest number of new areoles (2.33 areoles). However, the number of new areoles of the genus *Mammillaria* and *Echinopsis* was not significantly different (6.42 – 7.33 and 7.00 – 8.00 areoles, respectively).

Table 4 The number of new areoles of all 4 genera of cacti after planting in different growing media for 6 months.

Treatment	Number of new areoles			
	Gymnocalycium	*Astrophytum*	*Mammillaria*	*Echinopsis*
1	3.75^{b}	2.67^{bc}	6.50	7.42
2	4.67^{a}	2.33^{c}	6.42	8.00
3	4.67^{a}	3.08^{ab}	7.33	7.00
4	3.67^{b}	3.58^{a}	6.58	7.42
C.V.%	22.84	27.91	19.00	16.65
LSD$_{0.05}$	0.79	0.67	ns	ns

$^{a, b, c}$ different characters in the same column are statistically different at 95% confidence level ($P \leq 0.05$)

ns = not statistically different

note: treatment 1 = FRTL: perlite: vermiculite: pumice: vermicompost (1: 1: 1: 1: 1)
treatment 2 = FRTL: rice husk: coconut coir: charcoal: vermicompost (1: 1: 1: 1: 1)
treatment 3 = FRTL: rice husk ash: coconut husks chips: expanded clay: vermicompost (1: 1: 1: 1: 1)
treatment 4 = rice husk ash: vermicompost (1: 2)

The number of roots of all four genera of cacti were significantly different (Table 5; Figure 1). The genus *Gymnocalycium* grown with T1 had the highest number of roots (2.67) while T2 had the lowest number of roots (1.83). In the genus *Astrophytum* grown on T4 had the highest (2.83) while growing on T1 had the minimum number of roots (1.92). In the genus *Mammillaria* grown on T4 had the highest number of roots (9.83) while T1 had the lowest (7.50). In the genus, *Echinopsis* grown on T1 had the maximum number of roots (4.75) while T4 had the lowest (3.58).

Table 5 The number of roots of all 4 genera of cacti after planting in different growing media for 6 months.

Treatment	Number of roots			
	Gymnocalycium	*Astrophytum*	*Mammillaria*	*Echinopsis*
1	2.67^{a}	1.92^{b}	7.50^{b}	4.75^{a}
2	1.83^{c}	2.67^{a}	8.58^{ab}	4.17^{b}
3	2.08^{bc}	2.17^{b}	9.67^{a}	3.92^{bc}
4	2.17^{b}	2.83^{a}	9.83^{a}	3.58^{c}
C.V.%	18.12	16.55	28.57	10.23
$LSD_{0.05}$	0.33	0.33	2.09	0.35

^{a,b,c} different characters in the same column are statistically different at 95% confidence level ($P \leq 0.05$)

The root lengths of all four genera of cacti were significantly different (Table 6; Figure 1). The *Gymnocalycium* grown on T1 had the highest root length (6.65 cm) whereas T2 had the shortest roots length (5.28 cm)). In *Astrophytum* grown on T1 had the longest root (6.68 cm), while the T4 has the lowest roots length (5.21 cm). *Mammillaria* grown on T2 had the longest roots length (5.55 cm) while T1 had the shortest roots (4.40 cm). In *Echinopsis* planted with T3 had the highest roots length (14.46 cm) while T2 had the lowest roots length (9.63 cm).

Table 6. The root length of all 4 genera of cacti after planting in different growing media for 6 months.

Treatment	Root length (cm)			
	Gymnocalycium	*Astrophytum*	*Mammillaria*	*Echinopsis*
1	6.65^{a}	6.68^{a}	4.40^{b}	10.24^{b}
2	5.28^{b}	5.85^{bc}	5.55^{a}	9.63^{b}
3	5.43^{b}	6.05^{ab}	5.48^{a}	14.46^{a}
4	5.74^{ab}	5.21^{c}	4.70^{b}	10.67^{b}
C.V.%	19.99	13.13	9.74	23.59
$LSD_{0.05}$	0.95	0.64	0.40	2.18

^{a,b,c} different characters in the same column are statistically different at 95% confidence level ($P \leq 0.05$)

note: treatment 1 = FRTL: perlite: vermiculite: pumice: vermicompost (1: 1: 1: 1: 1)
treatment 2 = FRTL: rice husk: coconut coir: charcoal: vermicompost (1: 1: 1: 1: 1)
treatment 3 = FRTL: rice husk ash: coconut husks chips: expanded clay: vermicompost (1: 1: 1: 1: 1)
treatment 4 = rice husk ash: vermicompost (1: 2)

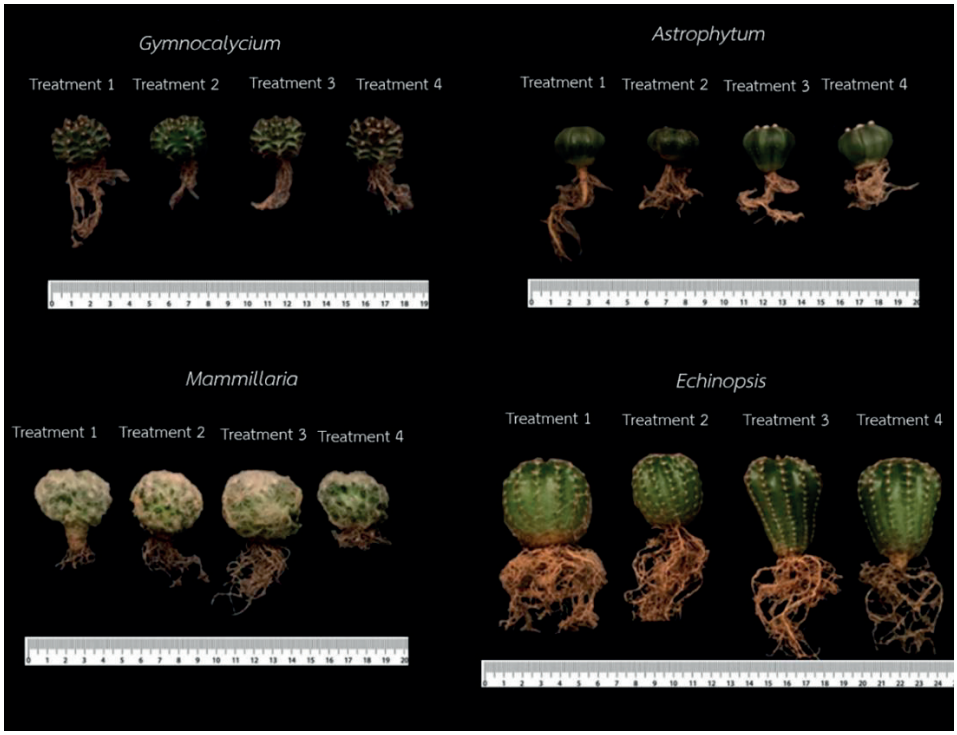

Figure 1. The stem growth of all 4 genera of cacti in 4 different growing media, namely: treatment 1) FRTL: perlite: vermiculite: pumice: vermicompost (1: 1: 1: 1: 1), treatment 2) FRTL: rice husk: coconut coir: charcoal: vermicompost (1: 1: 1: 1: 1), treatment 3) FRTL: rice husk ash: coconut husks chips: expanded clay: vermicompost (1: 1: 1: 1: 1) and treatment, and 4) rice husk ash: vermicompost (1: 2)

3.2 Discussion

The result of different growing media on the growth of 4 genera of cacti were found that T3 and T4 gave the best growth in all cacti such as stem diameter, number of roots and root length. Which were suitable for the growth of the cacti. Due to some properties of growing media were not significant difference after 6 months of planting such as follows: The pH before planting was 7.77, while after planting was in the range of 7.38 – 7.83 (T3) and 6.84 – 7.79 (T4). EC before planting was 0.54 (T3) and 0.81 (T4) mS/cm while after planting was in the range of 0.44 – 0.55 (T3) and 0.49 – 0.71 (T4). Before planting, the growing media moisture was 46.18% (T3) and 40.62% (T4), while after planting, the growing media moisture was in the range of 43.88 - 52.61% (T3) and 32.29 – 40.09% (T4). The bulk density before planting was 0.58 and 0.70 g/cm^3, while the bulk density after planting was in the range of 0.81 – 0.93 and 0.69 – 0.90 g/cm^3. The total porosity before planting was 54.03 % and 34.84% while the total porosity after planting was in the range of 43.18 – 64.75% and 38.89 – 58.30%, respectively. These properties were not different from the control treatment (T1). In the previous research reported that EC was in the range of 0.4 – 0.7 mS/cm [15], and the composition of the growing media was suitable for planting with total porosity of 50% and the rice husk ash with high porosity and low density [16]. It has enough macronutrients with 0.38% phosphorus and 1.28% potassium [17]. The FRTL have properties to help retain water and nutrients better. It contains approximately 0.5 - 0.1% nitrogen by weight [18]. Vermicompost comprises 1.15 % nitrogen, 0.38 % phosphorus, and 0.86 % potassium [19]. Coconut husks chips have good water absorption properties. It has a fibrous nature, thus allowing the growing media to be airy and loose [20]. The expanded clay can store water and nutrients [21]. Cacti were plants that prefer a low-density potting media and good drainage [10]. Their results were similar supported by Anuwong (2022), who studied the five genera of cacti grown in rice husks: vermicompost at a ratio of 1: 2 resulted in the highest height, stem diameter, number of roots and root length [22]. Although T3 and T4 gave the same results as an appropriate growth, but T3 had a lower cost than T4 and the control (T1). T3 can reduce the production cost of growing media around 0.72 baht/2-inch pot (33% of reduce cost) when compared with T1 as a commercial media.

4. Conclusions

The growth of all four genera of Cacti found that the planting material consisting of FRTL : rice husk ash: coconut husks chips: expanded clay: vermicompost had the most optimum growth in all four genera and can reduce the cost of growing media about 0.72 baht (33%) for cacti in 2-inch pot.

5. Acknowledgements

Thank you Faculty of Agricultural Technology, King Mongkut's Institute of Technology Ladkrabang for supporting research equipment and Asst. Prof. Dr. Sukunya Yampracha for her suggestions.

Author Contributions: Conceptualization, C.A.; methodology, K.R.; software, K.R.; validation, C.A.; formal analysis, K.R.; investigation, C.A.; resources, K.R. and C.A.; data curation, K.R. and C.A.; writing—original draft preparation, K.R. and C.A.; writing—review and editing, K.R. and C.A.; visualization, K.R.; supervision, C.A.; project administration, C.A.; funding acquisition, K.R. and C.A.

Funding: This research received no external funding.

Conflicts of Interest: The authors declare no conflict of interest.

References

[1] A Working List of All Plant Species. Available online: http://www.theplantlist.org/browse/A/Cactaceae/. (20 October 2021).

[2] Catus. Available online: https://www.Britannica.com/plant/cactus. (20 October 2021).

[3] Nobel, P.S. *Environmental Biology of Agaves and Cacti*, 1st ed.; Cambridge University Press: New York, USA, 1988; 10-15.

[4] Barthlott, T.; Hunt, D. Cactaceae. In *The family and genera of vascular plants* 3rd ed.; Kubitzki, K., Rohwer, J., Bittrich, V., Eds.; Springer: New York, USA, 1993; 2, 161-165.

[5] Hunt, D. *CITES Cactaceae Checklist*, 3rd ed.; Royal Botanic Gardens, Kew, UK, 1999; 9.

[6] Anderson, E.F.; *The Cactus Family*, 1st ed.; Timber Press, Portland, USA, 2021; 26-27.

[7] Cactus in Thailand. Available online: http://www.unclechorn.com/. (20 October 2021).

[8] Tariq, U.; Rehman, S.; Khan, M.A.; Younis, A.; Yaseen, M.A. Agricultural and municipal waste as potting media components for the growth and flowering of *Dahlia hortensis* 'Figaro'. *Turkish Journal of* Botany, 2012; *36*, 378-385.

[9] Yasmeen, S.; Younis, A.; Rayit, A.; Riaz, A.; Shabeer, S. Effect of different substrates on growth and flowering of *Dianthus caryophyllus* cv. 'Chauband Mixed'. *American-Eurasian Journal of Agricultural & Environmental Sciences*, 2012; *12*, 249-258.

[10] What is Cactus Soil and How Does It Differ from Regular Potting Mix?. Available online: https://www.thespruce.com/what-is-cactus-soil-5113988 (20 November 2022).

[11] Business is Spiking for This Thai Cactus Seller Amid a Covid-19 Gardening Boom. Available online: https://lot.dhl.com/business-is-spiking-for-this-thai-cactus-seller-amid-a-covid-19-gardening-boom/. (25 September 2022).

[12] Baldwin, D.L. *Designing with succulents*, 1 st ed.; Timber Press, Portland, USA, 2007; 304.

[13] 15 of the Best Types of Cactus You Can Grow at Home. Available online: https://www.countryliving.com /gardening/g28365636/types-of-cactus-species/ (1 September 2021).

[14] Spomer, L.A. Three simple demonstrations of the physical effects of soil amendment. *HortScience*, 1979; *14(1)*, 75-77.

[15] Joelma, D.F.; Santo, M.D.; Junior, C.D.; Neto, E.B.; Lida, M.D.; Cunha, M.D.; Santos, D.D.; Amorim, S.D.; Mello, A.C. Growth of cactus pear cv. Miúda under different salinity levels and irrigation frequencies. *Anais da Academia Brasileira de Ciencias*, 2018; *90(4)*, 3893–3900.

[16] Sutas, J.; Manad, A.; Pitakc, L. Effect of rice husk and rice husk ash to properties of bricks. *Procedia Engineering*, 2012; *32*, 1061-1067.
[17] Hashim, A.B.; Aminuddin, H.; Siva, K.B. Nutrient content in rice husk ash of some Malaysian rice varieties. *Pertanika Journal of Tropical Agricultural Science*, 1996; *19*(1), 77-80.
[18] Using Leaf Compost. Available online: https://njaes.rutgers.edu/fs117/. (10 September 2022).
[19] Khomami, A.M.; Haddad, A.; Alipoor, R.; Hojati, S.I. Cow manure and sawdust vermicompost effect on nutrition and growth of ornamental foliage plants. *Central Asian Journal of Environmental Science and Technology Innovation*, 2021; *2*, 68-77.
[20] Mariotti, B.; Martini, S.; Raddi, S.; Tani, A.; Jacobs, D.F.; Oliet, J.A.; Maltoni, A. Coconut coir as a sustainable nursery growing media for seedling production of the ecologically diverse *Quercus* species. *Forests*, 2020; *11*, 522.
[21] What are Hydroton Expanded Clay Pebbles, and How Do They Compare to Other Growing Media. Available online: https://planteli.com/clay-pebbles/. (10 September 2022).
[22] Anuwong, C.; Samran, N.; Kosinwattana, S. Effect of planting materials on growth of cactus. *Khon Kaen Agriculture Journal*, 2022; *50(4)*, 1019-1032.

JSTR
ASEAN Journal of Scientific and Technological Reports

Research article

Effect of Supplementation Yeast Fermented *Acacia mangium* Leaf in Diets on Growth Performance, Carcass Quality, and Haematology of Climbing Perch (*Anabas testudineus*)

Warrapong Nalinanon[1*], Saichon Lerdsuwan[2] and Duangjai Pisuttharachai[3]

[1] Fishery Science and Aquatic Resources, Disciplines of Technology Agriculture, King Mongkut's Institute of Technology Ladkrabang, Prince of Chumphon Campus, Chumphon, 86160, Thailand; warrapong.na@kmitl.ac.th
[2] Animal Science, Disciplines of Technology Agriculture, King Mongkut's Institute of Technology Ladkrabang, Prince of Chumphon Campus, Chumphon, 86160, Thailand; saichon.le@kmitl.ac.th
[3] Fishery Science and Aquatic Resources, Disciplines of Technology Agriculture, King Mongkut's Institute of Technology Ladkrabang, Prince of Chumphon Campus, Chumphon, 86160, Thailand; duangjai.pi@kmitl.ac.th
* Correspondence: warrapong.na@kmitl.ac.th

Abstract: A total of 360 juvenile *Anabas testudineus* of mean weight (2.88 ± 0.02 g/fish) were randomly distributed in triplicate of 20 fish per tank. *Acacia mangium* leave meal (AM) and yeast-fermented *Acacia mangium* leave meal (FAM) were used at 0, 2.5, 2.5, 5, 7.5, and 10 % supplemental in the experimental diets. They were fed for 12 weeks to *A. testudineus* fingerling stocked in 18 plastic tanks (200 liters) set up to recirculation system. Results indicated that the final body weight, weight gain, FCR, SGR, and PER were the best in treatment 4 (FAM 5.0%), significantly different ($P < 0.05$) from other FAM and AM treatments. There was no significant difference ($P > 0.05$) in HSI, FR, VSI, L*, a*, and b* across the test diets. The hematological indices' result showed no significant difference($P > 0.05$) in hematocrit and red blood cells among the experimental groups. However, the thrombocyte and lymphocyte were significantly different ($P < 0.05$) in experimental diets FAM 5.0% and FAM 7.5% compared to AM 2.5%, FAM 2.5%, and FAM 10%. The study showed that the inclusion of yeast-fermented *Acacia mangium* leave meal (FAM) at 5% had the best-enhanced growth performance and feed utilization without any adverse effect on the fish carcass quality and hematological indices.

Keywords: Yeast fermented; *Acacia mangium*; Growth performance; *Anabas testudineus*

Citation:
Nalinanon, W.; Lerdsuwan, S.; Pisuttharachai, D. Effect of Supplementation Yeast Fermented *Acacia mangium* Leaf in Diets on Growth Performance, Carcass Quality, and Haematology of Climbing Perch (*Anabas testudineus*). *ASEAN J. Sci. Tech. Report.* **2022**, *25*(4), 68-78. https://doi.org/10.55164/ajstr.v25i4.247547

Article history:
Received: October 10, 2022
Revised: December 9, 2022
Accepted: December 17, 2022
Available online: December 22, 2022

1. Introduction

The culture of climbing perch (*Anabas testudineus*) has long been implemented in Chumphon, Thailand. This fish has become the most popular cultural species in this region, with high economic value and demand. The climbing perch is commercially important and its value in Thailand was USD 19.13 million in 2010 [1]. This is due to its reasonable growth rate and resistance to pathogens, a favorite for consumption in Thailand. Besides that, scientists have focused their research on genetics development and the use of immunostimulants to improve growth performance and enhance fish disease resistance [2]. Using an immunostimulant could also potentially promote fish

growth [3]. Moreover, Immunostimulant does not leave any residue in fish bodies and the environment and is not harmful to human health. Baker's yeast (*Saccharomyces cerevisiae*) is a natural product from the baker's yeast industry that contains various immunostimulating compounds such as β-glucan, nucleic acid, mannan oligosaccharides, and chitin [4]. Fermentation of baker's yeast cells in *Acacia mangium* leaves meal and supplement the combination in diets has been proven to enhance fish growth and immunity [5].

Acacia mangium is a fast-growing species that can maintain active growth during the dry season and is used for reforestation in tropical regions [4]. It is the most common tree in many areas in southeast Asia and other tropical countries. Despite the documented low intake and degradability of *Acacia mangium*, there is an interest in finding the optimal way to feed this foliage[6]. The crude protein content in acacia foliage is relatively high, from 162 g to 170 g CP/kg dry matter [7]. The *Acacia mangium* leaves meal (AM) so obtained contained, on a dry weight basis, 15.97% crude protein, 2.25 % lipid, 4.04% ash, and 25% crude fiber [8]. Supplemented with 10% *Acacia mangium* leaves meal mixed with 10% coconut meal was found to have a suitable level to fulfill the growth performance of Nile tilapia(*Oreochromis nilitcus*) [9]. The nutrient digestibility of *Acacia mangium* leave is also low but was improved by fermentation with Baker's yeast (*Saccharomyces cerevisiae*) [10]. The use of brewer's yeast has positively affected several fish species' performance and welfare. The inclusion of 30–50% brewers yeast in the diet improved the feed efficiency of European seabass [11]

The objectives of this study were to examine the effect of supplementation of yeast-fermented *Acacia mangium* leaves meal on growth performance, carcass quality, and hematology of climbing perch (*Anabas testudineus*).

2. Materials and Methods

2.1 Sample preparation

The Baker's yeast (*Saccharomyces cerevisiae*) was purchased from a store at Pathiu market in Chumphon, Thailand. Mature *Acacia mangium* (AM) leaves were collected from the Inland Aquaculture field, King Mongkut's Institute of Technology Ladkrabang, Prince of Chumphon Campus (KMITL PCC), Chumphon, Thailand and dried in a hot air oven in 60 °C for 36 hours, and ground into powder using an electric blender. After passing through a 550 mm mesh sieve, the AM was fermented with *S. cerevisiae* yeast.

2.2 Solid state fermentation of Acacia mangium leave using S. cerevisiae

Eighty grams of *Acacia mangium* leaves were weighed into a 250 ml conical flask. The powdered leaves were mixed with liquid basal medium containing distilled water, 0.8 g of urea, 24 g of molasses, 16 g of tapioca starch, 0.56 g of $MgSO_4.2H_2O$ and 1.04 g KH_2PO_4 to obtain a final moisture content of 60%. The mixture was sterilized at 121 °C for 15 minutes and then cooled to room temperature (27 ± 2 °C). Four grams (6.77×10^6 CFU/g) of fermented yeast powder was added to the sterilized *Acacia mangium* leaves in the 250 ml conical flasks, mixed gently, loosely covered with aluminum foil, and incubated at 27 °C for 5 days with intermittent manual shaking. During incubation, samples were collected at 24 h for yeast cell count, spread on metallic trays, and oven-dried at 600 °C for 5 h, cooled to 27 ± 2 °C, milled, and packaged in air-tight containers [11].

2.3 Diet formulation and preparation

The formulations of the experimental diets for the supplementation of yeast-fermented *Acacia mangium* leaves meal (FAM) study are shown in Table 1. The fermented *Acacia mangium* leaves meal (FAM) was serially included at the rates of 2.5, 5, 7.5, and 10%, whereas unfermented *Acacia mangium* leaves meal (AM) was included at 2.5%. The control diet had no added AM or FAM. All diets were formulated to be isonitrogenous (40% crude protein) and isoenergetic (4,500 kcal/kg diet) [12]. The experimental diets were prepared following the procedure described by Nalinanon et al. [13]. The FAM was randomized for initial yeast cell count before supplementing to the experimental diets.

Table 1. The formulations and composition of the experimental diets are shown in Table 1.

Ingredient (%) As-fed basis	Treatments					
	Control 0%	**AM 2.5%**	**FAM 2.5%**	**FAM 5%**	**FAM 7.5%**	**FAM 10%**
Corn starch	2	1.5	1.5	1.5	1.5	1.5
Brocken rice	12.6	11.3	11.3	10.0	9.8	9.6
Rice bran	15.4	15.2	15.1	14.2	12.0	9.8
Fish meal (60% CP)	40.0	40.0	40.0	40.0	40.0	40.0
Soybean meal (45% CP)	27.0	26.5	26.6	26.3	26.2	26.1
AM	0	2.5	0	0	0	0
FAM	0	0	2.5	5.0	7.5	10.0
DCP (P17)	0.5	0.5	0.5	0.5	0.5	0.5
Premix[1]	1.0	1.0	1.0	1.0	1.0	1.0
Binder	1.0	1.0	1.0	1.0	1.0	1.0
Palm oil	0.5	0.5	0.5	0.5	0.5	0.5
Total (g)	100	100	100	100	100	100
Nutrient analysis [10]						
Moisture (%)	8.92	9.03	9.12	9.05	8.98	9.00
Crude protein (%)	40.02	40.03	40.02	40.04	40.01	40.05
Gross energy (Kcal/Kg)	4442.80	4466.69	4460.10	4473.34	4475.62	4477.89
Crude fat (%)	12.51	12.40	12.43	12.10	12.16	12.31
Fiber (%)	15.06	15.34	15.08	15.13	15.32	15.41
Ash (%)	11.81	12.02	12.51	12.60	12.83	12.86
NFE[2] (%)	11.68	11.18	10.84	11.08	10.70	10.37

[1] Vitamin-mineral premix provides per kg of diet: vitamin A 15,000 IU; vitamin D3 3,000 IU; vitamin E 25 IU; vitamin K30.5 g; vitamin B1 2.5 mg; vitamin B2 7 mg; vitamin B6 4.5 mg; vitamin B12 0.025 mg; pantothenic acid 35 mg; nicotinic acid 35 mg; choline chloride 0.25 g; biotin 0.025 mg; Cu 1.6 mg; folic acid 0.5 mg; Mn0.06 g; Se 0.15 mg; Fe 0.08 g; I 0.4 mg and Zn 0.045 g.
[2] NFE = Nitrogen-free extract = 100 - (moisture + protein + lipid + fiber + ash)
[2] NFE = Nitrogen-free extract = 100 - (moisture + protein + lipid + fiber + ash)

2.4 Experimental procedure

Juvenile climbing perch (*Anabas testudineus*) was provided by The Chumphon Aquaculture Genetics Research and Development Center. Before the study, The fish were maintained in an indoor oxygenated (1,000 L) tank in the Inland Aquaculture Laboratory, King Mongkut's Institute of Technology Ladkrabang, Prince of Chumphon Campus (KMITL PCC), Chumphon, Thailand. A domesticated strain of climbing perch was used in this study. The experimental fish were fed a control diet (40% crude protein and 4,500 kcal/kg gross energy) during the 2-week acclimatization period before starting the experiment. At the start of the investigation, 20 juvenile climbing perch (mean weight 2.88 ± 0.02 g) were reared in recirculation aquaculture tanks (RAT) for the experiment. The RAT was integrated into a single system of 15 (200-L) rearing tanks. Each rearing tank supplied 8 L/min of treated water, constant temperature (28 °C) with an aqua heater, and constant DO (6.0 mg/L). The six dietary treatments of AM and FAM in the experiment were fed to randomly assigned triplicate groups of fish and to apparent satiation twice a day. Fish were batch-weighed by tank once every two weeks and the daily ration was adjusted accordingly for 12 weeks.

2.5 Sample collection chemical analysis and color determination

At the start of the experiment, 60 fish were sacrificed, weighed, and measured in length. At the end of the feeding trial, 15 fish per treatment (5 fish per replicate) were randomly chosen, starved for 24 h, weighed, measured length, killed, and dissected. Liver, gut, and flesh were weighed to determine Hepatosomatic (HSI) and Viscerosomatic (VSI) indexes and Flesh ratio (FR) as described in Tawakalitu et al. [14]. Analysis of crude protein, crude fat, fiber, ash, moisture, NFE, and GE contents of the test diets followed the methods of Association of Official Analytical Chemists (AOAC) [15]. The fish fillets were analyzed for color by Konica Minolta CR-400 Chroma Meter. The samples were put into the glass dish, and

the measuring head of the meter was carefully placed in three different locations on the fillet. Means and standard deviations were determined from triplicate measurements.

2.6 Haematology studies

At the end of the trial, three fish per replication (n=9/treatment) were randomly captured, and blood samples were collected using a 2 ml syringe from the caudal vein to evaluate hematology studies. Before the blood samplings, fish were starved for 24 h. Hematocrit values were determined using microhematocrit heparinized capillary tubes. Red and white blood cells were counted in a Neubauer hemocytometer[16]. To estimate the differential leucocyte count, blood smears were prepared, air-dried, fixed in methanol, and stained using Giemsa (Merck, Germany) [17]. Leucocytes in blood smears were categorized into thrombocytes, eosinophils, basophils, neutrophils, lymphocytes, and monocytes.

2.7 Calculations and statistical analysis

Growth, survival rate, feed utilization, and some physical qualities were calculated using the following equations[13].

(1) WG = Wf – Wi; where WG is the weight gain, Wi and Wf is the initial and final mean body weights.

(2) FCR = [sum of dried diet consumed /weight gain]; FCR is the feed conversion ratio.

(3) SGR = [100 × [(ln(FW) – ln(IW)] /day]; where SGR is the specific growth rate measured in percent per day and IW is the initial weight, and FW is the final weight both measured in grams.

(4) PER = wet weight gain (g)/total protein intake (g); where PER is the protein efficiency ratio

(5) SR = [100 × (remaining number of fish)/ (initial number of fish)], where SR is the survival rate measured in percent.

(6) HSI = [100 × liver weight / total body weight]; where HSI is the hepato-somatic index measured in percent.

(7) FR = [100 × flesh weight / total body weight]; where FR is the flesh ratio measured in percent.

(8) VSI = [100 × visceral mass weight / total body weight]; where VSI is the visceral-somatic index measured in percent.

All data were calculated as mean ± SD and subjected to one-way variance analysis. Duncan's new multiple-range test was used to test for significant differences at the ($P < 0.05$) level.

3. Results and Discussion

3.1 Results

The growth performance of *A. testudineus* juveniles over the period is presented in Table 2. The final body weight was significantly higher ($P < 0.01$) in FAM 5.0% and control, respectively, compared with other treatments. In the present study, dietary supplementation of yeast (*S. cerevisiae*) fermented *Acacia mangium* leaves meal at 5.0% level significantly enhanced the growth (weight gain and SGR), PER, and reducing trend of FCR in climbing perch. However, the final body weight of the group AM 2.5% (7.78 ± 0.17 g), FAM 7.5% (7.68 ± 0.20 g), and FAM 10% (7.50 ± 0.21g) were not differenced significantly ($P > 0.05$) between the group. Feed conversion ratio (FCR), specific growth rate (SGR), and protein efficiency ratio (PER) showed a highly significant difference ($P < 0.01$) among the treatment. A better FCR, 1.52 ± 0.16, was observed in FAM 5.0%, which was significantly lower from AM 2.5% (1.83 ± 0.09), FAM 7.5% (1.88 ± 0.10) and FAM 10% (1.97 ± 0.12). Similarly, significantly higher PER, 2.57 ± 0.15, was registered in FAM 5.0% compared to 1.89 ± 0.10, 2.18 ± 0.09, 1.87 ± 0.10, and 1.84 ± 0.08 in AM 2.5%, FAM 2.5%, FAM 7.5% and FAM 10% respectively. However, no significant difference in final body weight, weight gain, FCR, SGR, and PER was observed between FAM 5.0% and control.

Table 2. Growth performance of *Anabas testudineus* juveniles fed with yeast-fermented *Acacia mangium* leaves meal (FAM) supplemented diets

Growth parameters	Control	AM 2.5%	FAM 2.5%	FAM 5.0%	FAM 7.5%	FAM 10%	Level of significance
Initial wt. (g)	2.86 ± 0.04	2.88 ± 0.02	2.90 ± 0.01	2.88 ± 0.02	2.87 ± 0.02	2.87 ± 0.03	NS
Final wt. (g)	8.77 ± 0.18^{a}	7.78 ± 0.17^{c}	8.47 ± 0.14^{b}	8.78 ± 0.23^{a}	7.68 ± 0.20^{c}	7.50 ± 0.21^{cd}	**
Weight gain (%)	206.64 ± 5.36^{a}	170.14 ± 5.06^{c}	192.07 ± 5.12^{b}	204.86 ± 5.24^{a}	167.60 ± 5.03^{c}	161.32 ± 5.04^{cd}	**
FCR	1.58 ± 0.13^{a}	1.83 ± 0.09^{b}	1.56 ± 0.11^{a}	1.52 ± 0.16^{a}	1.88 ± 0.10^{b}	1.97 ± 0.12^{b}	*
SGR	2.56 ± 0.07^{a}	1.96 ± 0.05^{c}	2.20 ± 0.04^{b}	2.54 ± 0.04^{a}	1.98 ± 0.05^{c}	1.91 ± 0.06^{c}	**
PER	2.58 ± 0.11^{a}	1.89 ± 0.10^{c}	2.18 ± 0.09^{b}	2.57 ± 0.15^{a}	1.87 ± 0.10^{c}	1.84 ± 0.08^{c}	*
SR (%)	100 ± 0.00	98.33 ± 2.89	100 ± 0.00	100 ± 0.00	100 ± 0.00	100 ± 0.00	NS

The means with no superscript letter in common per factor indicate significant difference; Values are presented as mean ± SD; If the effect were significant, ANOVA was followed by the Duncan test. *P < 0.05; **P < 0.01; NS, not significant.

Table 3. Water quality parameters in the experimental tanks during the study period (mean ± SD)

Parameters	Control	AM 2.5%	FAM 2.5%	FAM 5.0%	FAM 7.5%	FAM 10%	Level of significance
Temperature (°C)	26.85 ± 0.42	26.83 ± 0.46	26.72 ± 0.43	26.90 ± 0.48	26.76 ± 0.39	26.78 ± 0.45	NS
pH	7.10 ± 0.16	7.13 ± 0.11	7.13 ± 0.12	7.11 ± 0.13	7.12 ± 0.18	7.11 ± 0.15	NS
Alkalinity (mg/l $CaCO_3$)	85.32 ± 1.83	86.10 ± 2.01	85.26 ± 1.76	86.11 ± 1.95	85.42 ± 2.08	85.58 ± 2.02	NS
Total hardness (mg/l)	55.52 ± 1.52	54.34 ± 2.11	55.12 ± 1.83	55.20 ± 1.24	55.39 ± 1.46	54.42 ± 2.01	NS
Total ammonia-N (mg/l)	0.25 ± 0.02	0.25 ± 0.02	0.25 ± 0.01	0.25 ± 0.01	0.25 ± 0.02	0.25 ± 0.01	NS
Nitrite-N (mg/l)	0.08 ± 0.01	0.08 ± 0.01	0.08 ± 0.01	0.08 ± 0.01	0.08 ± 0.01	0.08 ± 0.01	NS
Nitrate-N (mg/l)	0.21 ± 0.01	0.20 ± 0.01	0.20 ± 0.01	0.21 ± 0.01	0.21 ± 0.01	0.20 ± 0.01	NS
Dissolved oxygen (ppm)	5.69 ± 0.18	5.67 ± 0.12	5.65 ± 0.11	5.60 ± 0.15	5.59 ± 0.14	5.66 ± 0.10	NS

The means with no superscript letter in common per factor indicate a significant difference; If the effect were significant, ANOVA was followed by the Duncan test; NS was not significant.

The water quality parameters during the study period are presented in Table 3. No significant difference ($P > 0.05$) among the treatments was observed in water quality parameters during the experimental period.

The proximate composition (%) of FAM and experimental diets are presented in Tables 4 and 5. The dried FAM contained 14.47 ± 0.1% crude protein, 2.55 ± 0.18% crude lipid, and 49.67 ± 0.23% nitrogen-free extract (NFE). The mean ash content and organic matter were 5.97 ± 0.02% and 94.03 ± 0.78% of dried FAM, respectively. Experimental diets did not significantly differ ($P > 0.05$) in crude protein, lipid, ash, and crude fiber. However, the nitrogen-free extract (NFE) content was significantly higher ($P < 0.01$) in experimental diets FAM 7.5% and FAM 10% compared to control, AM 2.5%, FAM 2.5%, and FAM 5.0%. The crude protein and gross energy content ranged from 39.78 ± 0.16 to 40.02 ± 0.08% and 4,490.10 ± 2.64 to 4,497.89 ± 3.06 Kcal/Kg in the experimental diets.

Table 4. Proximate composition of yeast-fermented *Acacia mangium* leaves meal (FAM) and *Acacia mangium* leaves meal (AM) (mean ± SD)

Nutrients	FAM (%)	AM (%)
Organic matter[1]	94.03 ± 0.78	95.96 ± 0.83
Moisture	6.71 ± 0.01	8.56 ± 0.02
Crude protein	14.47 ± 0.1	15.97 ± 0.08
Crude lipid (EE)	2.55 ± 0.18	2.25 ± 0.21
Ash	5.97 ± 0.02	4.04 ± 0.01
Crude fiber	20.63 ± 0.52	25.00 ± 0.62
Total NFE[2]	49.67 ± 0.23	44.18 ± 0.26
Gross energy (Kcal/Kg)[3]	4,720.64 ± 2.85	4,963.14 ± 3.15

[1] Organic matter = 100-Ash; [2] NFE = 100 – (CP + EE + CF + ash + moisture) [3] Gross energy (GE) = (CP x 5.56) + (EE x 9.44) + (CF x 4.1) + NFE x 4.1) Kcal/Kg.

The carcass quality and fillet color parameters are presented in Table 6. No significant difference ($P > 0.05$) among the treatments was observed in carcass quality and fillet color at the end of the experiment. But also, The hepato-somatic index and flesh ratio ranged from 1.94 ± 0.06 to 2.05 ± 0.05% and 48.82 ± 2.98 to 50.04 ± 1.91% in the experimental diets. There was no difference in chromatic component a* (ranging from 7.11 ± 0.49 to 7.76 ± 0.54) and b* (ranging from -0.78 ± 0.11 to -0.62 ± 0.21) between fish fillets among the treatments

Table 7 shows the hematological indices of *Anabas testudineus* juveniles at the end of the trial. White blood cells were significantly higher in FAM-fed groups than in control and AM 2.5% diet-fed groups ($P < 0.01$). There was no significant difference in hematocrit and red blood cells among the experimental groups ($P > 0.05$). However, the thrombocyte and lymphocyte significantly differed ($P < 0.05$) in experimental diets FAM 5.0% and FAM 7.5% compared to AM 2.5%, FAM 2.5%, and FAM 10%. No significant difference ($P > 0.05$) among the treatments was observed in eosinophil, basophil, and monocyte at the end of the trial.

Table 5. Proximate composition (%) of experimental diets supplemented with graded levels of yeast-fermented *Acacia mangium* leaves meal (FAM) and *Acacia mangium* leaves meal (Am) (mean ± SD)

Nutrients	Control	AM 2.5%	FAM 2.5%	FAM 5.0%	FAM 7.5%	FAM 10%	Level of significance
Organic matter[1]	94.28 ± 0.73	94.43 ± 0.68	94.63 ± 0.70	94.74 ± 0.62	95.24 ± 0.34	95.51 ± 0.21	NS
Moisture	10.03 ± 0.10	10.12 ± 0.06	10.32 ± 0.21	9.96 ± 0.24	10.08 ± 0.11	10.15 ± 0.05	NS
Crude protein	39.89 ± 0.18	39.92 ± 0.12	39.78 ± 0.16	39.96 ± 0.20	40.02 ± 0.08	39.86 ± 0.13	NS
Crude lipid (EE)	11.34 ± 0.28	11.42 ± 0.16	11.32 ± 0.12	11.50 ± 0.21	11.56 ± 0.22	11.70 ± 0.10	NS
Ash	5.72 ± 0.41	5.57 ± 0.42	5.37 ± 0.60	5.26 ± 0.25	4.76 ± 0.67	4.49 ± 0.70	NS
Crude fiber	12.12 ± 0.35	12.08 ± 0.48	12.34 ± 0.26	12.67 ± 0.08	12.52 ± 0.11	12.78 ± 0.03	NS
NFE[2]	20.90 ± 0.05[b]	20.89 ± 0.02[b]	20.87 ± 0.04[b]	20.65 ± 0.13[b]	21.06 ± 0.02[a]	21.02 ± 0.01[a]	**
Gross energy[3]	4,492.80 ± 3.18	4,496.69 ± 3.10	4,490.10 ± 2.64	4,493.34 ± 2.88	4,495.62 ± 3.04	4,497.89 ± 3.06	NS

[1]Organic matter = 100-Ash; [2]NFE = 100 – (CP + EE + CF + ash + moisture); [3]Gross energy (GE) = (CP x 5.56) + (EE x 9.44) + (CF x 4.1) + NFE x 4.1) Kcal/Kg; The means with no superscript letter in common per factor indicate significant difference; Value is presented as mean ± SD; If the effect were significant, ANOVA was followed by Duncan test. *P < 0.05; **P < 0.01; NS, not significant.

Table 6. Carcass quality and fillet color (L*, a*, b*) of *Anabas testudineus* fed with yeast-fermented *Acacia mangium* leaves meal (FAM) supplemented diets (mean ± sd)

Parameters	Control	AM 2.5%	FAM 2.5%	FAM 5.0%	FAM 7.5%	FAM 10%	Level of significance
[1]HSI (%)	2.04 ± 0.07	2.00 ± 0.06	2.05 ± 0.05	2.01 ± 0.02	1.94 ± 0.06	1.97 ± 0.05	NS
[2]FR (%)	49.60 ± 2.81	49.02 ± 2.90	49.66 ± 2.06	50.04 ± 1.91	49.63 ± 2.54	48.82 ± 2.98	NS
[3]VSI (%)	24.13 ± 3.14	24.90 ± 3.02	26.65 ± 3.51	22.32 ± 3.97	21.76 ± 4.08	24.17 ± 3.21	NS
L* (lightness)	41.40 ± 1.97	40.14 ± 1.42	41.18 ± 1.47	39.55 ± 1.99	40.64 ± 1.82	41.24 ± 1.84	NS
a*	7.32 ± 0.57	7.76 ± 0.54	7.24 ± 0.52	7.11 ± 0.49	7.70 ± 0.46	7.67 ± 0.50	NS
b*	-0.62 ± 0.21	-0.77 ± 0.16	-0.74 ± 0.27	-0.66 ± 0.18	-0.68 ± 0.20	-0.78 ± 0.11	NS

[1] HSI = [100 × liver weight / total body weight]; where HSI is the hepato-somatic index measured in percent; [2]FR = [100 × flesh weight / total body weight]; where FR is the flesh ratio measured in percent; [3]VSI = [100 × visceral mass weight / total body weight]; where VSI is the viscero-somatic index measured in percent.

Table 7. The blood parameters of *Anabas testudineus* fed with yeast-fermented *Acacia mangium* leaves meal (FAM) supplemented diets

Parameters	Control	AM 2.5%	FAM 2.5%	FAM 5.0%	FAM 7.5%	FAM 10%	Level of significance
Hematocrit (%)	38.67 ± 3.06	40.00 ± 7.21	35.84 ± 1.58	35.84 ± 5.86	37.22 ± 5.00	36.30 ± 1.53	NS
Red blood cell (1×10^6cell/mm^3)	4.07 ± 0.56	4.35 ± 0.74	4.14 ± 0.85	4.30 ± 0.92	4.24 ± 0.79	4.44 ± 0.87	NS
White blood cell (1×10^4cell/mm^3)	6.10 ± 0.38^{d}	5.73 ± 0.21^{d}	8.08 ± 0.35^{c}	8.38 ± 0.23^{bc}	8.83 ± 0.49^{b}	10.49 ± 0.55^{a}	**
Thrombocyte (%)	44.33 ± 9.29^{ab}	54.00 ± 10.15^{a}	52.00 ± 1.00^{a}	39.00 ± 4.00^{b}	38.33 ± 2.08^{b}	54.67 ± 7.37^{a}	*
Eosinophil (%)	3.00 ± 1.73	2.67 ± 1.53	6.00 ± 4.00	2.00 ± 1.00	6.67 ± 4.16	6.67 ± 4.16	NS
Basophil (%)	0.00 ± 0.00	0.33 ± 0.58	1.00 ± 1.00	0.33±0.58	1.00 ± 1.00	1.00 ± 1.00	NS
Neutrophil (%)	0.33 ± 0.58^{b}	2.00 ± 0.00^{a}	1.33 ± 0.58^{ab}	1.67±1.15^{a}	2.33 ± 0.58^{a}	1.67 ± 0.58^{a}	*
Lymphocyte (%)	48.00 ± 9.64^{a}	34.00 ± 8.72^{b}	31.67 ± 4.73^{b}	52.33±5.03^{a}	45.67 ± 5.51^{a}	29.67 ± 0.58^{b}	*
Monocyte (%)	4.33 ± 1.53	7.00 ± 6.00	8.00 ± 6.08	4.67±0.58	6.00 ± 1.73	6.33 ± 5.03	NS

The means with no superscript letter in common per factor indicate significant difference; values are presented as mean ± SD; If the effect were significant, ANOVA was followed by the Duncan test. *P < 0.05; **P < 0.01; NS, not significant.

3.2. Discussion

The present study illustrates the role of FAM as a dietary supplement on growth performance, carcass quality, and hematology of climbing perch (*Anabas testudineus*). Including baker's yeast (*Saccharomyces cerevisiae*) as a dietary ingredient in the fish diet improved the growth performance of African Catfish [18]. In the present study, dietary supplementation of yeast (*S.cerevisiae*) fermented *Acacia mangium* leaves meal at 5.0% level significantly decreased the trend of crude fiber in diets and enhanced the growth (weight gain and SGR), PER, and reduced the FCR in climbing perch. These results agree with Israeli carp [19] and Nile tilapia [20]. Similar results were obtained when *S.cerevisiae* was added to the fish diet of hybrid striped bass [21]. The improved fish growth and feed utilization may be due to enhanced nutrient digestibility. In this regard, [18] found that adding yeast improves diet and protein digestibility, which may explain the better growth and feed efficiency recorded with yeast supplements. As inasmuch, dried yeast is a source of nucleic acids and non-starch polysaccharides, including β-1,3 glucan. In avian species, β-glucans may affect the absorption of nutrients, possibly by increasing gut viscosity, while the high concentration of nucleic acids may affect nutrient metabolism in monogastric animals. [22] On the other hand, [23] reported a linear decrease in growth performance and efficiency in nutrient utilization when juvenile tilapia were fed above 15% yeast. HSI (Hepato-Somatic Index), FR (Flesh Ratio), VSI (Viscero-Somatic Index), and fillet color (L*, a*, b*) of the fish were not significantly affected by the supplementation of yeast-fermented *Acacia mangium* leaves meal in the diet ($P > 0.05$). This study reveals that FAM does not influence the color attributes of climbing perch fillet, wherewith, As fish is not capable of synthesizing carotenoids de novo, there is a need to incorporate carotenoids in the diet of cultured species. According to Bustari et al. [24], the carcass quality of fish at the end of their experiment showed that edible flesh, dress-out percentage, carcass waste, fillet color, and sensory quality of the fish slightly fluctuated among all the experimental diets without significant differences. These results followed the same trend as those obtained by Olvera-Novoa, et al. [25]. A linear increase trend in white blood cells when climbing perch were fed FAM component diets significant difference ($P < 0.01$) with control and *Acacia mangium* leaves meal AM 2.5% diet. The highest value of white blood cells was observed in diet 6 (FAM 10%), while a high level of thrombocyte, eosinophil, and basophil was observed in diet 6 (FAM 10%). Several workers [26-28] reported that *S. cerevisiae* improved the efficacy of the immune system, improved intestinal lumen health, and increased digestion and absorption of nutrients, which resulted in better performance.

4. Conclusions

The present study indicates that yeast (*S.cerevisiae*) fermented *Acacia mangium* leaves meal at 5.0% (FAM 5.0%) in diet positively enhanced growth performance and feed utilization of Climbing perch (*Anabas testudineus*) without any adverse effect on the fish health and carcass quality.

5. Acknowledgements

The authors would like to thank Asst. Prof. Dr. Sitthipong Nalinanon for his help in proofreading the manuscript.

Author Contributions: Conceptualization, W. N.; performed the experiments, W. N., S. L., and D. P.; formal analysis, W. N.; data collection, S. L. and D. P.; writing—original draft preparation, W. N.; writing—review and editing, W. N.; supervision, W. N. All authors have read and agreed to the published version of the manuscript.

Funding: This research received no external funding.

Conflicts of Interest: The authors declare no conflict of interest.

References

[1] Information Technology Center. Fisheries Statistic of Thailand 2010. Department of Fisheries, Ministry of Agriculture and Cooperatives. Thailand. Technical Paper No 12. 2012.

[2] Burrels, C.; Williams, P.D.; Soutthgate, P.J.; Wadsworth, S.L. Dietary nucleotide: A novel supplement in fish feed. 2. Effects on vaccination, salt water transfer, growth rates and physiology of Atlantic salmon (*Salmo salar* L.). *Aquaculture*. 2001; 199, 171-178.

[3] Ian, B.; Roy, A.D. The use of immunostimulants in fish larval aquaculture. *Fish and Shellfish Immunology*. 2005; 19, 457-472.

[4] Tukmechi, A.; Andani, H.R.R.; Manaffar, R.; Sheikhzadeh,N. Dietary administration of beta -mercaptoethanol treated Saccharomyces cerevisiae enhanced the growth, innate immune response and disease resistance of the rainbow trout, Oncorhynchus mykiss. Fish and Shellfish Immunology. 2011; 30, 923-929.

[5] Henky, M.; Magdalena, E.F.K. The use of baker's yeast to promote growth of carp (*Cyprinus carpio* L). *International Journal of PharmTech Research.* 2016; 9, 415-420.

[6] Man, N.V.; Hao, N.V.; Tri, V.M. Biomass production of some leguminous shrubs and trees in Vietnam. Livest. *Research for Rural Development.* 1995; 7, 1-9.

[7] Do,T.T.V.; Nguyen, T.M.; Inger, L. Effect of method of processing foliage of Acacia mangium and inclusion of bamboo charcoal in the diet on performance of growing goats. *Animal Feed Science and Technology*. 2006; 34, 18-27.

[8] Van, D.T.T.; Mui, N.T.; Ledin, I. Tropical foliages: effect of presentation method and species on intake by goats. *Animal Feed Science Technology*. 2005; 118, 1-8.

[9] Nalinanon, W.; Lerdsuwan, S. Study on the effect of coconut (by-product) meal and Acacia mangium leaf in diets on growth and carcass quality of nile tilapia (Oreochromis niloticus). *Khon Kaen AgriculturevJournal*.2018; 46, 1026-1032.

[10] Oliva-Teles, A.; Goncalves, P. Partial replacement of fishmeal by brewers yeast (*Saccaromyces cerevisae*) in diets for sea bass (*Dicentrarchus labrax*) juveniles. *Aquaculture*. 2001; 202, 269-276.

[11] Tawakalitu, E. A.; Ogugua, C. A.; Akeem, O. R.; Aderonke, I. O. Protein enrichment of yam peels by fermentation with *Saccharomyces cerevisiae* (BY4743). *Annals of Agricultural Science.* 2017; 12, 56-63

[12] Hossain, M.A.; Sultana, Z.; Kibria, A.S.M.; Azimuddin, K.M. Optimum Dietary Protein Requirement of a Thai Strain of Climbing Perch,*Anabas testudineus* (Bloch, 1792) Fry. *Turkish Journal of Fisheries and Aquatic Sciences*. 2012; 12, 217-224.

[13] Nalinanon, W.; Lerdsuwan, S. Effect of dietary salt (NaCl) supplementation on growth, feed utilization and carcass quality of Nile tilapia (*Oreochromis niloticus*). The Proceedings of Suratthani Rajabhat University Conference 2018: International Conference on Innovations in Interdisciplinary Research (ICIIR), Suratthani Province, Thailand. 331 012012 http://doi.org/11.1098/1745-1325/335/1/012033. 2018.

[14] Tawakalitu, E. A.; Ogugua, C. A.; Akeem, O. R.; Aderonke, I. O. Protein enrichment of yam peels by fermentation with *Saccharomyces cerevisiae* (BY4743). *Annals of Agricultural Science.* 2017; 12, 56-63.

[15] Association of Official Analytical Chemists (AOAC). Official Methods of Analysis, 16th edn (ed. by P. A. Cunniff). AOAC International, Arlington, VA. USA. 1997.

[16] Ta'ati, R.; Soltani, M.; Bahmani, M.; Zamini, A.A. Growth performance, carcass composition, and immunophysiological indices in juvenile great sturgeon (*Huso huso*) fed on commercial prebiotic, Immunoster. *Iranian Journal of Fisheries Sciences*. 2011; 10, 324-332.

[17] Zorriehzahra, M. J.; Hassan, M. D.; Gholizadeh, M.; Saidi, A.A. Study of some hematological and biochemical parameters of rainbow trout (*Oncorhynchus mykiss*) fry in western part of Mazandaran province, Iran. *Iranian Journal of Fisheries Sciences*. 2010; 9, 185-193.

[18] Aderolu, A.Z.; Lawal, M.O.; Ali, T. O.; Aarode, O.O. Utilization of baker's yeast (*Saccharomyces cerevisiae*) in the diet of juvenile African catfish (*Clarias gariepinus*). *Journal of Science Research and Development*. 2011; 13, 19-28.

[19] Noh, S; Gagne, J.P.;Kaspar, V. Models of health behaviors and compliance: applications to audiological rehabilitation research. *Journal of Acad Rehabil Audiol Monograph Supplement*. 1994; 27, 375-389.

[20] Lara-Flores, M.; Olivera-Novoa, M.A.; Guzman-Mendez, B.E.; Lopez-Madrid, W. Use of the bacteria *Streptococcus faecium* and *Lactobacillus acidophilus*, and the yeast *Saccharomyces cerivisiae* as growth in Nile tilapia (*Oreochromis niloticus*). *Aquaculture*. 2003; 219, 193-201.

[21] Li, P.; Gatlin, D.M. III. Evaluation of the prebiotic grobiotic-A and brewer'syeast as dietary supplements for sub-adult hybrid striped bass (*Morone chrysops* x *M.saxatilis*) challenged in-situ with *Mycobacterium marinum*. *Aquaculture*. 2005; 248, 197-206.
[22] Bedford, M.R.; Classen, H.L. Reduction of intestinal viscosity through manipulation of dietary rye and pentosanase concentration is effected through changes in the carbohydrate composition of the intestinal aqueous phase and results in improved growth rate and food conversion efficiency of broiler chicks. *Journal of Nutrition*. 1992; 122, 560-571.
[23] Rodrigo, O.A.O.; Leandro, P.; Ricardo, B.; José, E.P.C. Effects of dietary yeast (*Saccharomyces cerevisia*) supplementation in practical diets of Tilapia (*Oreochromis niloticus*). *Animals*. 2012; 2, 16-24.
[24] Bustari, H.; Iskandar, P.; Indra, S.; Dian, I.; Zainal, A. M. Growth performance and carcass quality of river catfish *Hemibagrus nemurus* fed salted trash fish meal. *Egyptian Journal of Aquatic Research*. 2019; 45, 259-266.
[25] Olvera-Novoa, M.A.; Martinez-Palacios, C.A.; Olivera-Castillo, L. Utilization of torula yeast (*Candida utilis*) as a protein source in diets for tilapia (*Oreochromis mossambicus* Peters) fry. *Aquaculture Nutrition*. 2002; 8, 257-265.
[26] Oyofo, B.A.; De Loach, J.R.; Corrier, D.E.; Norman, J.O.; Ziprin, R.L.; Molenhauer, H. H. Prevention of *Salmonella typhimurium* colonization of broilers with Dmannose. *Poultry Science*. 1989; 68,1357-1366.
[27] Newman, K. Mannan-oligosaccharides: Natural polymers with significant impact on the gastrointestinal microflora and the immune system. Master degree. Biotechnology in the Feed Industry.Nottingham University, Nicholasville, Kentucky,USA. 2/12/1994.
[28] Spring, P.; Wenk, C.; Dawson, K.A.; Newman, K.E. The effects of dietary manna oligosaccharides on cecal parameters and the concentration of enteric bacteria in the ceca of Salmonella challenged broiler chicks. *Poultry Science*. 2000; 79, 205-214.

JSTR
ASEAN Journal of Scientific and Technological Reports

Research article

Impact of Using Blue Crab Shell Powder (BCSP) on Alteration of EC, pH, Leaf Greenness, and Growth of *Cucumis melo* var. Hamigua TA215 Seedlings

Pimpan Pimonrat[1], Dowroong Watcharinrat[2] Nattapong Chanchula[3], and Pornpimol Pimolrat [4*]

[1] Faculty of Agricultural Technology, Rajamangala University of Technology, Thanyaburi, Thailand; pimpan_p@rmutt.ac.th
[2] Shinawatra University, Bangtoey, Pathum Thani, Thailand; dowroongw@hotmail.com
[3] Expert Center of Innovative Agriculture, Thailand Institute of Scientific and Technological Research (TISTR), Khlong Luang, Pathum Thani, Thailand; lorchula@gmail.com
[4] Department of Coastal Aquaculture, Faculty of Maejo University at Chumphon, Maejo University, Lamae, Chumphon, Thailand; paqua50@gmail.com
* Correspondence: paqua50@gmail.com

Citation:
Pimonrat, P.; Watcharinrat, D.; Chanchula, N.; Pimolrat, P. Impact of Using Blue Crab Shell Powder (BCSP) on Alteration of EC, pH, Leaf Greenness, and Growth of *Cucumis melo* var. Hamigua TA215 Seedlings. *ASEAN J. Sci. Tech. Report.* **2022**, *25*(4), 79-85. https://doi.org/10.55164/ajstr.v25i4.247640

Article history:
Received: October 31, 2022
Revised: December 13, 2022
Accepted: December 17, 2022
Available online: December 22,2022

Abstract: Seedling is the most important starting material for muskmelon production. Healthy seedling production can be addressed by finding appropriate seedling substrates. Blue crab shell powder (BCSP) has been used as a substrate additive to increase the growth and yield of agricultural produce. This research aimed to investigate the impact of using BCSP on the alteration of EC, pH, leaf greenness, and growth of *Cucumis melo* var. Hamigua TA215 seedlings. The substrates making up the treatments were 5, 10, and 15% BCSP, and peat moss was used as a control. Four treatments replicated three times were laid out in a Completely Randomized Design (CRD). The results showed that increasing EC and pH were attributed by increasing the BCSP. After 9 days of watering, a reduction of EC was found. On the contrary, pH in 15% BCSP adding treatment was gradually increased and reached the highest point at day 9. Alteration of EC and pH affected leaf greenness. The highest point of leaf greenness was found on day 1, consistent with increasing EC. Final growth was most significant for seedlings grown in peat moss (control) and tended to decrease as the percent BCSP increased. These are indicative that essential elements in BCSP resulted in leaf greenness appearance. It was growing of pH impact growths of seedlings. Reduction of the amount of BCSP might provide favorable conditions around root environments for the seedling development of muskmelon with healthy growth.

Keywords: Blue crab shell powder (BCSP); Melon; EC; pH; Leaf greenness

1. Introduction

Muskmelon (*Cucumis melo* L.) is a crop belonging to the Cucurbitaceae family. People worldwide relish it due to its flesh fruits with plenty of sweetness, aroma, and nutritional compounds, which share an economic value of 181.79 million United States dollars [1-3]. It originated in Africa and is dispersed to the rest of the economic zone of the world nowadays. Muskmelon is commercially

cultivated as horticultural crops instead of growing under tropical or subtropical conditions, as it was done early [4]. Seedling is the most important starting material for the steps of muskmelon production. The longer hardening stage before transplanting and shortage of nutrition in seedling substrates affect the reduction of growth, yield, and taste of the produce. Healthy seedling production can be addressed by finding appropriate seedling substrates.

Blue swimming crab (BSC) is a global-demand seafood product harvested in several Indo-Pacific regions, such as Indonesia, Philippines, Vietnam, Cambodia, Malaysia, Thailand, India, and Sri Lanka [5]. In Thailand, major commercial fishing grounds distribute in the Gulf of Thailand provinces; Pattani, Prachuab-Kirikhan, Phetchaburi, Rayong, Surat Thani, Chonburi, Chanthaburi, Chumphon, Nakhon Si Thammarat, Narathiwat, Trat, and Songkhla as well as the Andaman Sea regions; Krabi, Phang Nga, Phuket, Trang, Satun, and Ranong [6]. The total catch of BSC was estimated at 25,712 tons, with 19,216 tons from the Gulf of Thailand and 6,496 tons from the Andaman Sea in 2013, and steadily increased every year since the 1960s. BSC is exported as fresh-cut crab, frozen, and canned products. There are shells as byproducts from fresh-cut crab product processing which have several advantages in rising productivity of agricultural production, low cost, and high biocompatibility named blue crab shell (BCS).

BCS has been used as a solid eliminator of toxins from wastewater [7-8], stabilizer of heavy metal contaminated soil and water [9-10], crab shell powder (CSP) as a plant diseases controller [11], growth substrate for insect-pathogenic fungus [12], growth substrate for bacteria which use as plant disease control [13-14], organic fertilizer [15-16], plant disease suppressor [11, 17], reducer of acidity soil [18], Meloidogyne suppressor [19], increasing seed germination [20-21].

We successfully used blue crab shell powder (BCSP) to increase the growth and yield of kaiware and sunflower microgreens [22]. However, no report has evaluated the impact of using BCSP on musk melon seedlings. Therefore, this research aimed to investigate the alteration of EC, pH, leaf greenness, and growth of *Cucumis melo* var. Hamigua TA215 seedlings.

2. Materials and Methods

Preparation of BCSP

Crab shells were cleaned under running tap water. The shells were dried at room temperature, then crushed into powder using a blender. After the shell powders were ground, they were maintained in a dry place at room temperature. The shell powders were used as solid substrates in the experiment. The experiment was carried out in a greenhouse at the Rajamangala University of Technology Thanyaburi in October 2021. Four treatments replicated three times were laid out in a Completely Randomized Design (CRD). The substrates making up the treatments were 5, 10, and 15% BCSP, and peat moss was used as a control.

Preparation of seedlings and growth performance analysis

We selected *Cucumis melo* var. Hamigua TA215 F1 by Known-you Seed (Thailand) Co., LTD. For testing, substrates were filled differently in the seed tray, which was placed over on drainage tray. The substrates were soaked overnight with water to achieve about 70-80% moisture. Germinated seeds, three days after seeding by incubation at room temperature without light, were planted into a seed tray. Each seedling was fed with 20 ml of water daily. Alterations of EC, pH, Leaf greenness, growth parameters, seedling height, leaf width, leaf length, stem fresh and dry weight, and root fresh and dry weight were recorded.

EC and pH analysis

During the experiment, the EC and pH of the substrates were measured for each treatment by taking the solution from the drainage tray with a syringe after daily watering. Measurements were carried out 3 times on day 1, day 5, and day 9 of the experiment.

Leaf greenness Analysis

The leaf greenness was measured by SPAD portable leaf greenness meter. Three SPAD measurements were averaged per expanded leaf in each treatment to represent one observation. Measurements were carried out 3 times on day 1, day 5, and day 9 of the experiment.

Statistical analysis

Analytical measurements and all collected data were presented by mean value with standard deviation. Each parameter was subjected to analysis of variance (ANOVA) by using CRD as an experimental design. Duncan's multiple range test (DMRT) was used to determine of differences between the treatment at 95% confidential ($p \leq 0.05$).

3. Results and Discussion

An increase in EC was attributed to an increase in BCSP. EC Alteration was found on days 5 and 9 (Table 1). On day 5, EC was higher than on day 1. On the contrary, the least amount of EC was observed on day 9, indicating essential elements dissolved daily since day 1. Consequently, solubility was therefore reduced on day 9. The appropriate EC for melon production under a hydroponic system is about 2.5 mS/cm [23]. Higher EC dues to adding BCSP at day 5 may affect unbalance of the nutrient requirement of vegetative growth. BCSP might contain more nutrients needed for the reproductive growth stage than the vegetative stage, such as Ca and Mg.

Table 1. Effect of different amounts of BCSP added into the substrate on electrical conductivity (EC) at days 1, 5, and 9.

Treatment	EC (mS/cm)		
	Day 1	Day 5	Day 9
Control	0.87	1.55	0.84
5%	1.80	2.27	1.10
10%	2.04	3.10	1.17
15%	2.10	3.19	1.25

For pH, the control treatment result was between 6.17 and 6.85 (Table 2). A higher pH was observed after adding BCSP. The most elevated pH was found in the amount of BCSP added (15%) on days 1, 5, and 9. A similar result was reported by studying the effect of crab residue in soil salinization and the development of melon. The increased crab residue concentration significantly increases the soil's pH [24]. An increase in pH was attributed to an increasing the day of the experiment, indicating the accumulation of essential element ions. The highest pH was found on day 9, adding 15% BCSP (8.34). On day 1, pH observation results of BCSP treatment were not reached 8.0 (6.17-7.31). pH observations over 8.0 were found on days 5 (6.80-8.23) and 9 (6.85-8.34), respectively. BCSP was the reason for the substrate pH value increase, which was unsuitable for growing melon seedlings. [25] reported that maintaining a pH between 6.0 and 6.5 is very important for muskmelon production.

Table 2. Effect of different amounts of BCSP added into the substrate on pH at days 1, 5, and 9.

Treatment	pH		
	Day 1	Day 5	Day 9
Control	6.17	6.80	6.85
5%	7.19	8.18	8.27
10%	7.29	8.18	8.31
15%	7.31	8.23	8.34

Leaf greenness analysis was relatively high across BCSP treatments at values of >45 SPAD units of the whole experiment (Table 3). At day 1, leaf greenness was highest for seedlings grown in 15% BCSP added substrate, indicating differences in foliage greenness. This result was also found on day 5. A similar result was reported by studying the effect of crab shell powder on pea, gram, and tomato leaf greenness which crab shell powder promoted higher leaf greenness accumulation [20]. At day 9, the highest value was observed in a minimal amount of 5% BCSP instead of 15%, indicating accumulation of pH and reduction of EC-affected greenness of the leaf.

Table 3. Effect of different amounts of BCSP added into the substrate on leaf greenness at day 1, 5, and 9 of seedling grown.

Treatment	Leaf greenness (SPAD unit)		
	Day 1	Day 5	Day 9
Control	45.87 ± 3.07^{b}	42.76 ± 5.66	42.68 ± 6.39
5%	54.70 ± 9.66^{ab}	46.77 ± 5.19	47.26 ± 1.81
10%	52.40 ± 1.47^{b}	48.80 ± 5.97	47.05 ± 2.58
15%	64.45 ± 0.64^{a}	51.35 ± 3.61	45.50 ± 3.96
F-test	*	ns	ns
C.V. (%)	10.25	11.61	8.78

All the data are expressed as mean ± standard deviations. This means the different superscript letters in a column differ significantly ($p \leq 0.05$). ns, *=nonsignificant or significant, respectively.

During the experiment, growth parameters were measured on days 1, 5, and 9. Seedling height decreased as the percent BCSP increased (Table 4). However, there was no statistically significant difference found between treatments. Consistent with trends observed for seedling height, leaf width tended to decrease as the percent BCSP increased (Table 5). Different results were obtained by studying the effect of a crab shell on germination and plant height which found that crab shell promoted plant height [21]. According to [15], fresh crab shell fog dramatically increased Cucurbitaceae's plant height.

Table 4. Effect of different amounts of BCSP added into the substrate on the seedling height at day 1, 5, and 9 of seedling grown.

Treatment	Seedling height (cm.)		
	Day 1	Day 5	Day 9
Control	3.18 ± 0.42	5.10 ± 1.02	5.92 ± 1.46
5%	3.30 ± 0.14	4.38 ± 1.02	5.47 ± 1.33
10%	3.00 ± 0.71	4.27 ± 1.24	5.17 ± 1.10
15%	3.00 ± 0.10	3.50 ± 2.26	4.60 ± 0.85
F-test	ns	ns	ns
C.V. (%)	16.84	29.44	22.12

All the data are expressed as mean ± standard deviations. This means the different superscript letters in a column differ significantly ($p \leq 0.05$). ns=nonsignificant.

Table 5. Effect of different amounts of BCSP added into the substrate on leaf width at day 1, 5, and 9 of seedling grown.

Treatment	Leaf width (cm.)		
	Day 1	Day 5	Day 9
Control	1.37 ± 0.15	1.70 ± 0.31	1.86 ± 0.17
5%	1.13 ± 0.21	1.63 ± 0.23	1.78 ± 0.10
10%	1.08 ± 0.45	1.63 ± 0.16	1.64 ± 0.42
15%	0.75 ± 0.07	1.55 ± 0.14	1.60 ± 0.07
F-test	ns	ns	ns
C.V. (%)	29.25	14.11	15.96

All the data are expressed as mean ± standard deviations. This means the different superscript letters in a column differ significantly ($p \leq 0.05$). ns=nonsignificant.

There were statistically significant differences between treatments at days 1, 5, and 9 of leaf length measurement. The highest severity was observed after adding 15% BCSP into peat moss. Leaf length was most significant for seedlings grown in peat moss (control) (Table 6).

Table 6. Effect of different amounts of BCSP added into the substrate on leaf length at day 1, 5, and 9 of seedling grown.

Treatment	Leaf length (cm.)		
	Day 1	Day 5	Day 9
Control	2.63 ± 0.42^{a}	3.73 ± 0.42^{a}	4.03 ± 0.10^{a}
5%	2.30 ± 0.17^{a}	2.98 ± 0.77^{a}	3.45 ± 0.59^{a}
10%	1.90 ± 0.60^{ab}	2.90 ± 0.47^{a}	3.41 ± 0.41^{a}
15%	1.20 ± 0.28^{b}	1.75 ± 0.35^{b}	2.60 ± 0.14^{b}
F-test	*	*	*
C.V. (%)	22.63	19.68	12.52

All the data are expressed as mean ± standard deviations. This means the different superscript letters in a column differ significantly ($p \leq 0.05$). *=significant.

Seedling growth tended to be susceptible to high percent BCSP added. Final stem fresh and dry weight was most significant for seedlings grown in peat moss (control) and managed to decrease as the percent BCSP increased (Table 7). Consistent with trends observed for stem fresh and dry weight, root new and dry weight was most significant for seedlings grown in peat moss (control) and tended to decrease as the percent BCSP increased. 5% BCSP was less severe to the growth of seedlings than other amounts. A similar result was reported by studying the effect of crab residue in soil salinization and the development of melon which the increase in the concentration of crab residue significantly reduces plant growth [24]. The EC and pH in the substrate changed during cultivation, while changes in the content of components in the leaf were maximum. Interferences of photosynthetic compounds may cause a reduction in growth. Therefore, proper pH and EC in the muskmelon root environment are essential. The results were unlike those reported in maize, where dry weight increases after cultivation in the amendment of acid soils using crab shell powder [18].

Table 7. Effect of different amounts of BCSP added into the substrate on stem fresh and dry weight and root fresh and dry weight at day 9 of seedling growth.

Treatment	Stem fresh weight (g)	Stem dry weight (g)	Root fresh weight (g)	Root dry weight (g)
Control	1.12 ± 0.34^{a}	0.10 ± 0.04^{a}	0.57 ± 0.23^{a}	0.04 ± 0.01^{a}
5%	1.03 ± 0.17^{ab}	0.11 ± 0.02^{a}	0.51 ± 0.26^{a}	0.04 ± 0.03^{a}
10%	1.02 ± 0.29^{ab}	0.09 ± 0.03^{ab}	0.27 ± 0.13^{ab}	0.02 ± 0.01^{ab}
15%	0.67 ± 0.03^{b}	0.05 ± 0.02^{b}	0.19 ± 0.06^{b}	0.01 ± 0.00^{b}
F-test	*	*	*	*
C.V. (%)	26.34	33.14	48.29	0.00

All the data are expressed as mean ± standard deviations. This means the different superscript letters in a column differ significantly ($p \leq 0.05$). *=significant.

4. Conclusions

Seedling is the most important starting material for the steps of muskmelon production. Healthy seedling production can be addressed by finding appropriate seedling substrates. Blue crab shell powder (BCSP) has been used as a substrate additive to increase the growth and yield of agricultural produce. However, no report has evaluated the impact of using BCSP on musk melon seedlings. The present study found that increased EC and pH were attributed to an increase in the amount of BCSP. 5% BCSP was less severe to the growth of seedlings than other amounts. The EC and pH in the substrate changed during cultivation, while changes in the content of components in the leaf were maximum. Interferences of photosynthetic compounds may cause a reduction in growth. Reduction of the amount of BCSP might provide favorable conditions around root environments for the seedling development of muskmelon with healthy growth.

5. Acknowledgements

This study was carried out with the support of the Crop Production Program, Faculty of Agricultural Technology, Rajamangala University of Technology Thanyaburi, Thailand. The authors offer particular thanks to MJU2T for the BCG project, Lamae district, Maejo University at Chumphon, responsible for BCSP support.

Author Contributions: Conceptualization, P.P. and P.P.; methodology, P.P.; software, P.P.; validation, P.P., and P.P.; formal analysis, P.P.; investigation, P.P.; resources, P.P. and C.N.; data curation, P.P.; writing—original draft preparation, P.P.; writing—review and editing, P.P.; visualization, W.D.; supervision, W.D.; project administration, P.P.; funding acquisition, P.P., and P.P. All authors have read and agreed to the published version of the manuscript.

Funding: This research received no external funding

Conflicts of Interest: The authors declare no conflict of interest.

References

1. Zhang, H.; Wang, H.; Yi, H.; Zhai, W.; Wang, G.; Fu, Q. Transcriptome profiling of *Cucumis melo* fruit development and ripening. *Hortic. Res.* 2016; 3, 1-10.
2. Abraham-Juarez, M.; Espitia-Vazquez, I.; Guzman-Mendoza, R.; Olalde-Portugal, V.; Ruiz-Aguilar, G.; Garcia-Hernandez, J.; Herrera-Isidron, L; Nunez-Palenius, H. Development, yield, and quality of melon fruit (*Cucumis melo* L.) inoculated with mexican native strains of *Bacillus subtilis* (EHRENBERG). *Agrociencia* 2018; 52, 91-102.
3. Manchali, S.; Murthy, K.; Vishnuvardana; Patil, B. Nutritional composition and health benefits of various botanical types of melon (*Cucumis melo* L.). *Plants 2021;* 10, 1-21.
4. Espinosa, F.; Vallejo, F.A.; Rizzo, L. Selection of half-sib families of creole melon (*Cucumis melo* L.) on the Ecuadorian coast. *Rev. Colomb. Cienc. Hortic.* 2019; *13*(2), 178-185.
5. Creech, S.; Bandara, J; Silva, D. Project proposal: An assessment of the ecological impact (habitats and ecosystem) of the blue swimmimg crab (*Portunus pelagicus*) fishery in the Palk bay (bay of Bengal), Sri Lanka. Sri Lanka blue swimming crab fishery improvement project. 2016; 11.
6. Banks, R; Trumble, R.J. Pre-assessment of the Thailand blue swimming crab (*Portunus pelagicus*) Fishery. May. 2012; 81.
7. Wen, F.S.; Li, C.L.; Jia, W.T.; Cheng, I.W. Applications of chitosan beads and porous crab shell powder combined with solid-phase microextraction for detection and the removal of colour from textile wastewater. *Carbohydr. Polym.* 2008, *72*(3), 550-556.
8. Rao, T.M.; Rao, V.V. Biosorption of Congo Red from aqueous solution by crab shell residues: a comprehensive study. *Springer Plus* 2016; 5, 2-14.
9. Rui, J.R.M.; Claudia, B.L.; Luciana, S.R.; Joao, P.C.; Armando, C.D.; Pereira, E. Sustainable approach for recycling seafood wastes for the removal of priority hazardous substances (Hg and Cd) from water. *J. Environ. Chem. Eng.* 2016; *4*(1), 1199-1208.
10. Feng, Y.; Zhong, Z.; Zhang, C. Stabilization of multiple heavy metal contaminated soils using discarded crab shell. *E3S Web of Conferences*. 2020; 194, 1-5.
11. Widodo.; Harti, H.; Wiyono, S. Control of banana wilt disease caused by *Fusarium oxysporum* Schlecht f.sp. cubense (E. F. Smith) using crab shell powder and chitosan. *J. Agric. Sci.* 2021; *43*(1), 56-68.
12. Oetari, A.; Khodijah, N.A.; Sumandari, O.; Wijaya, C.K.; Yama, G.S.; Sjamsuridzal. Crustaceous wastes as growth substrates for insect-pathogenic fungus Metarhizium majus UICC 295. 2019.
13. Yue-Horng, Y.; Pei-Ling, L.; Chuan-Lu, W.; San-Lang, W. An antifungal protease produced by *Pseudomonas aeruginosa* M-1001 with shrimp and crab shell powder as a carbon source. *Enzyme Microb. Technol.* 2006; *39*(2), 311-317.
14. Wen-Teish, C.; Yu-Chung, C.; Chia-Ling, J. Antifungal activity and enhancement of plant growth by *Bacillus cereus* grown on shellfish chitin wastes. *Bioresour. Technol*. 2007; *98*(6), 1224-1230.
15. Sarva, S.A.K.; Girl, A. Effect of freshwater crab shell fog as organic fertilizer to increase plant of Cucurbitaceae growth dramatically. *Agrotechnology*, 2015; *4*(1), 1-4.

16. Nekvapil, F.; Ganea, I.; Ciorita, A.; Hirian, R.; Ogresta, L.; Glumuzina, B.; Roba, C.; Pinzaru, S.C. Wasted biomaterials from Crustaceans as a compliant natural product regarding microbiological, antibacterial properties and heavy metal content for reuse in blue bioeconomy: A preliminary study. *Materials (Basel)*. 2021; *14*(16), 4558.
17. Escuadra, G.M.E.; Amemiya, Y. Suppression of Fusarium wilt of spinach with compost amendments. *J. Gen. Plant Pathol.* 2008; 74, 267-274.
18. Aydin, A; Sevinc, A. Amendment of acid soils using crab shell powder. *Asian J. Chem.* 2008; *20*(3), 2156-2162.
19. Yen, J.H.; Wu, H.Y.; Tsai, S.J.; Chen, D.Y.; Tsay, T.T. Effect of LT-M mixture on the yield, fruit quality of shaddock and the population of citrus nematode, tylenchulus semipenetrans cobb.in shaddock yard. *Plant Prot. Bull.* 2008; *50*(1-2), 31-36.
20. Rebecca, L.J.; Anbuselvi, S.; Prathiba, M.; Dola, S. Effect of marine waste on seed germination. *J. Chem. Pharm.* 2014; *6*(4), 581-584.
21. Rebecca, L.J.; Anbuselvi, S.; Sharmila, S.; Prathiba, M.; Dola, S. Effect of marine waste on plant growth. *Der Pharmacia Letter*. 2015; *7*(10), 299-301.
22. Pimonrat, P.; Rodnoi, N.; Sankum, K.; Pimolrat, P. Effect of ground blue crap shell on increasing growth and yield of microgreen. *Khon Kaen University Journal (Graduate Studies)*, 2022; *50*(1), 556-561.
23. Fatahian, V.; Halim, R.A.; Ahmad, I.; Chua, K.; Teh, C.B.S.; Awang, Y. Melon production using four hydroponic systems. *Acta. Hort.* 2013; 1004, 85-92.
24. Ferreira, F.J.; Amorim, A.V.; Araujo, F.J.F.; Lacerda, A.F.; Aquino, M.D.. Effects of crab residue in soil salinization and development of melon. *Revista Brasileira de Engenharia Agricola e Ambiental.* 2011; *15*(4), 359-364.
25. Warncke, D.D. Nutrient management for Cucurbits: melons, pumpkin, cucumber, and squash. *Indiana CCA conference proceeding,* 2007.

JSTR

ASEAN Journal of Scientific and Technological Reports

Lists of Reviewers

Manuscripts of research articles and academic articles of ASEAN Journal of Scientific and Technological Reports (AJSTR). ISSN 2773-8752 (Online), Volume 25, No. 1-4. (January – December 2022) were reviewed by the reviewers as follows:

1.	Prof. Dr. Pranut Potiyaraj	Faculty of Science, Chulalongkorn University
2.	Prof. Dr. Saksit Chanthai	Faculty of Science, Khon Kaen University
4.	Prof. Dr. Thawatchai Phaechamud	Faculty of Pharmacy, Silpakorn University
5.	Assoc. Prof. Dr. Burachat Chatveera	Faculty of Engineering, Thammasat University
6.	Assoc. Prof. Dr. Chalermchai Wongs-Aree	School of Bioresources and Technology, King Mongkut's University of Technology Thonburi
7.	Assoc. Prof. Dr. Charlie Navanugraha	Faculty of Environment and Resource Studies, Mahasarakham University
8.	Assoc. Prof. Dr. Dechrit Maneetham	Faculty of Technical Education Rajamangala University of Technology Thanyaburi
9.	Assoc. Prof. Dr. Dheerawan Boonyawan	Faculty of Science, Chiang Mai University
10.	Assoc. Prof. Dr. Jesada Is-haak	Faculty of Agricultural Technology and Agro-Industry, Rajamangala University of Technology Suvarnabhum
11.	Assoc. Prof. Dr. Kanokphorn Sangkharak	Faculty of Science, Thaksin University
12.	Assoc. Prof. Dr. Kiadtisak Saenboonruang	Faculty of Science, Kasetsart University
13.	Assoc. Prof. Dr. Kittiwet Kuntiyawichai	Faculty of Engineering, Khon Kaen Unversity
14.	Assoc. Prof. Dr. Klanarong Sriroth	Faculty of Agro-Industry, Kasetsart University
15.	Assoc. Prof. Dr. Manat Chaijan	School of Agricultural Technology and food Industry, Walailak University
16.	Assoc. Prof. Dr. Mayuree Kajayklang	Faculty of Agriculture, Natural Resources and Environment, Naresuan University
17.	Assoc. Prof. Dr. Nongnud Tangkrock-olan	Faculty of Science, Burapha University
19.	Assoc. Prof. Dr. Patchareeya Boonkorkaew	Faculty of Agriculture, Kasetsart University
20.	Assoc. Prof. Dr. Pattanapol Meena	Faculty of Science, Mahasarakham University
21.	Assoc. Prof. Dr. Pattarasinee Bhattarakosol	Faculty of Science, Chulalongkorn University
22.	Assoc. Prof. Dr. Rapeeporn Ruangchuay	Faculty of Science and Technology, Prince of Songkla University
23.	Assoc. Prof. Dr. Ratchadaporn Oonsivilai	School of Food Technology, Suranaree University of Technology
24.	Assoc. Prof. Dr. Sappasith Klomklao	Faculty of Agro-and Bio-Industry, Thaksin University
26.	Assoc. Prof. Dr. Sorapong Benchasri	Faculty of yechnology and community Development, Thaksin University
27.	Assoc. Prof. Dr. Sutthipoj Wongrerkdee	Faculty of Liberal Arts and Science, Kasetsart University
28.	Assoc. Prof. Dr. Usarat Thawornchaisit	Faculty of Science, King Mongkut's Institute of Technology Ladkrabang
29.	Assoc. Prof. Dr. Wara Taparhudee	Faculty of Fisheries, Kasetsart University

30.	Assoc. Prof. Dr. Wimonlak Sutapun	Institute of Engineering, Suranaree University of Technology
31.	Assoc. Prof. Dr. Worawut Koedprang	Faculty of Science and Fisherie, Rajamangala University of Technology Srivijaya
33.	Assoc. Prof. Dr. Wuttigrai Boonkum	Faculty of Agriculture, Khon Kaen University
34.	Assoc. Prof. Bundit Yuangsoi	Faculty of Agriculture, Khon Kaen University
35.	Asst. Prof. Dr. Apichart Sonthisombat	Faculty of Engineering, Rajamangala University of Technology Thanyaburi
36.	Asst. Prof. Dr. Apiwat WiSitsorasak	Faculty of Science, King Mongkut's University of Technology Thonburi
37.	Asst. Prof. Dr. Artit Chingsungnoen	Faculty of Science, Mahasakham University
38.	Asst. Prof. Dr. Catheleeya Mekjaruskul	Faculty of Pharmacy, Mahasarakham University
39.	Asst. Prof. Dr. Chutiphon Srisawat	Faculty of Science and Technology, Pibulsongkram Rajabhat University
40.	Asst. Prof. Dr. Daracha Thiammueang	Faculty of Fisheries Technology and Aquatic Resources, Maejo University
41.	Asst. Prof. Dr. Kitiyaporn Wittayanarakul	Faculty of Sciences, Khon Kaen University
42.	Asst. Prof. Dr. Komate Amphawan	Faculty of Informatics, Burapha University
43.	Asst. Prof. Dr. Kritsupath Sarnok	Faculty of Education Vongchavalitkul, University Nakornratchasima
44.	Asst. Prof. Dr. Kwanruthai Wongsaprom	Faculty of Science, Mahasarakham University
45.	Asst. Prof. Dr. Niraporn Chaiwang	Faculty of Agriculture, Khon Kaen University
46.	Asst. Prof. Dr. Niwat Muangkeow	School of Agricultural Technology and food Industry, Walailak University
47.	Asst. Prof. Dr. Noppamas Pukkhem	Faculty of Science, Thaksin University
48.	Asst. Prof. Dr. Orawan Chaowalit	Faculty of Science, Silpakorn University
49.	Asst. Prof. Dr. Orrarujee Muanwong	Faculty of Science, Khon Kaen University
50.	Asst. Prof. Dr. Pachara Pholna	Faculty of Science, Thaksin University
51.	Asst. Prof. Dr. Pathumwadee Yotmanee	Faculty of Science, Ramkhamhaeng University
52.	Asst. Prof. Dr. Pattamarat Rattanachuay	Faculty of Science, Prince of Songkla University
53.	Asst. Prof. Dr. Prasong Kessaratikoon	Faculty of Science, Thaksin University
54.	Asst. Prof. Dr. Prawit Kongjan	Faculty of Science and Technology, Prince of Songkla University
56.	Asst. Prof. Dr. Rattana Jariyaboon	Faculty of Science and Technology, Prince of Songkla University
57.	Asst. Prof. Dr. Santi Raksawong	Faculty of Science and Technology, Muban Chombueng Rajabhat University
59.	Asst. Prof. Dr. Saowapa Chotisuwan	Faculty of Science and Technology, Prince of Songkla University
60.	Asst. Prof. Dr. Siraya Sitthisarn	Faculty of Science, Thaksin University
61.	Asst. Prof. Dr. Somsak Siwadamrongpong	Institutes of Engineering, Suranaree University of Technology

62.	Asst. Prof. Dr. Sornchai Intachai	Faculty of Science, Thaksin University
63.	Asst. Prof. Dr. Suphada Kiriratnikom	Faculty of Science, Thaksin University
65.	Asst. Prof. Dr. Supoj Hengpraprohm	Faculty of Science and Technology, Nakhon Pathom Rajabhat University
68.	Asst. Prof. Dr. Suppakarn Chansareewittaya	School of Information Technology, Mae Fah Luang University
69.	Asst. Prof. Dr. Suthida Chamrat	Faculty of Education, Chiang Mai University
70.	Asst. Prof. Dr. Suwan Plaipichit	Faculty of Science, Srinakharinwirot University
71.	Asst. Prof. Dr. Thanya Panritdam	Faculty of Science, Thaksin University
72.	Asst. Prof. Dr. Thavorn Junthachote	Faculty of Agro and Bio Industry
74.	Asst. Prof. Dr. Thawatchai Tepnual	Faculty of Science, Thaksin University
75.	Asst. Prof. Dr. Visit Boonchom	Faculty of Science, Thaksin University
76.	Asst. Prof. Dr. Waraporn Rattanongphisat	Faculty of Science, Naresuan University
77.	Asst. Prof. Dr. Weerachai Sangchay	Faculty of Industrials Technology, Songkhla Rajabhat University
78.	Asst. Prof. Dr. Wichuda Klawech	Faculty of Sciences and Liberal Arts, Rajamangala University of Technology Isan
79.	Asst. Prof. Dr. Wiphada Wettayaprasit	Faculty of Science, Prince of Songkla University
80.	Asst. Prof. Dr. Yutthapong Sangnoi	Faculty of Agro-Industry, Prince of Songkla University
82.	Asst. Prof. Siriyaporn Sangaroon	Faculty of Science, Mahasarakham University
83.	Asst. Prof. Sittichoke Janyong	Faculty of Science and Fisheries Technology, Rajamangala University of Technology Srivijiaya
84.	Asst. Prof. Wirawut Lephon	Faculty of Industraial Technology, Pibulsongkram Rajabhat University
85.	Asst. Prof. Wittawat Molee	School of Animal Technology and Innovation, Suranaree University of Technology
86.	Asst. Prof. Yaowarat Sirisathitkul	School of Engineering and Technology, Walailak University
87.	Dr. Adisak Intana	College of Computing, Prince of Songkla University
88.	Dr. Chaipat Lapinee	School of Science, University of Phayao
90.	Dr. Jitsopa Chaliewsak	Faculty of Science, Srinakharinwirot University
91.	Dr. Korawit Prutsachainimmit	Faculty of Technology and Environment, Prince of Songkla University
92	Dr. Kornkanok Ubolchollakhet	Faculty of Engineering, Thaksin University
93.	Dr. Naphat Keawpibal	Faculty of Science, Thaksin University
96.	Dr. Nutt Nuntapong	Faculty of Natural Resources, Prince of Songkla University
97.	Dr. Wanida Petlamul	College of Innovation and Management, Songkhla Rajabhat University
98.	Dr. Weerawut Naebpetch	Faculty of Engineering, Thaksin University
99.	Dr. Win Win Myo	Faculty of Computing, University of Information Technology

100. Dr. Wirawut Lephon	Faculty of Industrial Technology, Phibunsongkhram Rajabhat
101. Nareenas Chehlaeh	Faculty of Science and Technology, Prince of Songkla University
102. Nopporn Poolyarat	Thailand Institute of Nuclear Technology (Public Organization)
103. Puji Irawati	National Astronomical Research Institute of Thailand (Public Organization)
104. Vutthichai Oniam	Faculty of Fisheries, Kasetsart University

JSTR
ASEAN Journal of Scientific and Technological Reports

Article type

Type of the Paper (Article, Review, Communication, etc.) *about 8,000 words maximum*

Title (Palatino Linotype 18 pt, bold)

Firstname Lastname[1], Firstname Lastname[2] and Firstname Lastname[2*]

[1] Affiliation 1; e-mail@e-mail.com
[2] Affiliation 2; e-mail@e-mail.com
* Correspondence: e-mail@e-mail.com; (one corresponding authors, add author initials)

Abstract: A single paragraph of about 400 words maximum. Self-contained and concisely describe the reason for the work, methodology, results, and conclusions. Uncommon abbreviations should be spelled out at first use. We strongly encourage authors to use the following style of structured abstracts, but without headings: (1) Background: Place the question addressed in a broad context and highlight the purpose of the study; (2) Methods: briefly describe the main methods or treatments applied; (3) Results: summarize the article's main findings; (4) Conclusions: indicate the main conclusions or interpretations.

Keywords: keyword 1; keyword 2; keyword 3 (List three to ten pertinent keywords specific to the article yet reasonably common within the subject discipline.)

1. Introduction

The introduction should briefly place the study in a broad context and highlight why it is crucial. It should define the purpose of the work and its significance. The current state of the research field should be carefully reviewed and critical publications cited. Please highlight controversial and diverging hypotheses when necessary. Finally, briefly mention the main aim of the work. References should be numbered in order of appearance and indicated by a numeral or numerals in square brackets—e.g., [1] or [2,3], or [4–6]. See the end of the document for further details on references.

2. Materials and Methods

The materials and methods should be described with sufficient details to allow others to replicate and build on the published results. Please note that your manuscript's publication implicates that you must make all materials, data, computer code, and protocols associated with the publication available to readers. Please disclose at the submission stage any restrictions on the availability of materials or information. New methods and protocols should be described in detail, while well-established methods can be briefly described and appropriately cited.

Interventional studies involving animals or humans, and other studies that require ethical approval, must list the authority that provided approval and the corresponding ethical approval code.

Citation:
Lastname, F.; Lastname, F.; Lastname, F. Title. *ASEAN J. Sci. Tech. Report.* **2022**, *25*(X), xx-xx. https://doi.org/10.55164/ajstr.vxxix.xxxxxx

Article history:
Received: date
Revised: date
Accepted: date
Available online: date

2.1 Subsection

2.1.1. Subsubsection

3. Results and Discussion

This section may be divided by subheadings. It should provide a concise and precise description of the experimental results, their interpretation, as well as the experimental conclusions that can be drawn.Authors should discuss the results and how they can be interpreted from previous studies and the working hypotheses. The findings and their implications should be discussed in the broadest context possible. Future research directions may also be highlighted.

3.1. Subsection

3.1.1. Subsubsection

3.2. Figures, Tables, and Schemes

All figures and tables should be cited in the main text as Figure 1, Table 1, etc.

Figure 1. This is a figure. Schemes follow the same formatting.

Table 1. This is a table. Tables should be placed in the main text near the first time they are cited.

Title 1	Title 2	Title 3
entry 1	data	data
entry 2	data	data [1]

[1] Table may have a footer.

3.3. Formatting of Mathematical Components

This is example 1 of an equation:

$$a = 1, \tag{1}$$

The text following an equation need not be a new paragraph. Please punctuate equations as regular text. This is example 2 of an equation:

$$a = b + c + d + e + f + g + h + i + j + k + l + m + n + o + p + q + r + s + t + u \tag{2}$$

The text following an equation need not be a new paragraph. Please punctuate equations as regular text. The text continues here.

4. Conclusions

Concisely restate the hypothesis and most important findings. Summarize the significant findings, contributions to existing knowledge, and limitations. What are the future directions? Conclusions MUST be well stated, linked to original research question & limited to supporting results.

5. Acknowledgements

Should not be used to acknowledge funders – funding will be entered as a separate. As a matter of courtesy, we suggest you inform anyone whom you acknowledge.

Author Contributions: For research articles with several authors, a short paragraph specifying their individual contributions must be provided. The following statements should be used "Conceptualization, X.X. and Y.Y.; methodology, X.X.; software, X.X.; validation, X.X., Y.Y. and Z.Z.; formal analysis, X.X.; investigation, X.X.; resources, X.X.; data curation, X.X.; writing—original draft preparation, X.X.; writing—review and editing, X.X.; visualization, X.X.; supervision, X.X.; project administration, X.X.; funding acquisition, Y.Y. All authors have read and agreed to the published version of the manuscript." Please turn to the CRediT taxonomy for the term explanation. Authorship must be limited to those who have contributed substantially to the work reported.

Funding: Please add: "This research received no external funding" or "This research was funded by NAME OF FUNDER, grant number XXX" and "The APC was funded by XXX". Check carefully that the details given are accurate and use the standard spelling of funding agency names at https://search.crossref.org/funding. Any errors may affect your future funding.

Conflicts of Interest: Declare conflicts of interest or state "The authors declare no conflict of interest." Authors must identify and declare any personal circumstances or interest that may be perceived as inappropriately influencing the representation or interpretation of reported research results. Any role of the funders in the design of the study; in the collection, analyses or interpretation of data; in the writing of the manuscript, or in the decision to publish the results must be declared in this section. If there is no role, please state "The funders had no role in the design of the study; in the collection, analyses, or interpretation of data; in the writing of the manuscript, or in the decision to publish the results".

References

References must be numbered in order of appearance in the text (including citations in tables and legends) and listed individually at the end of the manuscript. We recommend preparing the references with a bibliography software package, such as EndNote, ReferenceManager to avoid typing mistakes and duplicated references. Include the digital object identifier (DOI) for all references where available.

Citations and references in the Supplementary Materials are permitted provided that they also appear in the reference list here.

In the text, reference numbers should be placed in square brackets [ ] and placed before the punctuation; for example [1], [1–3] or [1,3]. For embedded citations in the text with pagination, use both parentheses and brackets to indicate the reference number and page numbers; for example [5] (p. 100), or [6] (pp. 101–105).

[1] Author 1, A.B.; Author 2, C.D. Title of the article. *Abbreviated Journal Name* Year, *Volume*, page range.

[2] Author 1, A.; Author 2, B. Title of the chapter. In *Book Title*, 2nd ed.; Editor 1, A., Editor 2, B., Eds.; Publisher: Publisher Location, Country, 2007; Volume 3, pp. 154–196.

[3] Author 1, A.; Author 2, B. *Book Title*, 3rd ed.; Publisher: Publisher Location, Country, 2008; pp. 154–196.

[4] Author 1, A.B.; Author 2, C. Title of Unpublished Work. *Abbreviated Journal Name* stage of publication (under review; accepted; in press).
[5] Author 1, A.B. (University, City, State, Country); Author 2, C. (Institute, City, State, Country). Personal communication, 2012.
[6] Author 1, A.B.; Author 2, C.D.; Author 3, E.F. Title of Presentation. In Title of the Collected Work (if available), Proceedings of the Name of the Conference, Location of Conference, Country, Date of Conference; Editor 1, Editor 2, Eds. (if available); Publisher: City, Country, Year (if available); Abstract Number (optional), Pagination (optional).
[7] Author 1, A.B. Title of Thesis. Level of Thesis, Degree-Granting University, Location of University, Date of Completion.
[8] Title of Site. Available online: URL (accessed on Day Month Year).

Reviewers sugestion

1. Name, Address, e-mail
2. Name, Address, e-mail
3. Name, Address, e-mail
4. Name, Address, e-mail

URL link:

Notes for Authors >> https://drive.google.com/file/d/1r0zegnIVeQqe4iLQyT1xDEIinNggINPD/view?usp=sharing
https://drive.google.com/file/d/1r0zegnIVeQqe4iLQyT1xDEIinNggINPD/view?usp=sharing

Online Submissions >> https://ph02.tci-thaijo.org/index.php/tsujournal/user/register

Current Issue >> https://ph02.tci-thaijo.org/index.php/tsujournal/issue/view/16516

AJSTR Publication Ethics and Malpractice >> https://ph02.tci-thaijo.org/index.php/tsujournal/ethics

Journal Title Abbreviations >> http://library.caltech.edu/reference/abbreviations

Research and Development Institute Thaksin University
222 M. 2 Ban-Prao sub-district,Pa-Pra-Yom district,
Phatthalung province, Thailand
Tel. 0 7460 9600 # 7242 , E-mail: aseanjstr@tsu.ac.th